5-2020

LOSS OF CASPASE-8 FUNCTION IN COMBINATION WITH SMAC MIMETIC TREATMENT SENSITIZES HEAD AND NECK SQUAMOUS CARCINOMA TO RADIATION THROUGH INDUCTION OF NECROPTOSIS.

Burak Uzunparmak

LOSS OF CASPASE-8 FUNCTION IN COMBINATION WITH SMAC MIMETIC TREATMENT SENSITIZES HEAD AND NECK SQUAMOUS CARCINOMA TO RADIATION THROUGH INDUCTION OF NECROPTOSIS.

by

Burak Uzunparmak, M.D.

Approved:

_____
Curtis R. Pickering, Ph.D.
Advisor

_____
Jeffrey N. Myers, M.D., Ph.D.

_____
Michael Andreeff, M.D., Ph.D.

_____
Andrew G. Sikora, M.D., Ph.D.

_____
Faye M. Johnson, M.D., Ph.D.

Approved:

_____
Dean, The University of Texas
MD Anderson Cancer Center UTHealth Graduate School of Biomedical Sciences

LOSS OF CASPASE-8 FUNCTION IN COMBINATION WITH SMAC MIMETIC TREATMENT SENSITIZES HEAD AND NECK SQUAMOUS CARCINOMA TO RADIATION THROUGH INDUCTION OF NECROPTOSIS.

A

DISSERTATION

Presented to the Faculty of

The University of Texas

MD Anderson Cancer Center UTHealth

and

The University of Texas

MD Anderson Cancer Center UTHealth

Graduate School of Biomedical Sciences in Partial Fulfillment

of the Requirements

for the Degree of

DOCTOR OF PHILOSOPHY

by

Burak Uzunparmak, M.D.

Houston, Texas

May, 2020

ACKNOWLEDGEMENTS

First and foremost, I would like to thank the University of Texas MD Anderson Cancer Center UTHealth, Graduate School of Biomedical Sciences (GSBS) for accepting me and all the support they have shown me throughout my Ph.D. career.

My sincere and deep gratitude goes to my supervisor, Dr Curtis R. Pickering, who opened the doors of his newly-established lab to me to perform my dissertation research under his mentorship. I am indebted to you for your continuous guidance and support over the course of my Ph.D. journey. Your passion for science, enthusiasm for generating new ideas to test in the lab, courage to address problems by imagining solutions and ability to see the big picture is a true inspiration to anyone working under your tutelage. Your approach to allow students to take independent decisions about research and then critique them has allowed me to become a better independent researcher. I am also grateful to you for offering me the emotional support and reassurance I needed at times of self-doubt and despair. Overall, this training under your guidance has been a tremendously rewarding experience.

Next, I would like to thank Dr Jeffrey N. Myers, the former chair of my thesis advisory committee who gave me the opportunity to train in his lab during the first one and a half years of my Ph.D. career. Dr Myers, who is undoubtedly one of the leading physician scientists in the country has been a true role-model to me for his commitment to pursuing cancer research for the greater cause of improving the quality of life of cancer patients.

I would like to extend my deepest gratitude to the members of my thesis advisory committee, Dr. Michael Andreeff, Dr Andrew G. Sikora and Dr Faye M. Johnson for their valuable suggestions and continued feedback during the course of my studies, which allowed my research project to stay on track and improved the quality of my dissertation and manuscript. My special thanks goes to Dr Sikora and his scientific team for helping me with immune profiling analysis we performed as part of a collaboration project that sparked a huge interest in me for the fascinating field of cancer immunology. I hope that our fruitful cooperation will continue in the future.

Next, I would like to thank all the past and present members of the Pickering and Myers labs, for sharing their research experiences and providing me with inputs and technical guidance throughout the course of my studies. I really enjoyed working with all of them. Herein, I would like to specifically acknowledge three names, Dr Antje Lindemann, Dr Meng Gao and Dr Abdullah Osman for their unconditional help and support, without which it would not have been possible to reach this milestone.

I would also like to thank GSBS, all the valuable GSBS staff, Cancer Biology Program and the Department of Head and Neck Surgery at MD Anderson Cancer Center for their support.

Last but not the least, I would like to thank my parents, my dear sister, the members of my family and my close friends for their continued blessings, love, and support during all these years, without which this journey would not have been possible.

LOSS OF CASPASE-8 FUNCTION IN COMBINATION WITH SMAC MIMETIC TREATMENT SENSITIZES HEAD AND NECK SQUAMOUS CARCINOMA TO RADIATION THROUGH INDUCTION OF NECROPTOSIS.

Burak Uzunparmak, M.D.

Advisor: Curtis R. Pickering

Caspase-8 (CASP8) is one of the most frequently mutated genes in head and neck squamous carcinomas (HNSCC), and mutations of CASP8 are associated with poor overall survival. The distribution of these mutations in HNSCC suggests that they are likely to be inactivating. Inhibition of CASP8 has been reported to sensitize cancer cells to necroptosis, a unique cell death mechanism. Here, we evaluated how CASP8 regulates necroptosis in HSNCC using cell line models and syngeneic mouse xenografts. *In vitro*, knockdown of CASP8 rendered HNSCCs susceptible to necroptosis induced by a second mitochondria-derived activator of caspase (SMAC) mimetic, Birinapant, when combined with pan-caspase inhibitors zVAD-FMK or emricasan. Strikingly, inhibition of CASP8 function via knockdown or emricasan treatment was associated with enhanced radiation killing by Birinapant through induction of

necroptosis. In a syngeneic mouse model of oral cancer, Birinapant, particularly when combined with radiation delayed tumor growth and enhanced survival under CASP8 loss. Exploration of the molecular underpinnings of necroptosis sensitivity confirmed that the level of functional receptor-interacting serine/threonine-protein kinase-3 (RIP3), a key enzyme in the necroptosis pathway was crucial in determining susceptibility to this mode of death. Although an *in vitro* screen revealed that many HNSCC cell lines were resistant to necroptosis due to low levels of RIP3, patient tumors maintain RIP3 expression and should therefore remain sensitive. Collectively, these results suggest that targeting the necroptosis pathway with SMAC mimetics, especially in combination with radiation, may be a relevant therapeutic approach in HNSCC with compromised CASP8 status, provided that RIP3 function is maintained.

TABLE OF CONTENTS

LIST OF FIGURES

LIST OF TABLES

CHAPTER-I : INTRODUCTION

CHAPTER-1: Introduction

1.1 Head and Neck Squamous Carcinoma

1.1.1 An Overview

Head and Neck Squamous Carcinoma (HNSCC) encompasses epithelial tumors originating from the mucosa of upper aerodigestive track and is the sixth most common cancer in the world, with the diagnosis of nearly 850,000 new cases and more than 450,000 cancer-related deaths annually (1). Global regions with the highest incidence rates for HNSCC include South and Southeast Asia, tropical areas of South America, and Sub-Saharan Africa (2). In the United States, HNSCC accounts for 3.7% of all cancers with an estimated 65,000 new cases and 14,500 cancer-associated deaths per year (3).

HNSCC can arise at a variety of subsites within the upper aerodigestive track, including the oral cavity, oropharynx, nasopharynx, hypopharynx, larynx, nasal cavity and paranasal sinuses with 40% of the tumors originating in the oral cavity (**Figure-1**). Throughout all the anatomical subtypes, men are significantly more affected by the disease than women with a 2:1 to 4:1 ratio (1). Despite advances in the diagnosis and treatment of cancers, HNSCC-related mortality rates have seen only a slight decline over the past 30 years, and 5-year overall survival (OS) rates for all stages of HNSCC combined remains at ~60% (3).
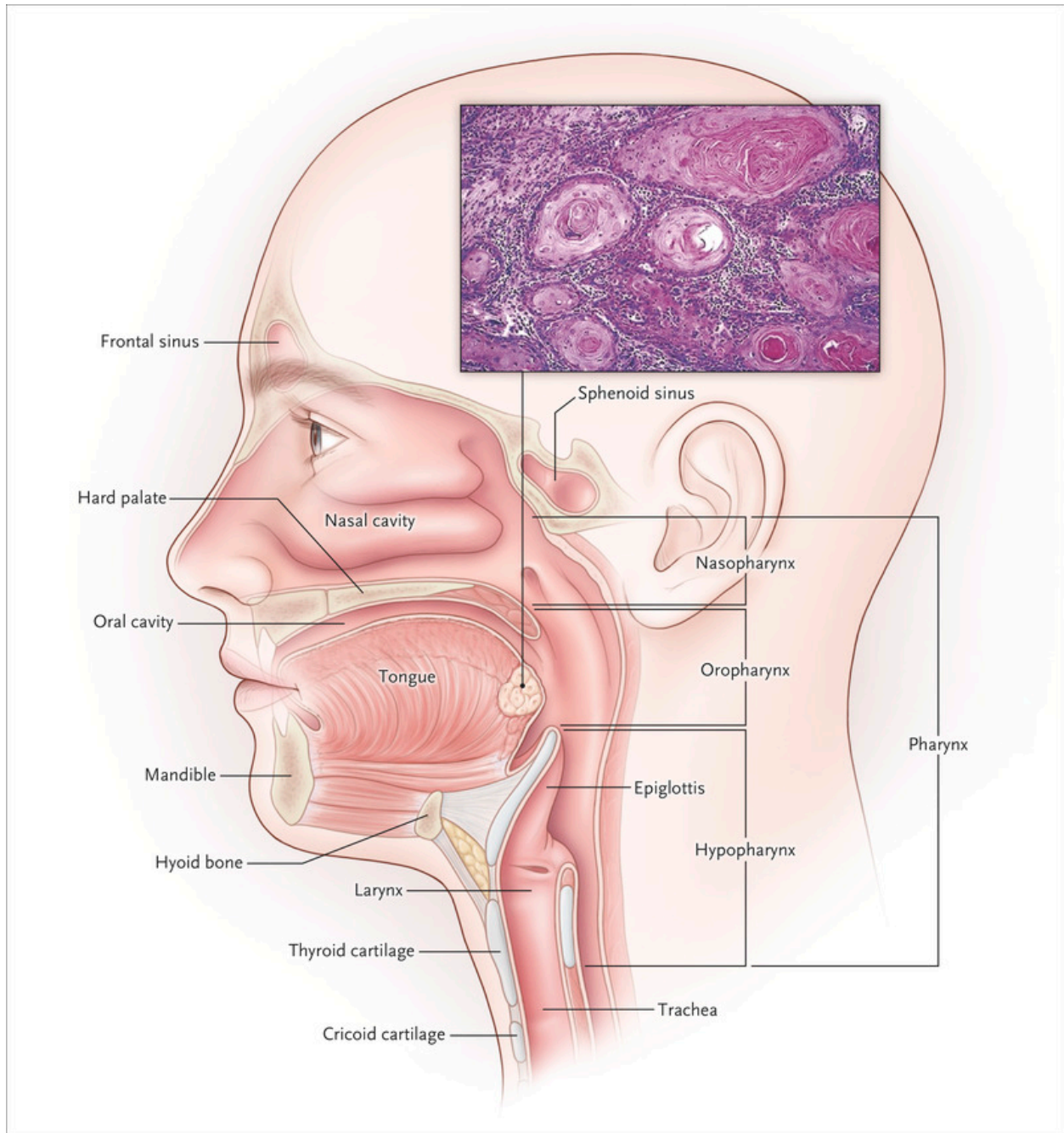
Figure-1: Anatomical sites of HNSCC

(Reproduced with permission from [Chow, L. Q. M. (2020) Head and Neck Cancer. *N.Engl. J. Med.* **382**, 60–72] Copyright Massachusetts Medical Society.)

1.1.2 Risk Factors for HNSCC

Although the etiology of HNSCC may vary depending on the subsite cancers originate from, tobacco use (either smoking or chewing tobacco) and alcohol consumption remain to be the two most common risk factors for the development of HNSCC, and their effects are exacerbated when combined (4–8). Chewing of betel nut, a prevalent habit in Southeast parts of Asia has also been implicated in the initiation of HNSCC, particularly in the oral cavity (9). Several hereditary diseases that are associated with chromosomal instability have been shown to increase the risk of developing HNSCC, including Fanconi's anemia, Bloom syndrome, ataxia telagiectasia and Li-fraumeni syndrome (10–13).

Infection with the human papilloma virus (HPV), especially HPV16, HPV33 and HPV35 is now a well-established causative factor for HNSCC (14). The incidence of HPV-associated HNSCC, a subtype that predominantly originates in the tonsils and base of tongue within the oropharynx has seen a dramatic increase in the past 30 years, particularly in the Western world (15, 16). HPV, which is found in >99% of cervical cancers, is a double-stranded DNA virus with an exclusive propensity to infect the basal layer of epithelia (17). HPV expresses two oncoproteins, E6 and E7, which upon infection of the target cells, bind to the products of p53 and Retinoblastoma (Rb) tumor suppressor genes of the host cell, respectively, leading to their degradation (18, 19). These molecular events enable HPV-infected epithelial cells to evade p53-dependent apoptotic death and enter cell cycle, hence promoting viral replication. The resulting genomic instability paves the way for accumulation of genetic alterations in the host

genome, ultimately causing malignant transformation of an HPV-infected cell into an invasive tumor cell (20). HPV-associated HNSCC is currently considered as a distinct entity from the HPV-negative subtype based on etiological factors, clinicopathological features and molecular characteristics of these cancers (21–23). Patients with HPV-associated HNSCC have, in general, more favorable prognosis than those with negative disease (24, 25). In recognition of that, the American Joint Committee on Cancer (AJCC) and the Union for International Cancer Control (UICC) introduced a separate staging system for p16-positive HNSCCs arising in the oropharynx (oropharyngeal squamous cell carcinoma [OPSCC]) in 2017, where p16 positivity was used as a surrogate marker to determine HPV status of the disease (26, 27). Ongoing treatment de-escalation trials of HPV-driven OPSCC will provide data that might lead to implementation of personalized treatment protocols based on HPV status for this cancer (28). Finally, Epstein–Barr virus (EBV) is a well-defined causative agent in HNSCCs that arise in the nasopharynx. Expression of EBV-linked viral gene products such as **l**atent **m**embrane **p**roteins (LMP1, LMP2A and LMP2B) and **EB**V-induced **n**uclear **a**ntigen-1 (EBNA-1) as well as EBV-associated microRNAs (including **B**am H1 **A r**ightward **t**ranscript [BART] microRNAs) have been shown to play important roles during oncogenic progression of nasopharynx cancer (367).

1.1.3 Treatment of HNSCC

The mainstay treatment options of HNSCC are surgery, radiation, chemotherapy and immunotherapy. Evaluation of the patients by a multispecialty medical team plays an important role in the choice of treatment for HNSCC, since treatment options may

change depending on the stage of cancer, anatomical site where it presents and the surgical accessibility of the lesion (4). Patients presenting with early stage disease (Stage I-II) usually receive surgery or radiation alone, each of which provide similar disease control with 5-year survival rates in 70 to 90% of the patients. Locally advanced disease (Stage III-IV) that comprise more than 60% of HNSCC cases, is characterized by large tumors with local invasion and/or metastasis to regional lymph nodes, and exhibits high risk for local recurrence (10-40%) and metastasis to distant organs with poor prognosis. Multi-modality treatment approaches, involving surgery, radiation and chemotherapy have improved cure rates for the patients presenting with locally advanced disease in the past two decades (29). Surgery is the primary choice of treatment for cancers originating in the oral cavity, followed by adjuvant radiotherapy or chemoradiotherapy. At other anatomical sites, surgery is considered for only small and accessible tumors. Under conditions whereby surgery is less feasible or would result in poor long-term morbidity, a definitive chemoradiotherapy regimen is the standard of care in the context of which cisplatin is administered with concurrent radiotherapy (30). Carboplatin, another platinum compound is preferred over cisplatin in patients with preexisting conditions such as kidney failure (31). Cetuximab, a monoclonal antibody targeting the epidermal growth factor receptor (EGFR) was the first targeted therapy approach approved by the US Food and Drug Administration (FDA) in HNSCC. A combination regimen including cetuximab and radiation was recommended for the treatment of patients with platinum-refractory locally advanced disease, although two clinical trials conducted in 2019 showed that cetuximab plus radiation is inferior to

cisplatin plus radiation in OPCC characterized by poorer overall and progression-free survival (32, 367).

Recent advances in immunotherapy, a treatment approach based on the modulation of immune system has revolutionized the practice of oncology. Two antibodies designed against programmed cell death protein-1 (PD1), an immune checkpoint receptor expressed on the surface of activated T cells, B cells and macrophages to limit immune responses, nivolumab and pembrolizumab showed efficacy in clinical trials for recurrent or metastatic HNSCC, leading to FDA approval of these two agents in 2016 (33).

Despite all the advances in diagnosis and treatment, the prognosis of HNSCC has improved very little over the past 3 decades with recurrent or metastatic disease developing in more than 65% of the patients in large part due to treatment failure, indicating a need for identification of new targets and biomarkers to guide therapy (4).

1.1.4 Pathogenesis of HNSCC

Accumulation of genetic and epigenetic alterations in genes whose protein products are involved in various signaling pathways plays a key role during the evolution of cancers from normal tissues (34). These genetic changes include mutations of genes that might occur at single base-pair level as well as insertions, deletions, duplications and translocations of large parts of the genome that sometimes involve entire chromosomes or chromosomal arms (35). Studies in the 1990s demonstrated the association between the progression of HNSCC from precursor lesions into invasive carcinoma and the accumulation of genetic alterations in that course (36). Leukoplakia, which is a white

lesion developing from the mucosal linings of oral cavity, is the most common precursor lesion for HNSCC. The classical risk factors defined for HNSCC involving smoking and alcohol consumption have also been implicated in the development of oral leukoplakia with the inclusion of additional risk factors such as immunosuppression and a personal and/or family history of cancers (37). The prevalence rate for leukoplakia ranges between 0.1% and 0.5% where only 1-2% of these lesions are expected to undergo malignant transformation into full-blown oral cancers annually (38). Besides leukoplakia, many precancerous mucosal alterations are not clinically recognizable and are identified as dysplastic mucosal epithelium only after microscopic examination. These precancerous morphological aberrations led scientists to develop the concept of 'field cancerization' in 1950s to not only describe these large dysplastic alterations but also to explain the high frequency of local recurrences and development of multiple primary tumors in the mucosal linings after the surgical removal of HNSCCs (39). Long-term exposure to carcinogens can lead to accumulation of pro-tumorigenic genetic changes in large areas throughout the upper aerodigestive tract, resulting in genetically altered 'cancerized fields' independent of the primary tumor site. These fields that may exhibit morphological alterations (for example, dysplasia) or appear normal contain a group of clonally expanding cancer-primed cells with the potential to evolve into invasive carcinoma and an abnormal microenvironment surrounding them (36, 40). Eventually, acquisition of additional mutations by these cells within these fields lead to evolution of invasive cancer in the context of a cancer-promoting microenvironment (41). Cancer-primed cells in a 'field' may constitute a source for local recurrences and second field carcinomas after surgical removal of the initial tumor and may even migrate

intraepithelially and/or via saliva throughout the entire upper aerodigestive tract to seed second primary tumors (42).

In the 1990s, comprehensive genetic studies investigating the molecular pathogenesis of HNSCC revealed a significant correlation between the number of genetic changes and the level of the dysplastic aberrations that lead to invasive cancer, allowing the development of a genetic progression model for HNSCC (36). The genetic events governing the development of HNSCC include loss of tumor suppressor gene function and/or activation of proto-oncogenes (**Figure-2**).
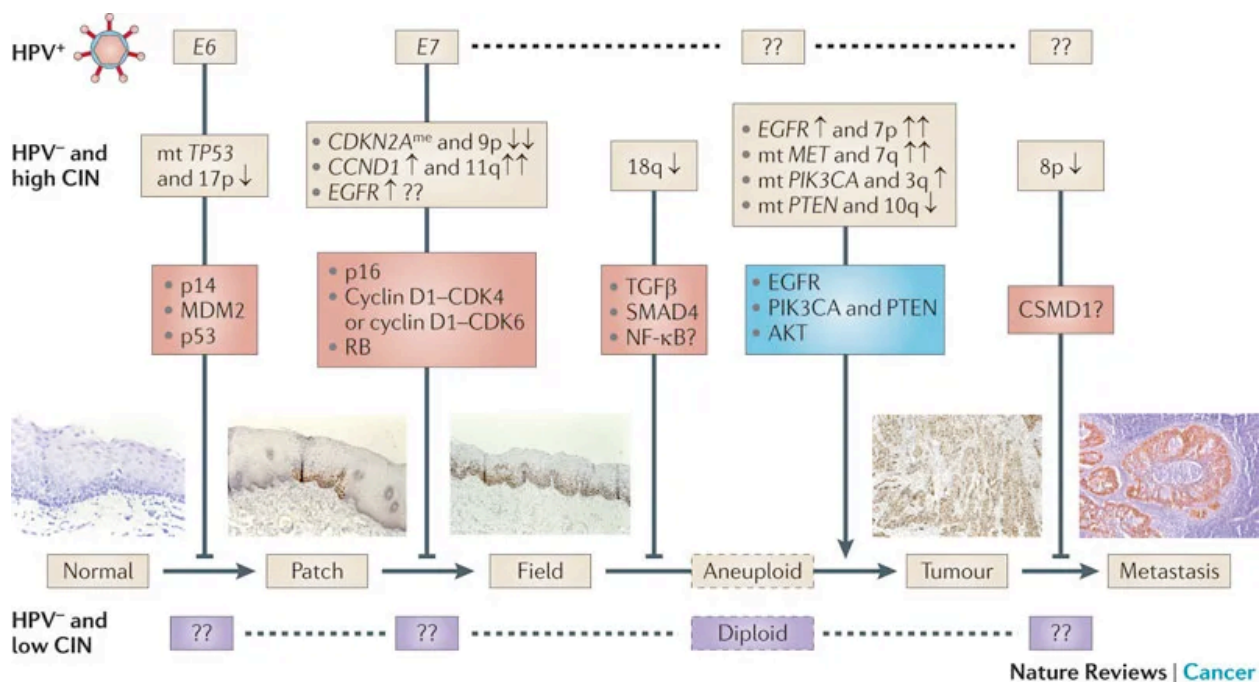
Figure-2: A hypothetical genetic progression model for HNSCC

The genetic alterations involved throughout the process are depicted (Reproduced with permission from [Leemans, C. R., Braakhuis, B. J. M., and Brakenhoff, R. H. (2011) The molecular biology of head and neck cancer. *Nat. Rev. Cancer*. **11**, 9–22] Copyright SpringerNature.)

First, a progenitor or stem cell within the mucosal linings acquires one (or more) genetic alterations, usually including a mutation in *TP53* and forms a patch containing *TP53-*mutant daughter cells through subsequent cell divisions (44, 45). The daughter cells undergo further genetic changes, including loss of heterozygosity (LOH) of 9p21 that harbors the CDKN2A gene, encoding p16^{INK4a} and p14^{ARF}, proteins that regulate G1/S cell cycle checkpoint and MDM2-mediated degradation of p53 (46, 47). Acquisition of these further genetic alterations enable the daughter cells to escape normal growth control and/or gain growth advantage, leading to development of this clonal unit into an expanding 'field' that replaces the normal mucosal epithelium laterally. Further genetic events altering the molecular circuitry around EGFR (48–50) as well as those that impact the PI3K–PTEN–AKT signaling pathway (51–53) transform the 'field' into an invasive carcinoma that progresses to metastasis. Both aneuploidy and the accumulation of cancer-associated alterations in genes contribute to malignant progression of HNSCC (54, 55).

1.1.5 Sequencing Studies in HNSCC

Early studies conducted to identify key genes/pathways whose alteration might contribute to the development and/or progression of HNSCC revealed that loss of cell cycle regulation and constitutive cell proliferation were important drivers for HNSCC. Key genes in these pathways, including *TP53*, *CDKN2A*, *CCND1*, *PIK3CA* and *PTEN* were found to be mutated and/or aberrantly expressed in HNSCC (22, 43, 47, 51, 53, 56–59). In early 2010s, use of next generation sequencing (NGS) led to identification of novel genetic alterations in HNSCC, opening new avenues for the development of

personalized therapy approaches (60, 61). These studies and a recent study by a large consortium, the Cancer Genome Atlas (TCGA) network (**Figure-3, 4**) confirmed that mutations in TP53 (mostly inactivating-type mutations) are found in vast majority (~85%) of HPV-negative HNSCC cases, making it the most frequently mutated gene in this cancer (62). One other prominent molecular abnormality noted in HPV-negative HNSCC was the disruption of the retinoblastoma pathway (RB pathway), which occurs through inactivation of CDKN2A by deletions, mutation or methylation (alterations in CDKN2A were found in 58% of the cases) and/or amplification of CCND1 (~31%). Another common molecular alteration identified was the activation of receptor tyrosine kinase pathway (RTK pathway) through amplifications in genes encoding growth factor receptors such as EGFR (15%), FGFR1 (10%) and ERBB2 (5%). Amplification of PIK3CA (34%) and loss of PTEN (12%), genetic changes that lead to the activation of the PI3K–PTEN–AKT signaling pathway were also common. Mutations in *TP53* were rarely detected in HPV-positive HNSCC, a phenomenon that can be explained by the fact that E6, a vital HPV-associated protein, prevents apoptosis through degradation and inactivation of p53 in host epithelial cells; albeit mutation/deletion of retinoblastoma 1 (RB1) is commonly observed in this cancer despite universal expression of E7, the HPV protein that targets RB1 (63, 366). Other molecular alterations in HPV-positive HNSCC included the amplification of PIK3CA (54%), fusion/mutation of FGFR3 (11%) as well as mutations in genes such as ZNF750, EP300, CASZ1, PTEN and CYLD that were found to be common in HPV-positive OSCCs (63, 366). Other highly enriched molecular changes found in HPV-negative HNSCC involved mutations in genes associated with WNT signaling such as FAT1 (23%) and AJUBA (6%), squamous cell

differentiation such as NOTCH1 (19%) and TP63 and oxidative stress response such as NFE2L2 (6%) and KEAP1. Intriguingly, these studies identified a distinct subgroup of HPV-negative HNSCC tumors with fewer genome-wide copy number alterations (CNA) and WT *TP53* status. This same subgroup, which was characterized on the basis of WT *TP53* and retention of chromosome 3p by a previous study (64), was shown to typically display mutations of HRAS and Caspase-8 (CASP8).
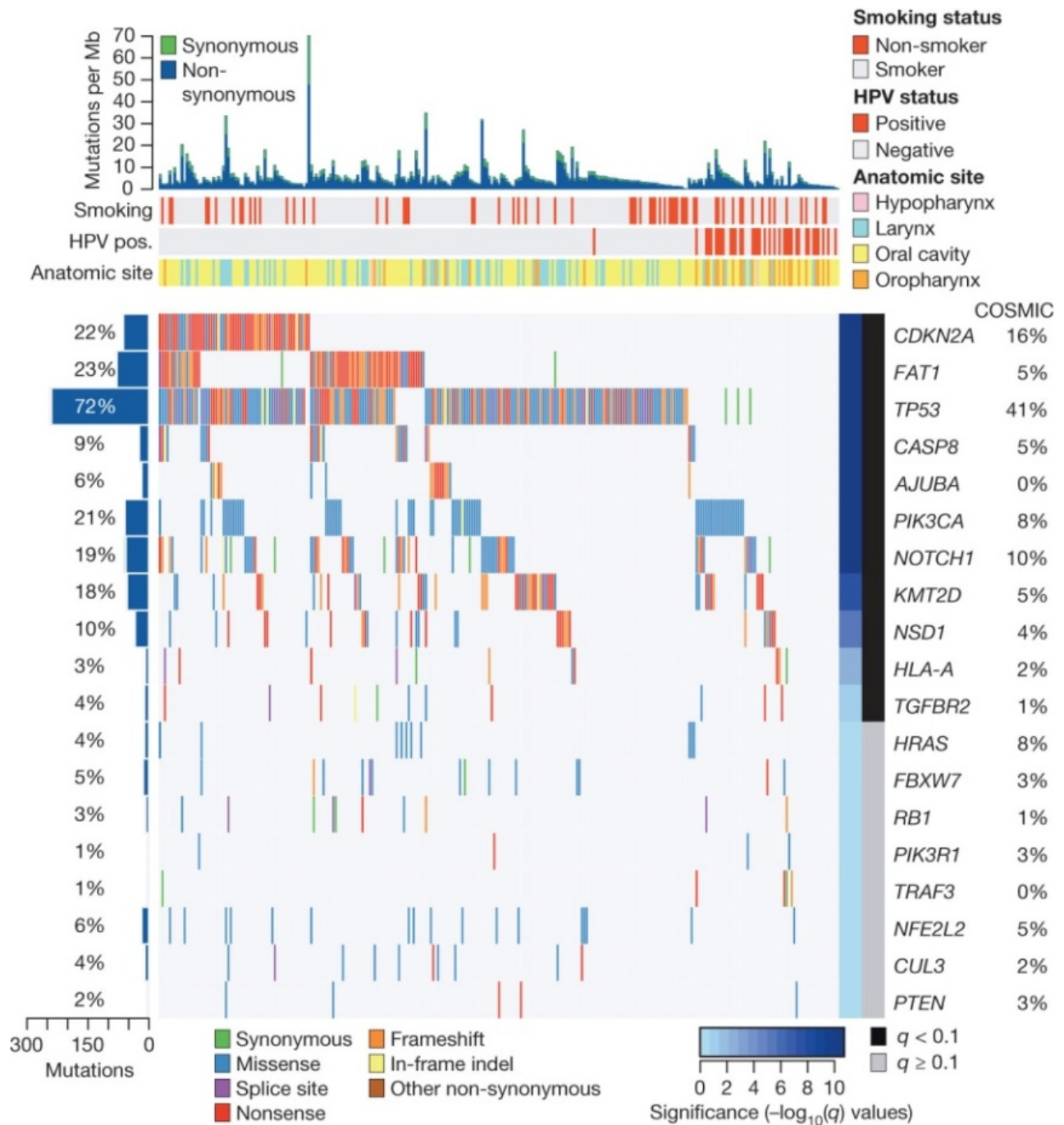
Figure-3: Significantly mutated genes in HNSCC

(Reproduced with permission from [Cancer Genome Atlas Network (2015) Comprehensive genomic characterization of head and neck squamous cell carcinomas. *Nature*. **517**, 576–82] Copyright SpringerNature.)
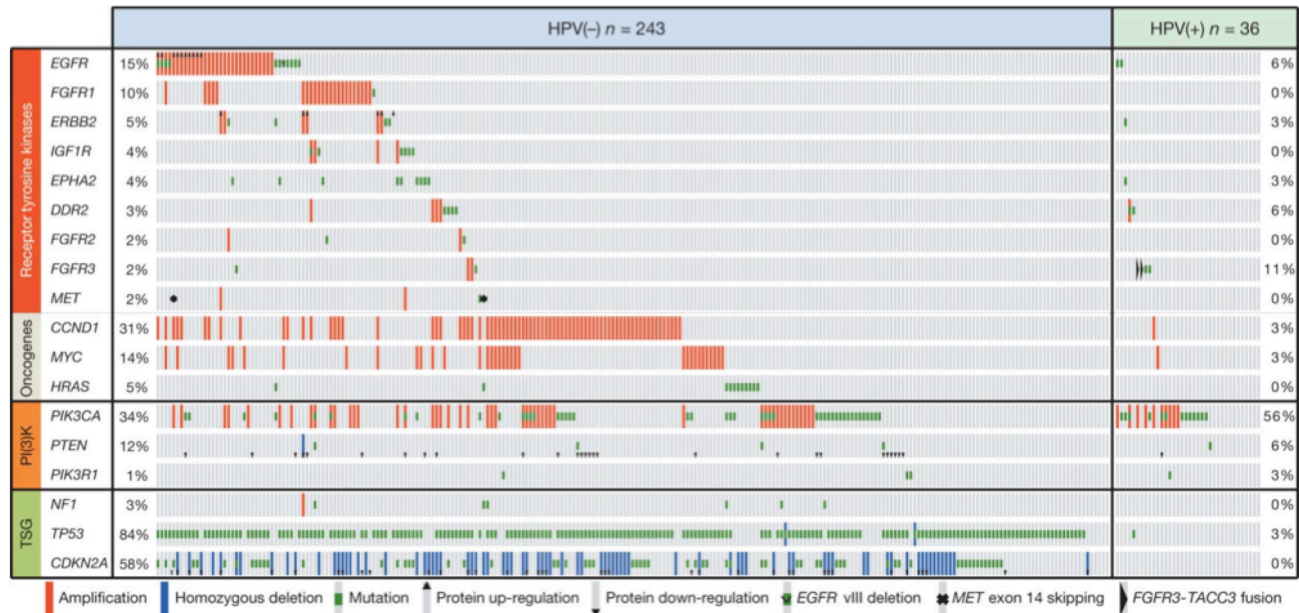
Figure-4: Driver oncogenic events in HNSCC

Caspase-8 is a **c**ysteine-**asp**artate specific prote**ase** (Caspase) that initiates programmed cell death (which is referred to as 'extrinsic apoptosis') in response to cell surface death receptor activation (65). Loss of CASP8 function has been shown to occur frequently in malignant neuroectodermal tumors, including neuroblastoma (66, 67) medullablastoma (68), glioblastoma (69), primitive neuroectodermal tumor (70) as well as small cell lung carcinoma (71). Mutations of CASP8 leading to reduction in Caspase-8 protease activity are commonly observed in epithelial-derived cancers such as colorectal carcinoma (72) and gastric cancer (73). In the TCGA consortium study, CASP8 was found to be mutated in approximately 10% of HNSCCs, with CASP8 mutations mostly occurring in oral cavity tumors. 18% of HPV-negative oral squamous cell carcinomas (OSCC) showed somatic mutations of CASP8. The spectrum of CASP8

mutations in patient tumors and human-derived HNSCC cell lines (nonsense, splice-site, and frame-shift mutations) indicates that they are likely to be inactivating mutations.

Although these mutations lead to compromise of CASP8 protein function, CASP8 expression is still maintained due in part to heterozygous nature of the mutations (74). The main objective of this thesis is to offer an insight into the inactivating mutations of CASP8 and provide data to help understand whether tumor responses to conventional and/or targeted therapy approaches in HNSCC might be influenced by these common genomic alterations.

1.2 Caspase-8

1.2.1 Introduction: Caspase family

Under physiological conditions, intrinsic genetic programs of eukaryotic cells allow cell death to occur in a regulated manner. This regulated form of death is referred to as programmed cell death (PCD), since this process is executed via a tightly regulated set of genetically encoded cellular mechanisms. Apoptosis is the most studied and well-defined form of PCD and is essential for cellular homeostasis and development. In apoptosis, intrinsic molecular programs govern cell death to prevent any damage to the surrounding, living cells. Apoptosis is facilitated by caspases, a family of evolutionarily conserved **c**ysteine-**asp**artate specific prote**ase**s (**Table-1**).

Caspase	Expression (Hu/Ms)	Domain architecture	Classification
Caspase-1	Hu, Ms	CARD — L — S	Inflammatory
Caspase-2	Hu, Ms	CARD — L — S	Apoptotic
Caspase-3	Hu, Ms	L — S	Apoptotic
Caspase-4	Hu	CARD — L — S	Inflammatory
Caspase-5	Hu	CARD — L — S	Inflammatory
Caspase-6	Hu, Ms	L — S	Apoptotic
Caspase-7	Hu, Ms	L — S	Apoptotic
Caspase-8	Hu, Ms	DED — DED — L — S	Apoptotic/ inflammatory
Caspase-9	Hu, Ms	CARD — L — S	Apoptotic
Caspase-10	Hu	DED — DED — L — S	Apoptotic
Caspase-11	Ms	CARD — L — S	Inflammatory
Caspase-12	Hu, Ms	CARD — L — S	Inflammatory
Caspase-14	Hu, Ms	L — S	ND

Table-1: Classification of human caspases. <u>Abbreviations:</u> CARD, caspase activation and recruitment domain; DED, death effector domain; L, large domain; S, small domain; Hu, human; Ms, mouse   (Reproduced with permission from [Kesavardhana, S., Malireddi, R. K. S., and Kanneganti, T.-D. (2020) Caspases in Cell Death, Inflammation, and Gasdermin-Induced Pyroptosis. *Annu. Rev. Immunol.* 10.1146/annurev-immunol-073119-095439] Copyright ANNUAL REVIEWS, INC.)

The caspases are initially expressed as enzymatically inactive zymogens that are called procaspases, which undergo dimerization and oligomerization to become active. The effector domain of procaspases bearing protease activity (caspase domain) is cleaved into small and large units during the activation process to allow protein complex formations to exert proteolytic activity (75–80).

Mammalian caspases are categorized into two major subfamilies: apoptotic and inflammatory caspases. The apoptotic caspases are further divided into two subgroups: initiator and executioner (or effector) caspases depending on their order of action during apoptosis. Initiator caspases serve as signal amplifiers by cleaving peptide bonds after certain aspartate residues on effector caspases rendering them active, whereas effector caspases facilitate apoptosis through cleavage of several cellular proteins at their target sites (75–78, 81, 82). Inflammatory caspases, caspases -1, -4, -5, -11, and -12 are activated in the context of an oligomeric protein complex called the 'inflammasome', a process that triggers pyroptosis, an inflammatory form of cell death, which is characterized by secretion of danger associated molecular patterns (DAMPs) from cells to promote inflammation (75, 76, 83)

1.2.2 Caspase-8 and Apoptosis

Caspase-8 (CASP8) is an apical caspase that initiates apoptosis in response to cell surface receptor activation. This process, which is referred to as 'extrinsic apoptosis' is mediated by members of the Tumor necrosis factor (TNF) superfamily, a group of receptors called death receptors (DR), including TNF receptor 1 (TNFR1), tumor necrosis factor receptor superfamily member 6 (TNFRSF6 [also called apoptosis antigen 1 (APO-1, Fas/CD95)]), TNF receptor superfamily member 25 (TNFRSF25 [also called DR3]) TNF-related apoptosis-inducing ligand receptor 1 (TRAIL-R1 [also called

DR4]), and DR5 (TRAIL-R2) (76, 84, 93–95, 85–92). These receptors have extracellular (containing varying numbers of cysteine-rich residues), transmembrane and cytoplasmic components and are activated by death-inducing ligands that belong to the TNF superfamily of cytokines, including FasL (CD95L/APO-1L), TRAIL (APO-2L), TNFα and TL1A (96–100). FasL binding to Fas and TRAIL binding to TRAIL-R1/-R2 result in the recruitment of the adaptor protein, **F**as-**a**ssociated protein with **d**eath **d**omain (FADD), a process that induces apoptosis; whilst TNFα binding to its cognate receptor, TNFR1 leads to the recruitment of another adaptor protein, **T**NF **r**eceptor type 1-**a**ssociated **d**eath **d**omain protein (TRADD), a process whose primary output is induction of pro-inflammatory genes (76, 101). Like other caspases, CASP8 is translated as a monomeric procaspase that comprises an N-terminal prodomain and a C-terminal protease domain (caspase domain), consisting of a large (~18kD) α subunit (p18), a small (~10kD) β subunit (p10) and a short linker region in between them. These two subunits are non-covalently linked parts of the same caspase domain, consisting of 6-stranded β-sheets (one anti-parallel) associated with 5 α helices (**Figure-5**) (102, 103).
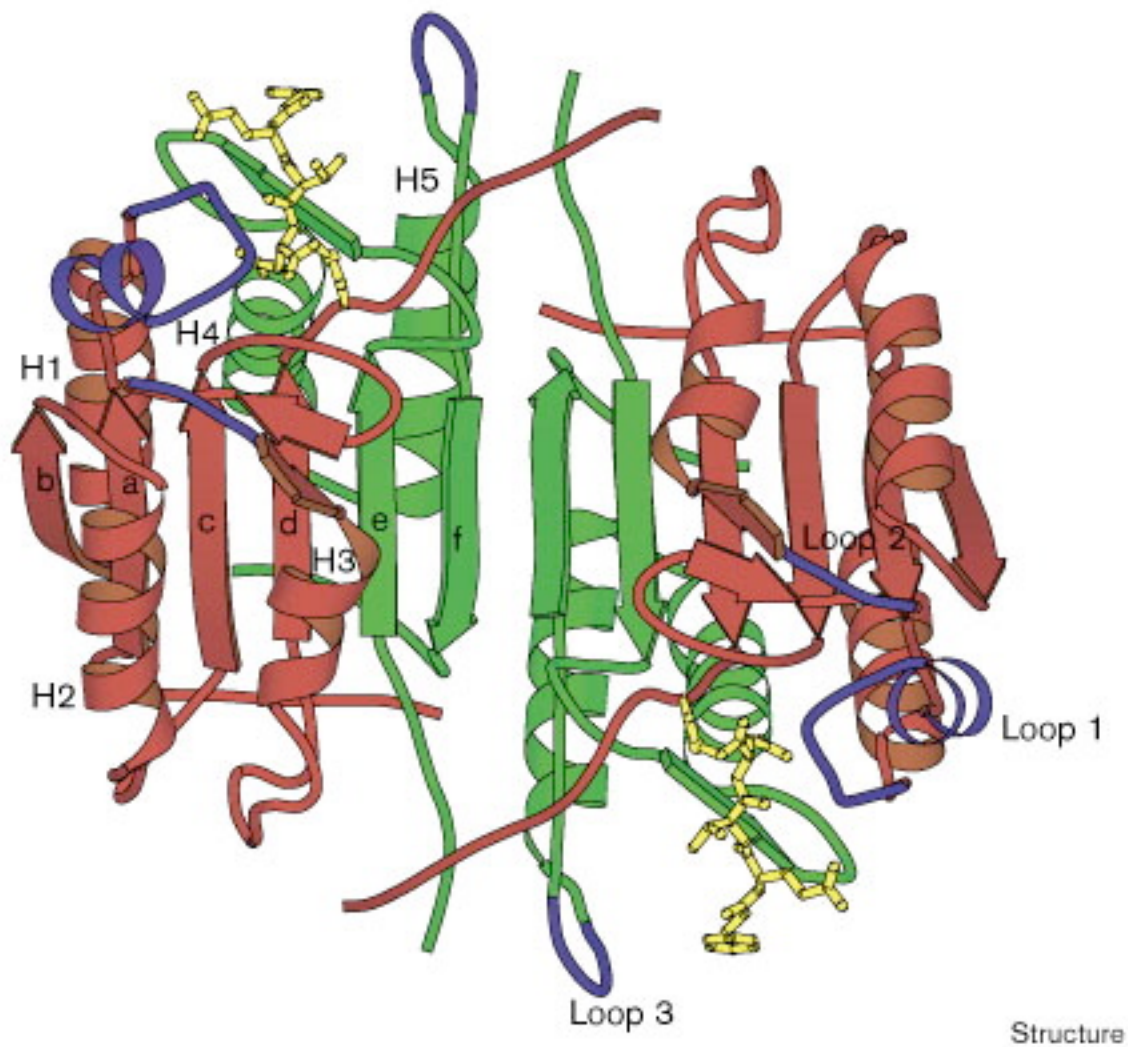
Figure-5: Ribbon diagram for the dimerized structure of Caspase-8's protease domain.

The large and small subunits are colored red and green, respectively. (Reproduced with permission from [Blanchard, H., Kodandapani, L., Mittl, P. R., Marco, S. D., Krebs, J. F., Wu, J. C., Tomaselli, K. J., and Grütter, M. G. (1999) The three-dimensional structure of caspase-8: an initiator enzyme in apoptosis. *Structure*. **7**, 1125–33] CopyrightElsevier.)

The prodomain of CASP8 includes two death effector domains (DEDs). The DED and

CARD domains (CARD domains are expressed by Caspases -1, -2, -4, -5, -9, -11, -12)

are members of a death domain (DD) superfamily, that play a key role in formation of

large oligomeric signaling complexes through homotypic (allowing self-association) and

heterotypic (allowing association of proteins containing DED/CARD domains) interactions (104, 105). Binding of death-inducing ligands to their cognate receptors (e.g. engagement of TRAIL-R1 by TRAIL) leads to trimerization of the receptors, allowing formation of high-order oligomers on cell surface. Despite the fact that overall sequence homology between members of the TNF superfamily ranges between 20 to 30%, once they are bound by their cognate ligands they can mediate overlapping signaling pathways (106–109). Following receptor trimerization, FADD, an adaptor protein bearing DD an DED domains (**Figure-6A**) is recruited to the cytoplasmic tails of death receptors, thanks to the homotypic interactions between DD domain of FADD and cytoplasmic DDs of Fas/CD95, TRAIL-R1 or TRAIL-R2 (From this point on TRAIL-R1 signaling will be used as a basis to explain the extrinsic apoptosis pathway in which CASP8 serves as the apical-most caspase). FADD, in turn recruits procaspase-8 via homotypic interactions between the DEDs of FADD and procaspase-8 to form the death-inducing signaling complex (DISC), composed of TRAIL-R1-FADD-CASP8 (110–112). Quantitative mass spectrometry analyses by several groups studying the DISC stoichiometry revealed that DDs of multiple TRAIL-R1 are required for the recruitment of FADD, which can recruit 6-9 procaspase-8 monomers by itself. Recruitment of so many procaspase-8 zymogens by a single FADD molecule prompted subsequent studies, which demonstrated that the
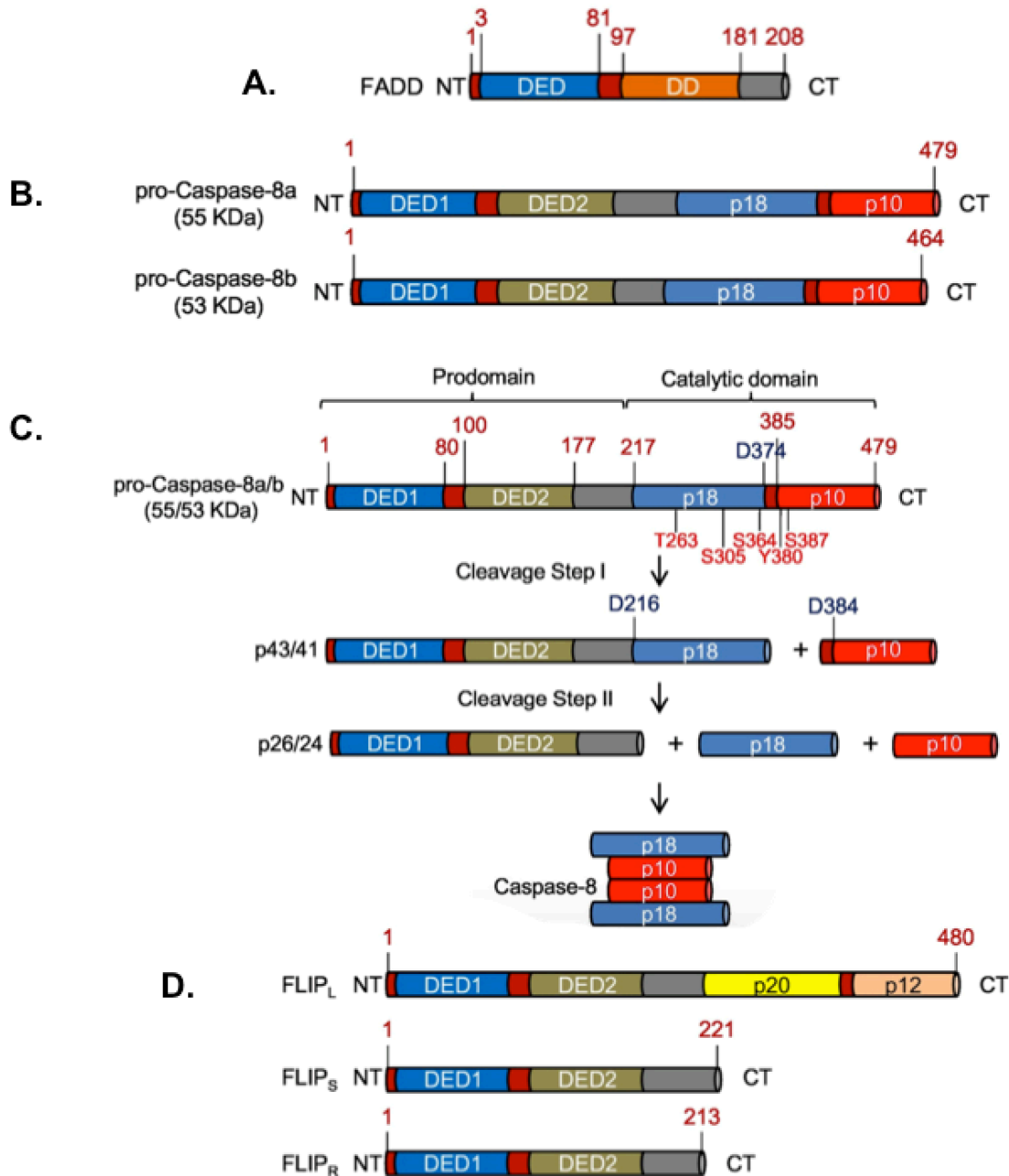
Figure-6: Activation of procaspase-8 and DISC-associated proteins

A. The structure of FADD **B.** The structure of two isoforms of procaspase-8, procaspase-8a and -8b **C.** The activation of procaspase-8. **D.** The structures of $FLIP_L$, $FLIP_S$ and $FLIP_R$ (Reproduced with permission from [Mandal, R., Barrón, J. C., Kostova, I., Becker, S., and Strebhardt, K. (2020) Caspase-8: The double-edged sword. *Biochim. Biophys. acta. Rev. cancer*. 1873, 188357] CopyrightElsevier.)

DED of FADD binds DED1 of a procaspase-8 monomer whose DED2 in turn recruits a second procaspase-8 via its DED1, culminating in the formation of a procaspase-8 DED chain (113–116).

The *CASP8* gene on chromosome 2q33.1 is expressed to generate several isoforms of procaspase-8 through alternative splicing of the *CASP8* mRNA. However, only two isoforms, procaspase-8a and –b (**Figure-6B**) are predominantly recruited to the DISC (Procaspase-8a has an additional 15-aminoacid long oligomer sequence [184-198] in the linker region between the pro- and catalytic [effector] domains) (117). Recruitment of inactive procaspase-8 zymogens to DISC brings them in close proximity to each other, allowing *trans* activation of the procaspase-8 monomers through homotypic interactions between their catalytic domains to form homodimers (110, 118–121). Formation of these stable homodimers leads to proteolytic activation of CASP8 zymogens, rendering them susceptible to cleavage by other homodimers through a two-step process. The first cleavage event occurring at the D374 aspartate residue creates two subunits: p43/41 and p12, followed by a second cleavage event at D216 and D384, resulting in the formation of three subunits: p26/24, p18 and p10 respectively. p18 and p10 fragments cleaved from the caspase domain of procaspase-8 during this process form a catalytically active tetramer, $p18_2$-$p10_2$ (This heterotetramer is referred to as active CASP8), which is released from the DISC into cytosol (**Figure-6C**) (110, 122–126).

A catalytically inactive homologue of procaspase-8, **F**LICE (FADD-like IL-1β-converting enzyme) **l**ike **i**nhibitory **p**rotein [FLIP] is also recruited to the DISC in response to

TRAIL-R1 stimulation through homotypic interactions involving the DEDs of FLIP (**Figure-6D**). 3 isoforms of FLIP have been identified: **FLIP$_L$**, a 55kD catalytically inactive monomer that is structurally the most similar isoform to procaspase-8 (The absence of a key cysteine residue in its large subunit renders FLIP$_L$ proteolytically inactive); **FLIP$_S$**, a 27kD isoform that competes with procaspase-8 for DED-mediated recruitment to the DISC, preventing the generation of active CASP8 in a dominant-negative fashion; **FLIP$_R$**, a 25kD isoform that lacks the additional C-terminal aminoacids present in FLIPs (A single nucleotide polymorphism [SNP] in the *CFLAR* gene has been implicated in the expression of FLIP$_R$). Although FLIP$_S$ and FLIP$_R$ are concurrently transcribed, FLIP$_S$, which is translated at a higher rate, is expressed more abundantly. Similar to FLIP$_S$, FLIP$_R$ also blocks the activation of procaspase-8 (110, 127–134).

It has conventionally been thought that, when present at high levels FLIP$_L$ competes with procaspase-8 for DED-mediated recruitment to the DISC, resulting in inhibition of apoptosis (135, 136). However, this view is now challenged by recent studies focusing on how FLIP isoforms differentially regulate the activation of procaspase-8. The findings of these studies indicate that FLIP$_{L/S}$ are recruited to the DISC in a procaspase-8 dependent manner through a co-operative and hierarchical mechanism that results in formation of procaspase-8: FLIP$_{L/S}$ heterodimers, whose composition determines the extent of activation of procaspase-8 and subsequent cell fate. Under physiological conditions whereby FLIP$_L$ levels are low, binding of FLIP$_L$ to procaspase-8 leads to conformational changes in the catalytic domain of procaspase-8, rendering the procaspase-8: FLIP$_L$ heterodimer catalytically active even in the absence of proteolytic

processing of either molecule. As levels of $FLIP_L$ become reduced, DED-mediated recruitment of procaspase-8 to the DISC sets in, facilitating *trans* activation, proteolytic cleavage and oligomer assembly of procaspase-8, promoting apoptosis. At high levels, $FLIP_L$ disrupts procaspase-8 oligomer formation and reduces the activity of procaspase-8, inhibiting cell death. Heterodimers that procaspase-8 forms with $FLIP_S$ and $FLIP_R$ through DED-mediated homotypic interactions lack catalytic activity. Therefore, at high levels, these FLIP isoforms preclude activation and oligomer assembly of procaspase-8, preventing cell death (110, 137, 138).

The enzymatic activity and apoptotic function of CASP8 can be regulated by additional post-translational mechanisms. Human procaspase-8b has phosphorylation sites on tyrosine residues Y273, Y293, Y380, Y448 and serine residues S287, S305 and S347 (123, 139–141). Polo like kinase-3 (Plk3), which interacts with Fas, FADD and procaspase-8, phosphorylates Y273 on procaspase-8 upon assembly of the DISC in response to Fas activation, promoting pro-apoptotic function of CASP8 (140). Conversely, Src-mediated phosphorylation of Y380 residue of procaspase-8 following engagement of the CD95 receptor interferes with autoproteolytic activity of procaspase-8, blocking apoptosis (142). Polyubiquitination of procaspase-8 by the E3 ligase Cullin-3 (CUL3) within DISC as part of TRAIL-R1 signaling leads to recruitment of the ubiquitin-binding protein p62 in certain cellular contexts. Subsequent p62-dependent aggregation of CASP8 leads to enhanced stability and activity, promoting apoptosis (76, 143–145).

While CD95, TNFRSF25 and TRAIL-R2 mediate procaspase-8 activation in a fashion akin to that of TRAIL-R1, TNFR1-mediated apoptosis is executed through a different mechanism, involving the recruitment of the adaptor protein TRADD, which in turn recruits **R**eceptor-**i**nteracting serine/threonine-**p**rotein kinase 1 (RIP1) to form a cell membrane bound signaling Complex-I. Deubiquinated RIP1 can form a cytosolic Complex-II, which triggers apoptosis, a mechanism that will be explained in detail in the later sections (110, 139).

Enzymatically active $p18_2$-$p10_2$ tetramers (active **CASP8**) released from the DISC into cytosol at the end of procaspase-8 activation process execute extrinsic apoptosis (**Figure-7**), following two distinct pathways. Cells in which active CASP8 alone is sufficient for the proteolytic maturation of executioner caspases, Caspase-3 (CASP3) and Caspase-7 (CASP7) to drive extrinsic apoptosis in response to death receptor activation, are termed as **Type-I cells** such as thymocytes and mature lymphocytes. In these cells, CASP3 and CASP7, caspases, which normally reside in the cytosol as pre-assembled homodimers, are activated through cleavage and removal of the linker sequence between their large and small subunits by CASP8, leading to conformational changes in their 3D structures, allowing generation of a substrate binding pocket. Active CASP3/7 homodimers cleave a large set of substrates including RhoGDI (**Rho** protein **G**DP **d**issociation **i**nhibitor), ROCK1 (**R**ho-associated, **c**oiled-coil-containing protein **k**inase-1), ICAD (**I**nhibitor of **c**aspase-**a**ctivated **D**Nase) and PARP1 (Poly [ADP-ribose]
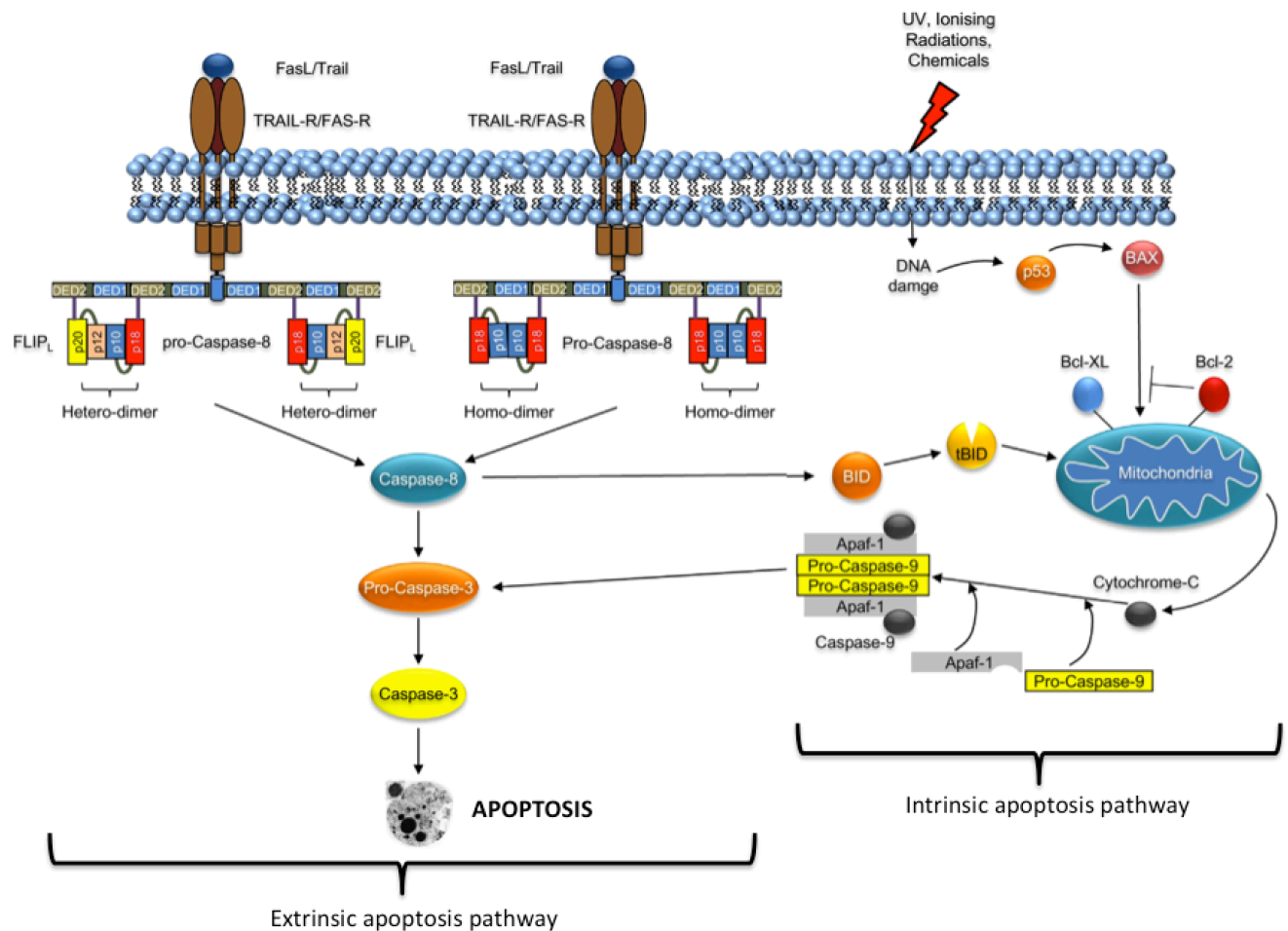
Figure-7: Schematic representation of the extrinsic and intrinsic apoptotic pathways.

In extrinsic apoptosis, cell surface death receptor activation facilitates recruitment of FADD and procaspase-8, which are assembled into DISC. CASP8 becomes activated in the DISC and is subsequently liberated into the cytosol where it cleaves and activates its downstream executioner caspases (CASP3/7) to engage apoptosis. Intrinsic apoptosis is induced by mitochondrial outer membrane permeabilization (MOMP) stimulated by intracellular stress factors, leading to Cytc release into the cytosol. Cytc binds to APAF1 to form the apoptosome complex, which facilitates activation of CASP9. This in turn promotes activation of CASP3/7 to execute apoptosis. (Reproduced with permission from [Mandal, R., Barrón, J. C., Kostova, I., Becker, S., and Strebhardt, K. (2020) Caspase-8: The double-edged sword. *Biochim. Biophys. acta. Rev. cancer*. 1873, 188357] CopyrightElsevier).

polymerase-1) (146–149). The fact that CASP3 and CASP7 demonstrate almost overlapping activity toward certain synthetic peptide substrates has led to the conventional view that they play functionally redundant roles during execution of apoptosis. This view has now been challenged by several observations suggesting that this overlap is not complete. For example, eye lenses of CASP7^{-/-} mice show a normal phenotype, whereas those from CASP3^{-/-} mice are characterized by marked cataract development (150). This notion was further supported by subsequent biochemical studies showing that CASP3 and CASP7 demonstrate differential sensitivity toward multiple peptide substrates, with CASP7 being more selective (One such peptide substrate is cochaperone p23, which is more susceptible to cleavage by CASP7 than CASP3) (146, 147, 151). One important substrate proteolytically processed by both CASP3 and CASP7 is PARP1, a nuclear enzyme involved in DNA repair, maintenance of DNA stability and regulation of the transcriptional machinery. Proteolytic cleavage of PARP1 by CASP3/7 is considered a hallmark of apoptosis (149, 152, 153). Upon translocation to the nucleus following their activation by CASP8, CASP3/7 cleave PARP-1 between its D214 and G215 residues, resulting in formation of two fragments: an 89kD catalytic fragment and a 24kD fragment bearing the DNA binding domain (DBD). The 89kD cleavage product has a significantly reduced DNA binding ability and is released into to the cytosol from the nucleus, whereas the 24kD DBD fragment binds to nicked DNA in an irreversible fashion, leading to inhibition of DNA repair enzymes

(including full-length/operational PARP1) and attenuation of DNA repair (149, 154–157) followed by manifestation of other apoptosis-associated cellular changes: chromosomal DNA fragmentation, nuclear condensation, degradation of cytoskeleton, cell shrinkage, membrane blebbing (resulting from CASP3/7-mediated cleavage and activation of ROCK1), loss of adhesion to cellular matrix or neighboring cells (149, 158, 159). In **Type-II cells** (e.g., hepatocytes, β cells of the pancreatic islets, and vast majority of the cancer cells), the activity of executioner caspases is restricted by XIAP (X-chromosome linked inhibitor of apoptosis protein) (76, 110, 160). In this scenario, CASP8 acts to enhance apoptotic signals to ensure full activation of CASP3/7 through cleavage and activation of the pro-apoptotic **B c**ell **l**ymphoma-2 (Bcl-2) family member BID (**B**cl-2 **h**omology-**3** [**B**H3] **i**nteracting-domain death agonist) into truncated BID (tBID), which in turn activates the intrinsic apoptosis pathway (**Figure-7**) (161–164).

Extrinsic apoptosis, which is mediated by death receptors, relies on external stimuli, whereas the intrinsic apoptosis pathway is triggered by internal and/or external stress factors causing DNA damage such as UV or γ-radiation, viral infections, hypoxia, hypothermia, heat shock, growth factor withdrawal, reactive oxygen species (ROS) overload and chemotherapeutic agents (110, 165, 166). The critical step in this mode of apoptotic cell death is irreversible mitochondrial outer membrane permeabilization (MOMP), which creates channels on the outer mitochondrial membrane leading to the release of apoptosis-inducing factors that are normally localized to the mitochondrial intermembrane space (161, 167, 168) These mitochondrial apoptogenic proteins include Cytochrome c (Cytc; a key protein that normally functions as an electron shuttle

as part of mitochondrial respiratory chain), **S**econd-**M**itochondria-derived **A**ctivator of **C**aspase (SMAC; also known as Diablo IAP-binding mitochondrial protein [DIABLO]) and Apoptosis-Inducing Factor (AIF) (161, 169–174). When released into the cytosol, Cytc binds to and activates **a**poptotic **p**eptidase **a**ctivating **f**actor-1 (Apaf-1), a member of the AAA+ ATPase family, through induction of nucleotide exchange of ADP/dADP for ATP/dATP. This is followed by assembly of seven individual Apaf-1/Cytc molecules into a wheel-like heptameric protein complex called apoptosome (175–177). The homotypic interactions between the N-terminal CARD domains present in both Apaf-1 and procaspase-9 target Procaspase-9 zymogens to the apoptosome, leading to proximity-induced homodimerization and autocatalytic maturation of caspase-9 (CASP9) (177–181). Processed CASP9 remains bound to the apoptosome, forming a haloenzyme. Simultaneously, procaspase-3 and -7 are targeted to the apoptosome where they are cleaved and activated by the CASP9/apoptosome haloenzyme (110, 182, 183). The extrinsic and the intrinsic apoptosis pathways merge at this step with the following steps being common between the two pathways.

Intrinsic apoptosis is primarily regulated by members of the Bcl-2 family, a group of pro- and anti-apoptotic proteins containing one to four **B**cl-2 **h**omology (BH) domains (i.e., BH1, BH2, BH3, and BH4) (161, 184). Bcl-2, Bcl-xL, Bcl-w, BCL-B, MCL1 (myeloid cell leukemia sequence-1) and A1 are the anti-apoptotic members of this family, all of which contain all BH domains. Pro-apoptotic Bcl-2 family members can be subdivided into two groups: The first subgroup consists of Bax, Bak and Bok, multi-domain Bcl-2 proteins that share four BH domains similar to pro-survival family members. The second

subgroup consists of BH3-only proteins, including BIM (Bcl-2-interacting mediator of cell death; also known as BCL2L11), PUMA (p53 upregulated modulator of apoptosis; also known as BBC3), BAD (Bcl-2 antagonist of cell death), NOXA (Latin for *damage*), BIK (Bcl-2 interacting killer), HRK (Activator of apoptosis Harakiri) and tBID (184, 185).

Studies in the late 1990s demonstrated that BID is a CASP8 substrate and its cleavage is crucial in Fas-mediated extrinsic apoptosis (76, 162, 164). Several other proteases including cathepsins, calpains and Granzyme-B have also been reported to cleave and therefore activate, BID (76, 186–189). CASP8 cleaves BID at its D60 residue, generating a 15kD cleavage product in which BH3 domain is exposed. This cleavage product, which is referred to as truncated BID (tBID, also known as p15) translocates to mitochondria and binds to the mitochondrial outer membrane (MOM) where it recruits multi-domain Bcl-2 proteins Bax and Bak via BH3-mediated homotypic interactions. Once targeted to MOM, Bax and Bak change their structure from inactive monomers into active homo-oligomers (This transition can be mediated by BH3-only proteins) and engage/perforate MOM through a mechanism that remains unresolved, resulting in MOMP and cell death (184, 190, 191) Thus, generation of tBID by CASP8 serves as a crucial link between the extrinsic and intrinsic apoptosis pathways, and therefore is of central importance to the onset of apoptotic cell death in Type-II cells.

1.2.3 Caspase-8 and Necroptosis

Until recently, apoptosis was considered the only regulated type of cell death that is tightly controlled through genetic and epigenetic mechanisms as opposed to necrosis,

which was classically described as a non-regulated, passive, accidental form of cell death. However, this view has now been challenged by evidence from recent genetic, biochemical studies that have redefined necrosis as a molecularly regulated mode of cell death (192, 193). Several forms of regulated necrotic cell death mechanisms have been recently identified that share common morphological features, including disruption of plasma membrane, swelling of cytoplasm due to influx of ions (calcium, sodium and potassium) and water, disintegration of cellular organelles; but are activated in response to different external stimuli and are driven by distinct biochemical pathways such as necroptosis, pyroptosis and ferroptosis (193, 194). Necroptosis (programmed necrosis) is a unique mode of regulated necrotic cell death mechanism that can be induced under loss and/or inactivation of CASP8. It has now become clear that necroptosis not only exerts adaptive functions upon cells' failing responses to stress stimuli, but also participates in defense against bacterial and viral infections (as part of developmental safeguard programs) as well as T-cell homoeostasis (161, 195–197).

At the molecular level, necroptosis is dependent on the enzymatic activity of **R**eceptor-**i**nteracting serine/threonine-**p**rotein kinases -1 (RIP1) and -3 (RIP3) to activate the pseudokinase **M**ixed-**l**ineage **k**inase domain-**l**ike (MLKL) (161, 198). Structurally aminoacid sequences of RIP1 and RIP3 show almost 50% homology. RIP1 consists of 671 aminoacids in humans and bears an N-terminal serine/threonine kinase domain, an **i**ntermediate **d**omain (ID), a **R**IP **h**omotypic **i**nteraction **m**otif (RHIM) and a C-terminal **d**eath **d**omain (DD), whereas RIP3 consists of 518 aminoacids (*H. sapiens*) containing

an N-terminal kinase domain, an ID and RHIM similar to RIP1 and a unique C-terminus

lacking a DD (**Figure-8**).
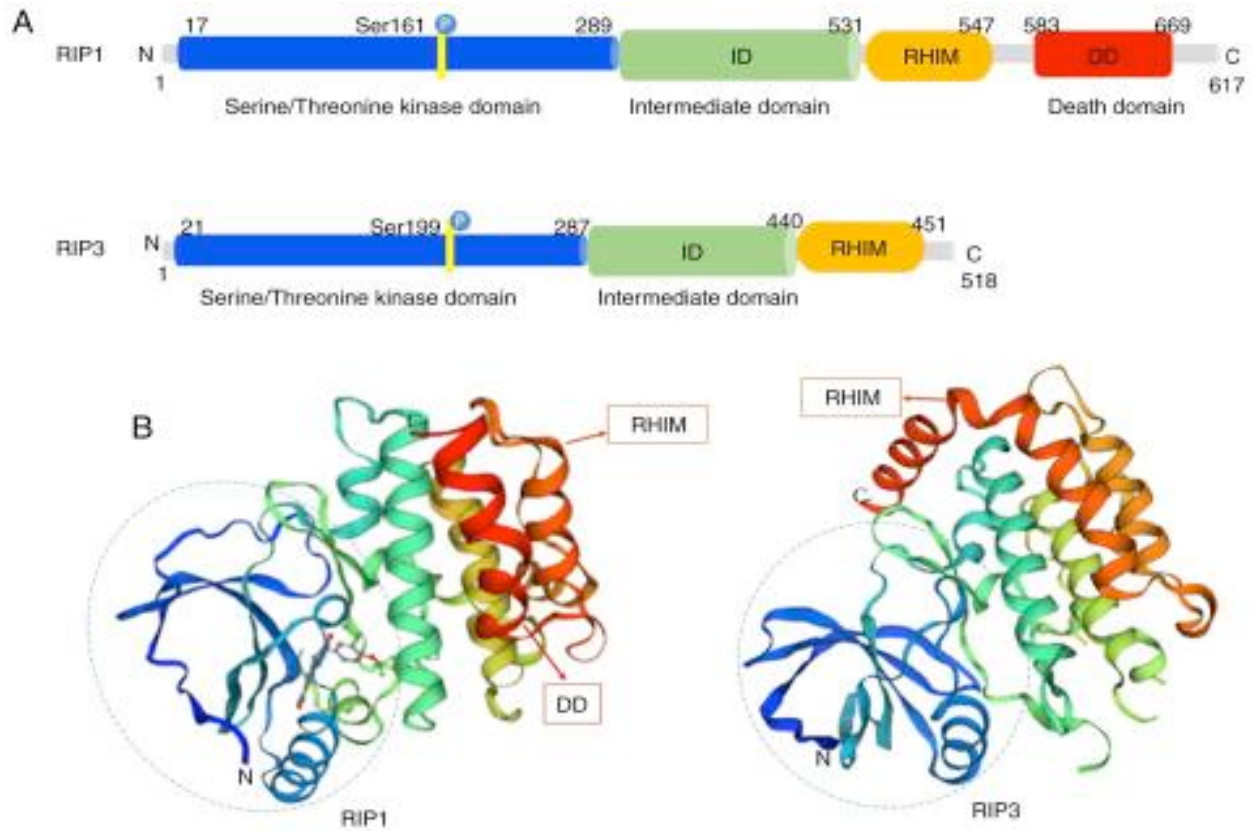
Figure-8: 2D and 3D structural diagrams of RIP1 and RIP3

A. Schematic representation of functional domains of RIP1 and RIP3. **B.** Ribbon diagrams showing tertiary protein structures of RIP1 and RIP3. (Reproduced with permission from [Liu, Y., Liu, T., Lei, T., Zhang, D., Du, S., Girani, L., Qi, D., Lin, C., Tong, R., and Wang, Y. (2019) RIP1/RIP3-regulated necroptosis as a target for multifaceted disease therapy (Review). *Int. J. Mol. Med.* **44**, 771–786] Copyright SpandidosPublications).

Necroptosis can be stimulated by RIP1-dependent and RIP1-independent mechanisms

(199). Death receptor engagement (in particular TNFR1) is the best characterized

necroptosis mechanism so far in which RIP1 functions as a bridge between death

receptor signaling and the activation of RIP3 and MLKL.

TNFα is predominantly expressed by macrophages and activated T cells as a membrane-bound 26kD protein, which is cleaved by **TNF-α-c**onverting **e**nzyme (TACE), culminating in the release of a 17kD soluble form (200, 201). Both membrane-bound and soluble forms of TNFα are biologically active. Binding of TNFα to its cognate receptor, TNFR1 leads to receptor trimerization and recruitment of the adaptor protein **T**NF **r**eceptor type 1-**a**ssociated **d**eath **d**omain protein (TRADD) through homotypic interactions between the C-terminal DD of TRADD and the intracellular DDs of TNFR1 (**Figure-9**). Once bound to TNFR1, TRADD serves as a binding platform to recruit key downstream proteins including the E3 ubiquitin ligases **T**NF-**r**eceptor-**a**ssociated **f**actor-2 (TRAF2) and -5 (TRAF5) as well as RIP1. TRADD's N-terminal TRAF2-binding domain and DD mediate its interaction with TRAF2 and RIP1, respectively (202). TRAF2/5 then recruit direct E3 ligases, **c**ellular **i**nhibitor of **a**poptosis **p**rotein-1 (cIAP1) and -2 (cIAP2) as well as **L**inear **u**biquitin **c**hain **a**ssembly **c**omplex (LUBAC) to RIP1 via a **c**IAP1/2-**i**nteracting **m**otif (CIM), leading to formation of the signaling **Complex-I.** TRAF2 has been shown to stabilize cIAP1 by inhibiting its autoubiquitination and subsequent proteasomal degradation (203). Once incorporated into Complex-I, cIAP1/2 and LUBAC catalyze K63-linked polyubiquitination of the intermediate domain of RIP1, allowing binding of **N**F-κB
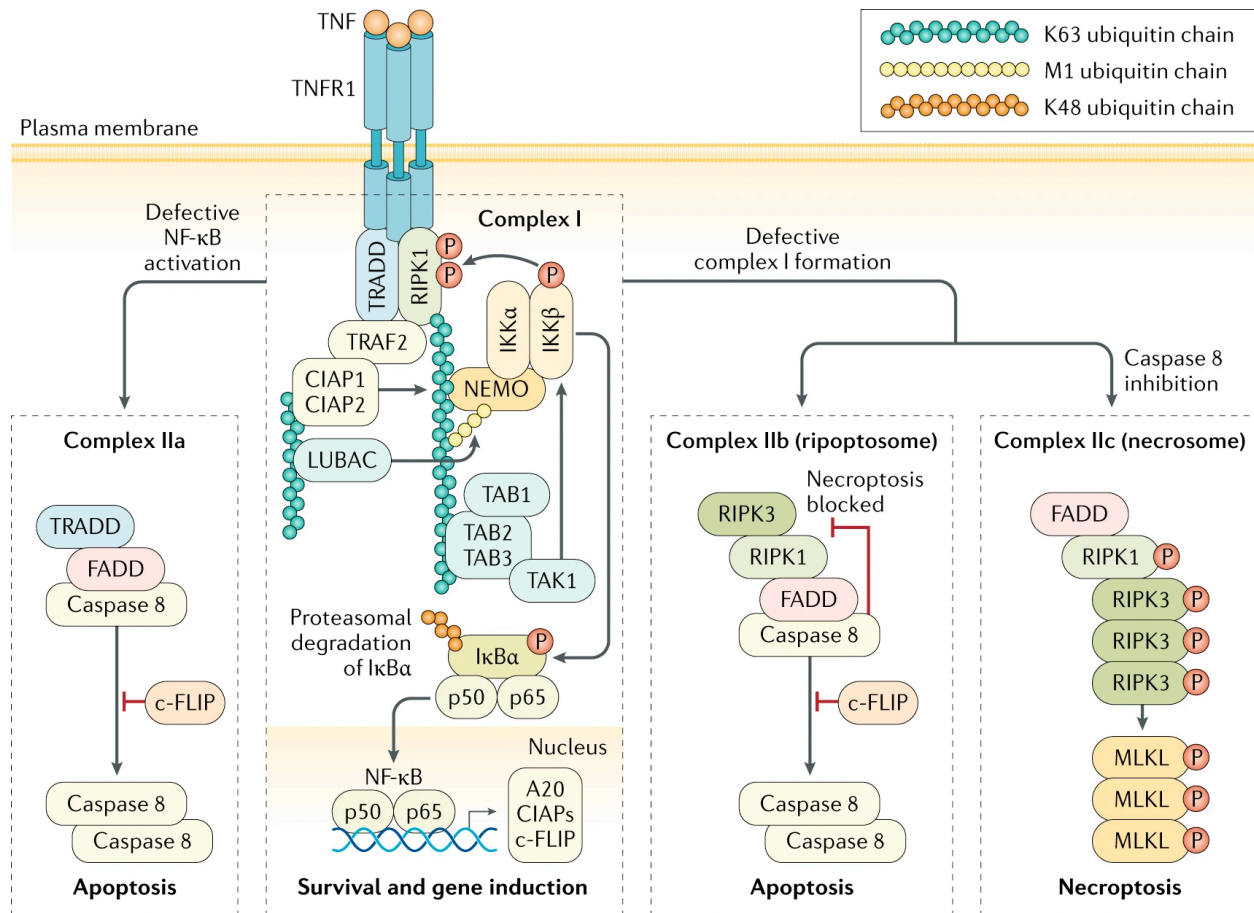
Figure-9: TNFR1-mediated survival and cell death pathways.

(Reproduced with permission from [Schwabe, R. F., and Luedde, T. (2018) Apoptosis and necroptosis in the liver: a matter of life and death. *Nat. Rev. Gastroenterol. Hepatol.* 15, 738–752] Copyright SpringerNature).

(**n**uclear **f**actor **k**appa-light-chain-enhancer of activated **B** cells) essential modulator (NEMO, also referred to as IKKγ [**i**nhibitor of I**κ**B **k**inase- γ]) to the K63 polyubiquitin chains of RIP1 through interactions involving its ubiquitin-binding domain, ultimately leading to recruitment of the IKK complex comprising IKKα and IKKβ (205, 206). K63 polyubiquitination of RIP1 is also crucial for the recruitment of TGFβ (**T**ransforming **g**rowth **f**actor-β) **a**ctivated **k**inase (TAK) complex (consisting of TAK1 and **TA**K1 **b**inding

proteins -1[TAB1] and -2[TAB2]) (207). TAK1 has been reported to phosphorylate and activate IKKβ, which in turn drives ubiquitylation and proteasomal degradation of the inhibitory protein IκBα (Nuclear factor of kappa light polypeptide gene enhancer in B-cells inhibitor alpha) allowing liberation and nuclear translocation of NF-κB dimers (consisting of p50 and p65) to transcriptionally activate the expression of pro-survival proteins (e.g. $FLIP_{S/R}$ and cIAPs) and cytokines (e.g. IL6 and TNFα) (204, 208). Phosphorylation of RIP1 by the IKK complex, occurring at its S25 residue inhibits RIP1 kinase activity, preventing formation of downstream death-inducing signaling complexes, Complex-II and/or necrosome, which will be discussed in the following paragraphs (209, 210) Thus, the assembly of Complex-I promotes cell survival through induction of NF-κB.

Genetic (e.g. genetic deletions of *Nemo* or *Rela* encoding IKKγ and p65 respectively) or pharmacological inactivation of NF-κB or other factors that mediate NF-κB activation (e.g. chemical inhibition of cIAP1/2 with SMAC mimetics) switches the outcome of TNFR1 signaling from survival toward apoptosis through assembly of a CASP8-activating cytosolic Complex-II (**Figure-9**) (204, 211–213). Hydrolysis of RIP3-bound K63 polyubiquitin chains by deubiquitinating enzymes such as cylindromatosis (CYLD) and A20 is implicated in the switch from Complex-I to Complex-II (214). Complex-II assembles in two different forms: Complex-IIA and Complex-IIB (also referred to as 'ripoptosome'). Complex-IIA forms upon release of TRADD from Complex-I into the cytosol, where it recruits FADD via DD-mediated homotypic interactions. FADD, then serves as a platform for recruitment (thanks to DED-mediated homotypic interactions)

and activation of CASP8, a process that is counterbalanced by NF-κB – driven transcriptional upregulation of pro-survival genes such as FLIP under physiological conditions (109, 215). Under conditions whereby K63-linked polyubiquitination events in Complex-I are compromised (e.g. pharmacological inhibition of the E3 ubiquitin ligases cIAP1/2 by SMAC mimetics), cells commit to apoptosis through Complex-IIB signaling (216–220). Complex-IIB, a large ~2MDa apoptosis-inducing platform contains RIP1, FADD and CASP8 as core components and can assemble independently of death receptor engagement in response to genotoxic stress-induced inhibition of IAPs (i.e. XIAP, cIAP1 and cIAP2). It can also form upon SMAC mimetic treatment without requiring autocrine TNFα signaling thanks to homotypic DD interactions between FADD and deubiquitinated RIP1 and DED interactions between FADD and CASP8. Complex-IIB formation relies on the kinase activity of RIP1 and can stimulate CASP8-mediated apoptosis independently of NF-κB target genes (221). Hence, Complex IIA/B signaling leads to CASP8-mediated apoptotic cell death.

Apoptosis, a highly conserved mechanism in metazoans operates to remove superfluous cells during organismal development. Consistent with this function, genetic deletion of pro-apoptotic genes in mice such as *Apaf1* or *Casp9* (whose protein products are drive intrinsic apoptosis) led to the aberrant accumulation of cells, resulting in craniofacial defects, overgrowth of the brain and embryonic lethality (199, 222–224). However, germline deletion of *Casp8* (or genes encoding its obligate adaptor FADD or the CASP8 paralogue FLIP) resulted in embryonic lethality in mice at embryonic day 10.5 (E10.5) as a result of excessive cell death (199, 225–228). Furthermore, conditional knockouts of *Casp8*, *Fadd* or *Cflar* (encoding murine FLIP) were associated

with suppression of T-cell receptor (TCR)-mediated T cell activation and proliferation (199, 229–231). Subsequent studies demonstrated that $Casp8^{-/-}$ T cells showed normal NF-κB activation and initial proliferation upon TCR engagement, but then rapidly underwent cell death that could be inhibited by the RIP1 inhibitor, Necrostatin-1 (Nec-1) or genetic deletion of *Rip3* (199, 232, 233). Strikingly, this finding was consistent with the observation that embryonic lethality in $Casp8^{-/-}$ mice was fully abrogated by concurrent deletion of *Rip3* (199, 234, 235). Furthermore, knockout of *Rip3* protected the skin and intestines of mice from severe inflammation resulting from organ-specific genetic deletion of *Casp8* or *Fadd* (199, 236–238). These studies implicated CASP8 in suppression of RIP3-mediated necroptosis. As discussed in the previous sections, autocatalytic processing of CASP8 is crucial for its apoptotic functions. $Casp8^{D387A/D387A}$ mice in which *Casp8* is mutated in the self-processing site (producing a non-cleavable form of CASP8 impaired in mediating apoptosis, but still capable of blocking necroptosis) are born and reach adulthood without any major complications, indicating that the primary role for CASP8 during development is inhibition of necroptosis rather than mediating apoptosis (139, 235, 239, 240). These findings also suggest that the catalytic activity of CASP8, rather than its self-processing is essential for the inhibition of necroptosis, a phenomenon which was corroborated by subsequent studies demonstrating that CASP8 is partially active in procaspase-8/FLIP$_L$ heterodimers. This observation indicates that uncleaved CASP8 blocks necroptosis without promoting apoptosis and that FLIP$_L$ plays a role in the switch in CASP8's catalytic function from induction of apoptosis to suppression of necroptosis (199, 239).

How CASP8 regulates necroptosis has not been fully uncovered, although CASP8-mediated cleavage of both RIP1 and RIP3 is widely believed to restrict necroptotic signaling (200). RIP1 and RIP3 each bear cleavage sites targeted by CASP8 and are substrates for procaspase-8/FLIP$_L$ heterodimers (139, 241, 242). CASP8-mediated cleavage of the deubiquitinating enzyme CYLD following TNFα stimulation has also been shown to suppress necroptotic death, promoting survival (243). When CASP8 is lost or inhibited (e.g. by the pharmacological pan-caspase inhibitors zVAD-FMK or IDN-6556 [emricasan] or viral FLIP$_S$ mimetics), Complex-IIC (also referred to as 'necrosome') is formed in the cytosol, resulting in necroptosis (139). Under conditions that favor the assembly of necrosome (e.g. dual inhibition of cIAP1/2 by SMAC mimetics [impairing Complex-I formation] and CASP8 by zVAD-FMK [disrupting Complex-II formation]), RIP3 is recruited to RIP1 via RHIM-mediated homotypic interactions. Oxidization of 3 key cysteine residues of RIP1 by ROS has been shown to activate RIP1 autophosphorylation on S161, enabling RIP1 to recruit RIP3 and form a functional necrosome (244). E3 ligase Pellino-1 (PELI1) mediates K63-linked ubiquitination on K115 of activated RIP1, facilitating recruitment of RIP3 to the necrosome, an event that is followed by phosphorylation and activation of RIP3 by RIP1, leading to RIP3 oligomerization (245, 246). Intriguingly, despite driving TNFα-mediated RIP3 activation, in the absence of death receptor signals, RIP1 can also block spontaneous RIP3 activation in the cytosol, through recruitment of CASP8/FLIP$_L$ complexes, leading to inhibition of RIP3 oligomerization and degradation of nascent RIP3 oligomers possibly via a cIAP-mediated mechanism (246). RIP3 oligomerization, which is arguably the most critical step of necroptosis induction stimulates further activation of RIP3 through

cis-auto phosphorylation (246–249). In a recent study, the transmembrane protease **A** **d**isintegrin **a**nd **m**etalloproteinase-17 (ADAM17) has been shown to play a role in this phosphorylation process in a murine model of **d**extran **s**ulfate **s**odium (DSS)-induced colitis (250). Furthermore, ubiquitination also regulates RIP3 activity during necroptosis. RIP3 is ubiquitinated at its K5 residue (possibly by cIAPs) in response to necroptotic signals, allowing necrosome formation. K5 ubiquitin levels are tightly controlled by the deubiquitinating enzyme A20. T cells deficient in A20 show increased susceptibility to necroptosis caused by significantly higher levels of RIP3 ubiquitination at K5 accompanied by faster assembly of RIP1-RIP3 heterodimers, suggesting that A20 negatively regulates necroptosis besides its role in Complex-II formation (251). Conversely, RIP3 ubiquitination at two lysine residues, K55 and K363 by the E3 ligase CHIP (**c**arboxyl terminus of **H**sp70-**i**nteracting **p**rotein) serves as a lysosomal degradation signal for RIP3, preventing necroptosis. Hence, phosphorylation and ubiquitination events play key roles in RIP3-mediated necroptosis. Activation of RIP3 is followed by recruitment of MLKL, the obligatory effector of necroptosis to the necrosome (**Figure-10**) (252).
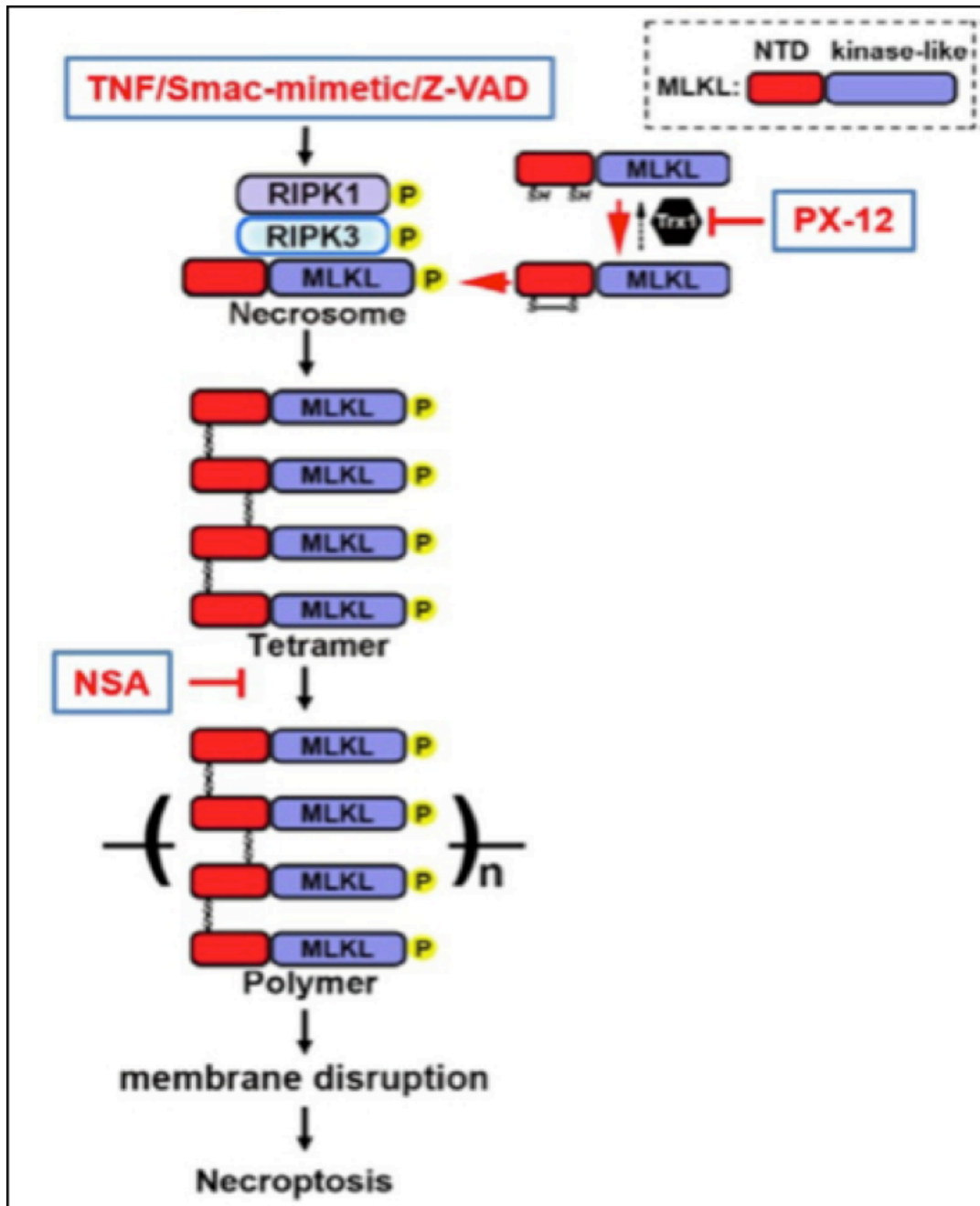
Figure-10: Schematic representation of MLKL polymerization during execution of necroptosis.

Trx1: Thioredoxin-1; NTD, N-terminal four-helical bundle domain; NSA, necrosulfonamide (Reproduced with permission from [Johnston, A., and Wang, Z. (2018) Necroptosis: MLKL Polymerization. J. Nat. Sci.])

MLKL is a pseudokinase that consists of an **N**-**t**erminal **d**omain (NTD) containing 4

helical bundles followed by a **b**race **r**egion (BR) with two α helices and a C-terminal

pseudokinase domain (PKD, also called **k**inase-**l**ike **d**omain [KLD]) that contains a helical activation loop and an ATP-binding pocket (205). Intriguingly, a recent work showed that the four-helical bundle region in the NTD of MLKL is required and sufficient for its polymerization and execution of necroptosis, a mechanism which was also demonstrated in mouse cells (253, 254). However, there have been no reports so far showing endogenous expression of the N-terminal fragment of MLKL to mediate necroptosis under normal and/or pathophysiological conditions. Once incorporated into the necrosome, MLKL is phosphorylated by RIP3 at T357 and S358 in the pseudokinase domain (murine MLKL is phosphorylated at S345, S347 and T349 among which phosphorylation of S345 is critical for RIP3-mediated MLKL activation) (255, 256). Upon phosphorylation, MLKL undergoes a series of conformational changes that result in the unfolding and release of the BR, triggering MLKL tetramer formation through generation of intermolecular disulfide bridges (**Figure-10**). MLKL tetramers further polymerize into octameric structures upon joining of two previously-formed tetramers in their side-by-side position, with MLKL N-terminal α-helices 4 and 5 being located in the interface of the two tetramers (256). Intermolecular disulfide bonds are crucial for the stability of MLKL polymers. In the absence of necroptotic stimuli, the cytoplasmic thiol oxidoreductase thioredoxin-1 (Trx1) restricts disulfide bond formation between monomeric MLKL. Necroptosis inhibitor necrosulfonamide (NSA) facilitates cross-linking between C32 residue of Trx1 and C86 of MLKL, blocking MLKL polymerization. Inhibition of Trx1 with the small molecule inhibitor PX-12 stimulates necrosome formation, phosphorylation and polymerization of MLKL and subsequent necroptotic death (257).

MLKL-induced disintegration of cellular membranes is a key element of necroptotic cell death. Once formed in the necrosome, MLKL octamers, which show propensity for binding to phosphatidylinositol lipids and cardiolipin (a hallmark lipid of mitochondria) translocate to plasma and intracellular membranes, where they create pores to impair membrane integrity, promoting necroptosis (258, 259). It was also reported that MLKL octamers can mediate influx of calcium (through activation of the calcium channel TRPM7 [**T**ransient **R**eceptor **P**otential Cation Channel, Subfamily **M**, Member-**7**]) or sodium ions to promote cell death (260, 261). Excessive production of ROS resulting from disruption of mitochondrial membrane integrity by MLKL oligomers has been shown to contribute to necroptosis as well (262). Therefore, although several mechanisms have been proposed, there is no definitive consensus as to the execution mechanism downstream of MLKL in necroptosis.

Contrary to TNFR1 signaling, which is associated with formation of a pro-survival complex first, and death-inducing complexes subsequently in stimulated cells, other death receptor-mediated pathways (e.g. TRAILR1, TRAILR2, Fas) execute apoptosis through assembly of the receptor-bound DISC and CASP8 activation (see earlier). Under conditions whereby cIAPs are lost or inactivated (e.g. inhibition of cIAP1/2 by SMAC mimetics), RIP1 is recruited to TRAILR1 or Fas, resulting in formation of a signaling complex akin to Complex-I, which can progress either toward generation of the cytosolic Complex-IIB (also called 'ripoptosome') that relies on the kinase activity of RIP1 and can stimulate CASP8-mediated apoptosis or, when CASP8 is inactivated (e.g.

pharmacological inhibition of CASP8 by the pan-caspase inhibitor zVAD-FMK) RIP1-mediated necroptosis through formation of the necrosome (192, 263, 264).

Cellular stress, damage and bacterial/viral infections are detected through germline-encoded pattern recognition receptors (PRRs) such as **T**oll-**l**ike **r**eceptors (TLRs), **N**ucleotide-binding and **o**ligomerization **d**omain (NOD*)*-**l**ike **r**eceptors (NLRs) and **R**etinoic Acid-**I**nducible **G**ene-1 Protein (RIG1)-**l**ike **r**eceptors (RGRs) some of which have been implicated in induction of necroptosis (192, 265). Upon activation, TLR3, a member of the TLR family that recognizes double stranded RNA (dsRNA), recruits **T**oll/**I**nterleukin-1 **r**eceptor (TIR) domain-containing adaptor inducing Interferon (IFN)-β (TRIF), which recruits additional signaling partners to activate NF-κB, leading to induction of type-I IFNs. TLR4, a sensor of bacterial lipopolysaccharide (LPS) signals through the adaptor proteins MyD88 (**my**eloid **d**ifferentiation primary response gene **88**) or TRIF, resulting in NF-κB-induced upregulation of proinflammatory cytokines such as IL-1β, IL6 and TNFα (192, 266). TRIF, a cytosolic adaptor protein shared by both the TLR3 and TLR4 signaling pathways bears a RHIM domain that allows interaction with RIP1 and RIP3. Activation of TLR3 by the synthetic dsRNA analog polyinosinic-polycytidylic acid (poly(I:C)), or TLR4 by LPS in the presence of the pancaspase inhibitor zVAD-FMK induces TRIF-mediated necroptosis in macrophages and fibroblasts that depends on RIP3 and MLKL (192, 267, 268). Other necroptosis mediators include the **D**NA-dependent **a**ctivator of **I**FN regulatory factors (DAI; also known as ZBP-1 [**Z**-DNA **b**inding **p**rotein-1]), a cytosolic PRR that senses viral double stranded DNA (dsDNA) to promote NF-κB-mediated expression of type-I IFNs. DAI has

been shown to form a complex with RIP3 through RHIM-mediated homotypic interactions to activate RIP3/MLKL-dependent RIP1-independent cytomegalovirus (CMV)-induced necroptosis (269, 270). Under conditions whereby either CASP8 or FADD is lost or inactivated, type-I (e.g. IFNα or IFNβ) and type-II (IFNγ) IFNs can induce transcriptional activation of the viral RNA-responsive **p**rotein **k**inase **R** (PKR) in mouse embryonic fibroblasts (MEFs), which then recruits RIP1 to initiate necrosome formation, leading to necroptotic cell death (192, 271). In macrophages, execution of necroptosis mediated by TLR3, TLR4 and TNFR1 (in response to poly(I:C), LPS and TNFα respectively) requires **IFN-α r**eceptor type-**I** receptor (IFNAR1) signaling, suggesting an autocrine loop of type-I IFNs (192, 272). Hence, regulation of necroptosis is important in controlling cellular responses to viral and bacterial infections, DNA damage as well as inflammation, where aberrations in necroptosis signaling have been implicated in the development of various human diseases with excessive cell death and inflammatory responses (273).

Uncontrolled necroptosis could be an underlying mechanism in neurodegenerative diseases such as Alzheimer Disease (AD), which is characterized by severe neuronal loss. Study of postmortem human AD brains has shown a significant increase in the levels of RIP1, MLKL, necrosome complex and MLKL oligomers, which positively correlated with the Braak stage of the disease and inversely correlated with the cognitive score of the patients (274). In a mouse mode of AD, treatment of animals with the RIP1 kinase inhibitor 7-Cl-O-necrostatin (also called as **Nec**rostatin-1s[Nec-1s]) blocked necroptosis, preventing axonal degeneration (275). Multiple Sclerosis (MS) is

another neurodegenerative disease characterized by oligodendrocyte dysfunction and loss of myelin sheaths around nerves. Study of white matter patient samples from control and MS tissue has revealed upregulation of necroptosis markers including phosphorylation of RIP1, RIP3 and MLKL, accompanied by a significant increase in MLKL oligomers in MS. Oral administration of Nec-1s inhibited degeneration of oligodendrocytes and reduced disease severity in an experimental mouse model of MS (276).

Rheumatoid arthritis (RA) is a common chronic inflammatory disease, characterized by autoimmunity that triggers joint inflammation, degradation of cartilage and bone tissue and ultimate joint destruction. In a mouse model of collagen-induced arthritis (CIA), levels of key elements of the necroptosis pathway, RIP1, RIP3 and MLKL were found to be significantly elevated in the synovium of CIA mice compared with their WT counterparts (277). In a subsequent study, treatment of CIA mice with Nec-1s reduced the expression of necroptosis mediators RIP1, RIP3, MLKL and proinflammatory cytokines IL-1β, IL6, IL17 and TNFα in the synovium, inhibiting development of RA (278). Therefore, targeting necroptosis might be a viable therapeutic approach for RA.

Necroptosis has been implicated in cardiac ischemia-reperfusion (IR) injury. In mouse and guinea-pig models of IR, treatment of animals with Nec-1 inhibited phosphorylation of RIP1/RIP3 and significantly reduced necroptotic cell death *in vivo*, leading to reduction in myocardial infarct size and preservation of cardiac performance (279, 280).

Findings from recent studies suggest that necroptosis is one of the underlying mechanisms for hepatic injury and hepatitis observed in chronic alcohol consumption and **n**on-**a**lcoholic **s**teato**h**epatitis (NASH), an aggressive form of fatty liver disease marked by liver inflammation that can progress to cirrhosis and hepatic failure (192, 281, 282). Liver samples obtained from patients with alcohol-induced liver disease and NASH showed RIP3 overexpression. RIP3 induction was also detected in liver in murine models of alcoholic liver disease and NASH, which was associated with development of hepatic injury, fibrosis and inflammation, rescued by genetic deletion of *Rip3* (281, 282).

Preclinical and clinical evidence suggests that the role necroptosis plays in disease conditions is not limited to pathologies that are characterized by an excessive cell death (see above) but extends to oncological conditions that will be discussed in more detail in the following sections.

1.2.4 Novel Roles for Caspase-8 in Immune Regulation

Interleukin-1β (IL-1β) is a pleiotropic cytokine, which is key for orchestration of inflammatory responses against pathogens. IL-1β has also been implicated in a variety of inflammatory diseases such as Rheumatoid Arthritis, Familial Mediterranean Fever (FMF) and Behçet's disease (283, 284). IL-1β, best characterized member of the IL-1 cytokine family (other members of the family include IL-1α, IL-18, IL-33, IL-36α, IL-36β,and IL-36γ) is typically expressed by innate immune cells (e.g. macrophages, monocytes and dendritic cells) as a 31kD cytosolic precursor protein (referred to as pro-IL-1β) and undergoes cleavage for activation. Once activated, IL-1β is secreted out of

cells to exert its activity, a process facilitated by large multi-protein complexes termed inflammasomes (285). Several recent studies have identified novel roles for CASP8 in regulating IL-1β directly or indirectly through modulation of inflammasomes depending on the nature of stimuli initiating the signaling pathway (286).

IL-1β is produced by myeloid cells (it is not constitutively expressed) in response to molecular patterns carried by a variety of pathogens called 'pathogen-associated molecular patterns' (PAMPs) that are recognized by 'pattern recognition receptors' (PRRs) on macrophages, such as Toll like receptors (TLRs) and **N**ucleotide-binding and **o**ligomerization **d**omain (NOD*)-***l**ike **r**eceptors (NLRs) (see earlier) (266). PRR signaling leads to activation of **N**F-κB and transcriptional activation of pro-inflammatory cytokines such as IL-1β, IL-6 and TNFα. Production of the precursor protein pro-IL-1β serves as a priming step. Encounter of the primed cell with further PAMP(s), or **d**anger **a**ssociated **m**olecular **p**atterns (DAMPs, endogenous molecules released from dying or dead cells such as ATP, calreticulin etc.) promotes the processing, activation and secretion of IL-1β (285). Cleavage of IL-1β is executed by Caspase-1 (CASP1), whose activation occurs through recruitment and incorporation into inflammasome (287). The term inflammasome was coined to describe a large molecular scaffold consisting of a cytosolic PRR, adaptor proteins and a protease (CASP1) (83). The **n**ucleotide-binding **o**ligomerization **d**omain (**N**OD), **l**eucine-**r**ich **r**epeat (**LR**R)-containing proteins (NLR) family members NLRP1, NLRP3, and NLRC4, as well as **a**bsent-**i**n-**m**elanoma 2 (AIM2) and pyrin are among the cytosolic PRRs that engage inflammasomes (288–290). NLRP3, the best characterized and well-studied inflammasome bears a tripartite

structure: a C-terminal LRR that senses PAMPs/DAMPs, a central nucleotide-binding domain (referred to as NACHT) and an N-terminal pyrin domain (PYD) (285). The N-terminal PYD of NLRP3 recruits a bipartite adaptor protein called **a**poptosis-associated **s**peck-like protein containing a **c**aspase activation and recruitment domain (ASC) via PYD-mediated homotypic interactions, which in turn recruits procaspase-1 thanks to homotypic interactions involving CARD domains (288). Once incorporated into the inflammasome, procaspase-1 undergoes proximity-induced autocatalytic processing to become activated. Active CASP1 proteolytically processes pro-IL-1β into its biologically active form (288, 291, 292). In addition to pro-IL-1β (and pro-IL-18), CASP1 can cleave and activate gasdermin D (GSDMD), a pore-forming protein, which upon activation facilitates the release of IL-1β into extracellular space from the cytosol (293). When formed in low numbers GSDMD pores serve as plasma membrane channels for secretion of IL-1β from living cells, whereas formation of GSDMD pores in high abundance triggers a lytic form of cell death known as pyroptosis, allowing release of numerous intracellular contents including IL-1β (293–295). Hence, depending on the context, GSDMD facilitates secretion of IL-1β from living or dead (pyroptotic) cells.

Although inflammasome-induced CASP1 activation constitutes the major source for IL-1β, serine proteases, such as cathepsins (e.g. cathepsin C, cathepsin D, cathepsin G), neutrophil elastases and collagenases also contribute to the processing and activation of IL-1β (286, 296–298). Importantly, recent studies have identified CASP8 as an alternative protease that can process pro-IL-1β directly (independently of inflammasome activation) in response to PAMP signaling that proceeds through canonical PRRs such

as TLR4 and concomitant death receptor signaling (e.g. CD95 signaling) (286, 299). TRIF-mediated activation of CASP8 in response to stimulation of TLR3/TLR4 signaling (see earlier) is key in CASP8-induced cleavage of pro-IL-1β (300). CASP8 serves as the major protease to proteolytically activate pro-IL-1β during inflammatory responses developed against pathogens, such as fungi species *Candida albicans* and *Aspergillus fumigatus* as well as bacteria such as *Mycobacterium bovis* and *Mycobacterium leprae* (**Figure-11A**) (301). Stimulation of the dectin signaling pathway during development of immune responses against fungal pathogens comprises a large multiprotein complex involving BCL-10 (**B c**ell **l**ymphoma-**10**), MALT1 (**m**ucosa-**a**ssociated **l**ymphoid **t**issue lymphoma translocation protein-**1**) and CARD9 (**c**aspase **a**ctivation **r**ecruitment **d**omain [CARD]-containing coiled-coil protein-9) that induces NF-κB signaling leading to upregulation of pro–IL-1β. Subsequent recruitment of ASC and procaspase-8 to the CARD9–BCL10–MALT1 complex induces activation of CASP8, which then processes pro–IL-1β into its biologically active form (286, 301). Although these results indicate that CASP8 acts as a major protease for proteolytic processing and activation of pro–IL-1β and that active CASP8 can promote inflammation in TLR-primed innate immune cells such as macrophages and dendritic cells in response to death receptor stimulation; they are paradoxical considering death receptor engagement induces apoptosis, whereas the release of IL-1β is associated with pyroptosis, an inflammatory mode of cell death. Therefore, future studies are warranted to elucidate how TLR priming coupled with death receptor stimulation induces CASP8-mediated inflammation.

Misfolded protein accumulation in the endoplasmic reticulum (ER) lumen activates the **u**nfolded **p**rotein **r**esponse (UPR, also referred to as ER stress) pathway, a tightly

controlled mechanism that is highly conserved among mammalian species. Upon activation of the UPR, normal cell functioning is restored by inhibition of protein translation, degradation of misfolded proteins and activation of signaling pathways leading to upregulation of chaperons that are involved in protein folding (286). CASP8 promotes inflammation through processing and activation of pro–IL-1β independently of CASP1 in macrophages during treatment with chemotherapeutic agents such as doxorubicin and oxaliplatin as well as ER stress-inducing agents such as tunicamycin and thapsigargin in the presence of LPS (**Figure-11B**) (299, 302, 303). Intriguingly, induction of ER stress by oxaliplatin also stimulates calreticulin (CRT) exposure through a CASP8-dependent mechanism. When elicited by oxaliplatin, CRT exposure pathway is activated upon phosphorylation of the **e**ukaryotic translation **i**nitiation **f**actor-**2α** (eIF2α) by the ER-sessile kinase PERK (**p**rotein kinase R [**P**KR]-like **e**ndoplasmic **r**eticulum **k**inase), followed by CASP8-mediated cleavage of the ER protein BAP31 (**B**-cell receptor-**a**ssociated **p**rotein-**31**), conformational activation of the pro-apoptotic Bcl2 proteins Bax and Bak and transport of CRT from ER to the plasma membrane through the Golgi apparatus. CRT exposure that occurs in dying tumor cells as part of a unique form of apoptosis called immunogenic cell death (ICD) serves as an 'eat me' signal, allowing macrophages to engulf and destroy them (304). Misregulation of the ER stress caused by aging or environmental factors can lead to numerous disease conditions ranging from diabetes to neurodegenerative disorders including Alzheimer's disease, Parkinson's disease, and bipolar disorder (305). Thus, exploring the roles of CASP8 during ER stress response is important for development of novel therapies.

NLRP3 inflammasome signaling proceeds through canonical and non-canonical pathways (**Figure-11C**). The canonical NLRP3 inflammasome signaling is activated in response to stimuli such as LPS/ATP, LPS/Nigericin (a potent bacterial toxin that functions as a potassium ionophore depleting intracellular potassium sources) or ATP/PAM3CSK4 (a synthetic triacylated **l**ipo**p**eptide [LP] that mimics bacterial LPs; abbreviated as PAM) and does not rely on Caspase-11 (CASP11) activity. The non-canonical NLRP3 inflammasome signaling can be activated during immune responses developed against bacterial pathogens such as *Citrobacter rodentium* and *Escherichia coli* and requires CASP11 (286, 306, 307). Binding of internalized LPS (released from endocytosed Gram negative bacteria) to procaspase-1 induces oligomerization, autoproteolytic processing and activation of procaspase-11 zymogens. Active CASP11 can then cleave and activate its downstream substrates such CASP1 and GSDMD, leading to CASP1-mediated cleavage and activation of pro–IL-1β and GSDMD-mediated formation of pores in the plasma membrane promoting pyroptosis (308).

Genetic studies confirmed CASP8's role in the regulation of NLRP3 inflammasome. Macrophages and dendritic cells from *Rip3/CASP8*$^{-/-}$ but not Rip3$^{-/-}$ mice demonstrated significantly reduced activation of both canonical (LPS/ATP, ATP/PAM) and non-canonical (*C. rodentium*, *E. coli*) NLRP3 inflammasomes (286, 309). CASP8 and its binding partner FADD are required in both priming and activation of the NLRP3 inflammasome (**Figure-11C**) Specifically, stimulation of the TLR signaling pathway activates NF-κB leading to transcriptional upregulation of pro–IL-1β and NLRP3, a priming process that partially relies on CASP8 activity. CASP8 is recruited to the NLRP3

inflammasome complex where it promotes cleavage and activation of procaspase-1. CASP8's involvement in promoting CASP1-mediated processing and activation of pro–IL-1β (as part of NLRP3 signaling complex) has been demonstrated during *Salmonella typhimurium*, *Yersinia pestis* and *Listeria monocytogenes* infections (286, 310, 311). CASP8 is also capable of directly binding and activating procaspase-1 (286, 309).

Intriguingly, data from several other reports suggest a negative regulatory role for CASP8 in inflammatory immune responses. In a study, conditional knockout of *Casp8* in dendritic cells resulted in a significant increase in LPS-induced NLRP3 inflammasome formation, CASP1 processing and subsequent IL-1β production (**Figure-11D**), which was abrogated upon genetic deletion of *Rip3,* siRNA (**s**mall **i**nterfering RNA) knockdown of *Mlkl* or Nec-1 treatment *in vitro* (312). In a study where the effect of CASP8 loss was investigated, conditional deletion or expression of an enzymatically inactive form of *Casp8* in mouse skin led to an inflammatory-type local disease characterized by marked immune cellular infiltration of the dermis (by eosinophils, granulocytes and T cells), a phenotype that was not rescued upon genetic deletions of TNFR1, IL-1β or TLR4 (313). Consistent with this observation, in a study by Li *et. al.* conditional epidermal knockout of *Casp8* resulted in an Atopic Dermatitis-like skin disorder in mice, characterized by infiltration of mast cells in the dermis with upregulation of Th2 cytokines (e.g. IL-9, IL-13) in the acute and Th1 cytokines (e.g. IL-12 and IL-18) in the chronic phases of the disease (314). In another study, tissue specific ablation of *Casp8* in the gut and skin was associated with disruption of tissue homeostasis and severe inflammation characterized by infiltration of macrophages, neutrophils and T cells at both sites.

Interestingly, deleterious effects of *Casp8* loss were rescued by *Rip3* deletion or neutralization of TNF, suggesting that repression of necroptosis (an inflammatory mode of cell death) might be a mechanism by which CASP8 regulates inflammation (238). Therefore, our current understanding of CASP8 functions in immune processes is far from complete, and future studies are warranted to dissect the differential roles of CASP8 in regulating inflammatory responses.
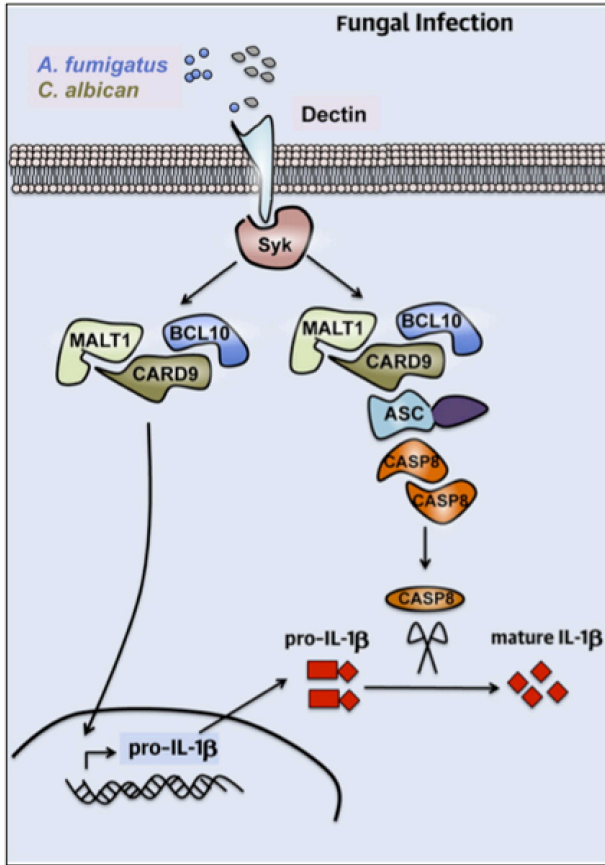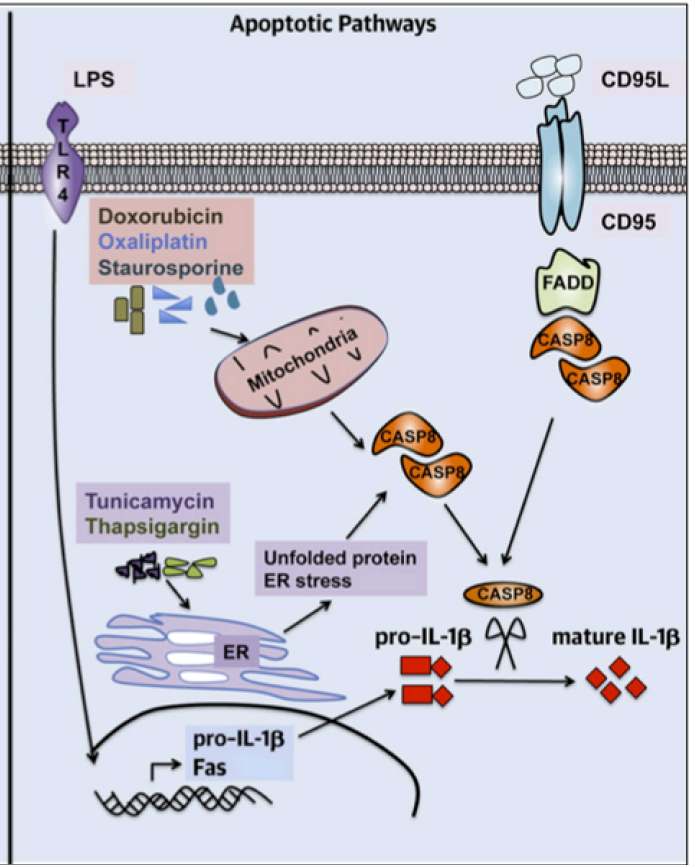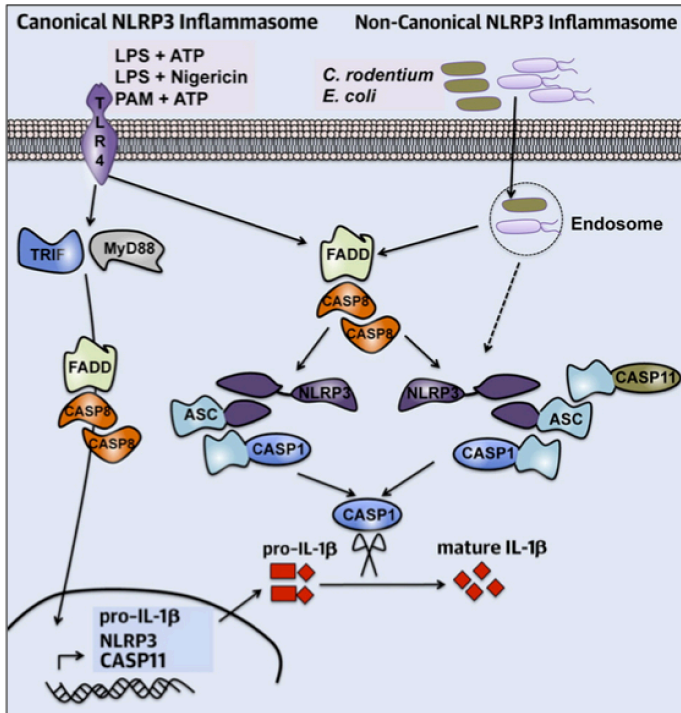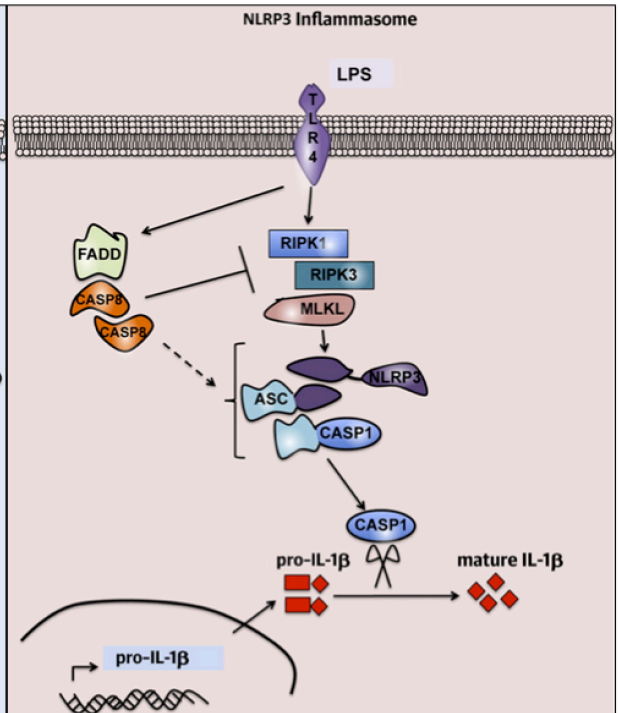
Figure-11: Novel roles for Caspase-8 in regulation of IL-1β and the NLRP3 inflammasome.

A. Upon binding of fungi-derived PAMPs to the dectin receptor (a natural killer (NK)-cell-receptor-like C-type lectin), it becomes tyrosine phosphorylated (presumably by Src kinases) and recruits the **s**pleen **t**yrosine **k**inase (Syk). Subsequent formation of the CARD9–BCL10–MALT1 complex induces NF-κB signaling leading to upregulation of pro–IL-1β. Recruitment of ASC and CASP8 to the CARD9–BCL10–MALT1 complex induces activation of CASP8, which then processes pro–IL-1β to its mature form. **B.** Under normal conditions, CD95 signaling leads to formation of the DISC within which CASP8 becomes activated to induce apoptosis. In the presence of LPS, CD95 signaling induces activation of CASP8 and CASP8–dependent processing and activation of pro–IL-1β. Under normal conditions chemotherapeutic drugs induce intrinsic apoptosis. In the presence of LPS, chemotherapeutic agents, doxorubicin and oxaliplatin as well as endoplasmic reticulum (ER) stress inducers, tunicamycin and thapsigargin promote CASP8 activation. Active CASP8 then cleaves pro–IL-1β into its mature form. **C.** CASP8 activity is necessary for both canonical and non-canonical NLRP3 inflammasome activation. Stimulation of TLR4 signaling leads to NF-κB activation and up-regulation of pro–IL-1β and NLRP3, an event that partially relies on CASP8 activity. Stimulation of canonical or non-canonical NLRP3 signaling requires CASP8 for the formation of NLRP3 inflammasome. CASP8 is required for activation of procaspases -1 and -11. **D.** CASP8 negatively regulates LPS-induced activation of the NLRP3 inflammasome. Inactivation of CASP8 renders dendritic cells hypersensitive to LPS that activates NLRP3 inflammasome through a RIP1-, RIP3- MLKL-dependent mechanism. (Reproduced with permission from [Mandal, R., Barrón, J. C., Kostova, I., Becker, S., and Strebhardt, K. (2020) Caspase-8: The double-edged sword. *Biochim. Biophys. acta. Rev. cancer*. 1873, 188357] CopyrightElsevier).

1.2.5 Caspase-8 and Cancer

Resistance to apoptosis is one of the hallmarks of cancer and it has been associated with both tumor development/progression and resistance to cancer therapy (315). Consistently, targeting of the apoptosis pathway has been proposed as a viable strategy to improve anti-cancer therapy response (316). CASP8, a canonical cysteine-aspartate specific protease, plays key roles during the initiation and execution of apoptosis (see earlier). Given its importance in death receptor-mediated apoptosis, CASP8 has been historically considered as a tumor suppressor (316). This notion is supported by the observation that CASP8 expression or its protease activity both of which are required for the execution of the apoptosis signaling pathway, are often impaired in cancer (65, 110). Loss of CASP8 expression is commonly observed in malignant neuroendocrine tumors. Deletion of *CASP8* has been linked to tumor aggressiveness and resistance to TRAIL-induced apoptosis in malignant neuroblastoma (66). CpG islands (the " 5'—C—phosphate—G—3' " sequence of nucleotides on one DNA strand) are short interspaced DNA sequences that are rich in 'GC' content. Most CpG islands serve as sites of transcription initiation. Methylation of cytosines in CpG dinucleotides by DNA methytransferases is an important mechanism by which tumor suppressor genes (TSG) are silenced (317). CASP8 loss due to CpG island methylation of the *CASP8* promoter has been shown to render primitive neuroectodermal brain tumors unresponsive to TRAIL-induced apoptosis (70). CpG island promoter hypermethylation underlies silencing of *CASP8* in medullablastoma, glioblastoma multiforme (GBM) and small cell lung carcinoma (SCLC) as well. Notably, these neuroendocrine tumors most of which develop during childhood, arise from cells that do not form extensive integrin-mediated

cell-cell, cell-ECM (**e**xtra**c**ellular **m**atrix) contacts, and thus are lacking access to potent

survival signals (65). Hence, it might be possible to speculate that expression of CASP8

is not well-tolerated in these tumors due to lack of a supportive microenvironment. Loss

of CASP8 expression is strongly associated with poor survival outcomes in

neuroendocrine tumors in contrast to epithelial-derived cancers in which an overt loss of

CASP8 function is rather rare. In these tumors, downregulation of CASP8 function that

occurs during disease progression is mainly caused by somatic mutations (**Figure-12**)

(65). These CASP8 mutations (missense and frameshift mutations as well as deletions

or allelic losses), most of which are loss-of-function in nature have been identified in

colorectal, gastric and hepatocellular carcinomas as well as esophagus cancer (72, 73,

318–320). During progression, carcinomas upregulate many different protumorigenic

pathways including overexpression of endogenous caspase inhibitors (i.e. inhibitor of

apoptosis proteins [IAPs]), activation of growth factor receptors (i.e. EGFR signaling)

and/or non-receptor tyrosine kinase signaling (Src kinases) which can contribute to

inhibition of CASP8 activity (65, 321–323). Thus, it is probable that the presence of

multiple mechanisms compromising CASP8 function allows maintenance of CASP8

expression in epithelial tumors. It is also reasonable to speculate that expression of

CASP8 could be selected for in a tumor microenvironment under conditions whereby its

pro-apoptotic activity is restricted, a phenomenon that can explain the upregulation of

CASP8 observed in cervical and renal cancers during early disease stages (324, 325).

Interestingly, expression of CASP8 is diminished with disease progression in these

cancers. A possible explanation for the observed change in CASP8 expression is that

cancers benefit from non-apoptotic activities of CASP8 (e.g. ability of CASP8 to

promote cell motility) during carcinogenesis, however, once established in a specialized

oncogenic niche where they have become less-dependent on these functions, CASP8

is downregulated allowing metastasis to occur (110).
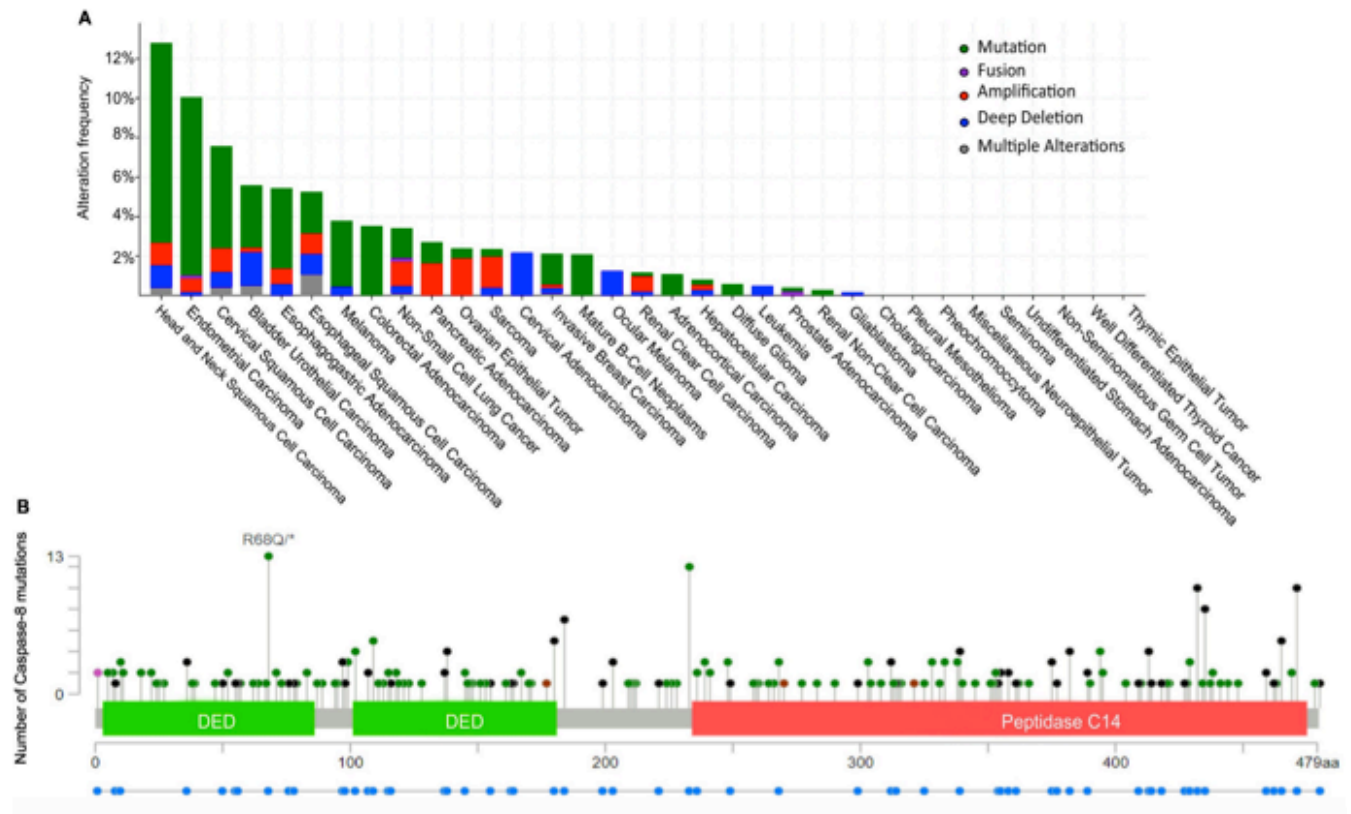
Figure-12: Caspase-8 mutations in various cancers

A. Types of CASP8 alterations in different cancers **B.** Distribution of CASP8 mutations
(Reproduced with permission from [Mandal, R., Barrón, J. C., Kostova, I., Becker, S.,
and Strebhardt, K. (2020) Caspase-8: The double-edged sword. Biochim. Biophys. acta.
Rev. cancer. 1873, 188357] CopyrightElsevier).

In a report by Helfer *et. al*., mouse embryonic fibroblasts (MEFs) derived from *Casp8*^{-/-}

mice showed impaired cell motility, which was restored upon inducible expression of

Casp8. Inhibition of Casp3, the downstream effector of Casp8 did not impact cell motility in WT MEFs, suggesting that the observed effect was independent of the pro-apoptotic function of Casp8. Rescue of cell motility upon expression of Casp8 in $Casp8^{-/-}$ MEFs was associated with activation of Rac (a member of the 'Rho family GTPases' that becomes active when bound to GTP, promoting cell movement through induction of structural changes in cytoskeleton), formation of lamellipodia and cell adhesion, cellular processes that are downstream of calpain activation (326). In another study, restoration of CASP8 in a CASP8-deficient neuroblastoma cell line promoted cell migration following activation of integrin signaling *in vitro*. Enhancement of cell migration by CASP8 did not rely on its catalytic activity; rather it was associated with recruitment of CASP8 to a multiprotein complex including focal adhesion kinase (FAK) and Calpain-2 (CPN2), leading to calpain activation and targeting of CASP8 to the periphery in a FAK-dependent fashion to potentiate cell migration (327). In a follow-up study by the same group, CASP8 was found to co-localize with Src at the leading edge of migrating cells upon stimulation of integrin signaling. Localization of CASP8 to the lamella of migrating cells was dependent on Src-mediated phosphorylation of its Y380, since a mutated CASP8-Y380F lacking the tyrosine residue targeted by Src kinase did not localize to the periphery or promote cell migration (328). The role CASP8 plays in promoting cell motility could contribute to tumor progression by enhancing migratory and/or invasive properties of cancer cells, providing a possible explanation for the upregulation of CASP8 in some cancer types. Therefore, CASP8 may act as a tumor suppressor or oncogene depending upon the specific cellular context.

1.2.6 Caspase-8 and HNSCC

Integrative genomic analysis of HNSCC has uncovered that CASP8 is one of the most frequently mutated genes in HNSCC (**Figure-12A**). Somatic mutations of CASP8 have been detected in ~10% of HNSCC cases, with CASP8 mutations mostly occurring in oral cavity tumors (60, 74). 18% of HPV-negative oral squamous cell carcinomas (OSCC) showed somatic mutations of CASP8. The spectrum of CASP8 mutations in patient tumors (**Figure-12B**) and human-derived HNSCC cell lines (nonsense, splice-site, and frame-shift mutations) indicates that they are likely to be inactivating mutations that compromise protein function of CASP8, possibly sensitizing cancer cells to necroptotic stimuli (74, 139).

SMAC (**S**econd-**M**itochondria-derived **A**ctivator of **C**aspase) mimetics are small-molecule inhibitors that promote caspase activation and apoptosis through neutralization of IAPs (**i**nhibitor of **a**poptosis **p**roteins) (329). Preclinical studies have highlighted the therapeutic potential of SMAC mimetics through induction of cancer cell death directly (218) or via synergistic interaction with a variety of cytotoxic therapy approaches, including chemotherapy (330, 331) radiotherapy (332, 333) or immunotherapy (334). The SMAC mimetic Birinapant was found to enhance cytotoxicity induced by death ligands in a panel of HNSCC cell lines (335). Birinapant also synergizes with radiation to prevent tumor growth in various xenograft models of HNSCC bearing genomic amplifications of FADD and cIAP1 *in vivo* (335). Other SMAC mimetic compounds such as LCL161 and ASTX660 have also been shown to confer *in*

vivo radiosensitivity to HNSCC xenografts (336, 337). However, how inactivating mutations of CASP8 impacts necroptosis in HNSCC and whether modulation of the necroptosis pathway with these small molecule agents might have potential clinical utility in the context of CASP8 loss have largely been unexplored. Thus, the main objective of this thesis is to offer an insight into the loss-of-function mutations of CASP8 and provide data to help understand whether necroptosis pathway could be used as a therapeutic target for enhancing anti-tumor response to conventional and/or targeted therapy approaches in HNSCC.

CHAPTER-II : MATERIALS AND METHODS

CHAPTER-2: Materials and Methods

HNSCC Cell Lines

Human derived-HNSCC cell lines were cultured in DMEM complete media supplemented with 10% FBS, Penicillin/Streptomycin, glutamic acid, non-essential amino acids, vitamins, pyruvate and Myco-Zap (Lonza), unless instructed otherwise. Cells were incubated in a 37^0C incubator, in 5% CO_2 atmosphere and maintained as previously described (338). Features of the cell lines used in experiments are outlined in **Table-2**. Murine oral cancer (MOC) 1 cell line was provided by Dr. R. Uppaluri (Washington University School of Medicine) (339). All cell lines were authenticated by short tandem repeat (STR) profiling and cultured for no longer than 15 passages before use in experiments.

Cell line	Primary site	Age	Sex	TNM stage	Culture media	Primary Source
Detroit-562	Pleural effusion (P)	–	F	–	DMEM, 10% FBS	ATCC
FADU	HP	56	M	–	DMEM, 10% FBS	ATCC
HN30	P	–	–	–	DMEM, 10% FBS	Dr. John Ensley, Wayne State University
HN31	LN (HN30)	–	–	–	DMEM, 10% FBS	Dr. John Ensley, Wayne State University
JHU–011	REC (L)	–	M	T3N0	RPMI 1640, 10% FBS	Dr. David Sidransky, Johns Hopkins University
TR146	REC (OC)	67	F	–	DMEM, 10% FBS	Dr. Thomas Rupniak, Imperial Cancer Research Fund, London
UMSCC-1	REC (OC)	73	M	T2N0M0	DMEM, 10% FBS	Dr. Thomas E. Carey, University of Michigan
UMSCC-17A	L	47	F	T1N0M0	DMEM, 10% FBS	Dr. Thomas E. Carey, University of Michigan
UMSCC-25	LN (L)	50	M	T3N0M0	DMEM, 10% FBS	Dr. Thomas E. Carey, University of Michigan

Table-2: HNSCC cell lines. L, larynx; **LN,** lymph node; **OC,** oral cavity; **P,** pharynx; **REC,** recurrence; **ATCC,** American Type Culture Collection

Genomic Analysis

The Cancer Genome Atlas (TCGA) data were obtained from the TCGA PanCancerAtlas Project (340) and analyzed for CASP8 mutations and RIP3 expression for HNSCC. Cell line RIP3 gene expression data is available through the Gene Expression Omnibus (GEO) (accession GSE122512) (341).

Engineering of stable cell lines

Cell lines were transduced with lentiviral shRNA constructs against CASP8 (shCASP8) or control scrambled shRNA, containing GFP and puromycin resistance gene (GE Dharmacon). shCASP8 and control cells were GFP-sorted and subjected to puromycin selection (1μg/ml). After antibiotic treatment, control and shCASP8 cells were assessed for protein expression of CASP8 by Western Blotting (WB). CRISPR/Cas9 sgRNA constructs were designed to knock out CASP8 in MOC1 cells (342). Knockout of *CASP8* was validated via WB screening and sequencing.

RIP3 was knocked down using lentiviral shRNA constructs (GE Dharmacon) in select MOC1 clonal cell lines carrying WT RIP3, as described above for *CASP8*. Select MOC1 clones that show lack of protein expression of RIP3 were transduced with inducible lentiviral vectors encoding WT (Plasmid #73701) or kinase-dead mutant (D143N) RIP3 (Plasmid #73703) purchased from Addgene (These plasmids were gifted by Dr. Francis Chen). Control pTRIPZ empty vector was obtained from MD Anderson Functional Genomics Core Facility. MOC1 cells transduced with control or RIP3 expression constructs were subjected to puromycin selection (1μg/ml). Expression of WT or D143N RIP3 was induced by Doxycycline (1μg/ml) for 72 hours and verified by WB.

For the *in vivo* experiments, inducible lentiviral shRNA constructs were designed against Luciferase (shLUC) or CASP8 *(*shCASP8*)* in collaboration with the MD Anderson Institute for Applied Cancer Science as described previously (343). MOC1 cells transduced with shLUC or shCASP8 vectors were subjected to puromycin selection (1μg/ml), treated with Doxycycline (50ng/ml) for 72 hours and verified by WB. shRNA/sgRNA oligo sequences are outlined in **Table-3.**

mouse *Casp8* CRISPR-Cas9 sgRNA sequences	DNA Sequence (5' to 3')
Casp8 for-1	CACCGGTGTCGTCTATGGAACGGAT
Casp8 rev-1	AAACATCCGTTCCATAGACGACACC
Casp8 for-2	CACCGCAAGAACTATATTCCGGATG
Casp8 rev-2	AAACCATCCGGAATATAGTTCTTGC
Casp8 for-3	CACCGTAGCTTCTGGGCATCCTCGA
Casp8 rev-3	AAACTCGAGGATGCCCAGAAGCTAC
human *CASP8* shRNA oligo sequences	
CASP8 shRNA#1 (shCASP8#1)	TAATTCGGAAGAGCAGCTC
CASP8 shRNA#1 (shCASP8#2)	TTCCTTCTCCCAGGATGAC
mouse *Casp8* shRNA oligo sequences	
Casp8 shRNA#1 (shCASP8#1)	AAACTTTGTCTGAAGTCCG
Casp8 shRNA#4 (shCASP8#4)	TTTCATTTGCAGTGCAGTC
mouse *Casp8* inducible shRNA oligo sequences	
Casp8 inducible shRNA#10 (shCASP8)	TTTCATTTGCAGTGCAGTC
Luciferase inducible shRNA oligo sequences	
luciferase inducible shRNA (shLUC)	CGCTGAGTACTTCGAAATGTC
mouse *Ripk3* shRNA oligo sequences	
Ripk3 shRNA (shRIP3)	TACCTCGGAGACAGCAGCA

Table-3: List of shRNA and CRIPSR-Cas9 sgRNA oligo sequences used in the study

Cell proliferation and viability assays

To evaluate cell proliferation, HNSCC cells were plated in 96-well plates at two densities: 50cells/well and 100cells/well. Cell density was measured using CellTiter-Glo (Promega). Luminescence reads were taken at the indicated time points and normalized to Day 0 reads to calculate cell doublings.

To assess cell viability following drug treatments, 3-10 X 10^3 cells were plated in 96-well plates and allowed to attach overnight. Cells were then treated with 0.01% DMSO (mock treatment) or Birinapant, Z-VAD-FMK (or emricasan), TNFα (or TRAIL) and Necrostatin-1s either alone or in combinations at the indicated doses for 24 hours, after which cell viability was measured by CellTiter-Glo. Average luminescence values taken for each treatment condition were normalized to that of mock-treated cells from the same experiment to calculate % cell density. All treatments were carried out in triplicates or greater. The list of drugs/reagents used in the study can be found in **Table-4**.

No.	Reagent/drug name	Catalog number	Company
1	Birinapant	S7015	Selleckchem
2	zVAD-FMK	FMK001	R&D Systems
3	human recombinant TNFα	210-TA	R&D Systems
4	human recombinant TRAIL	375-TEC	R&D Systems
5	murine recombinant TNFα	315-01A	Peprotech
6	murine recombinant TRAIL	315-19	Peprotech
7	Necrostatin-1s (7-Cl-O-Nec1)	10-4544	Focus Biomolecules
8	Puromycin dihydrochloride from Streptomyces alboniger	P8833	Sigma-Aldrich
9	Doxycycline	631311	Takara Bio USA

Table-4: List of reagents/drugs used in the study.

Clonogenic survival assays

HNSCC cells were seeded in 6-well plates at predetermined densities and allowed to adhere overnight. The next day, cells were treated with 0.01% DMSO (mock treatment) or Birinapant, Z-VAD-FMK (or emricasan) and Necrostatin-1s either alone or in combinations at the indicated doses. For radiosensitivity assays, treatments described above were followed by exposure to either 2, 4 or 6 Gray (Gy) radiation. 24 hour after treatments, media containing the drug dilutions were aspirated and replaced with fresh media. Colonies were allowed to form for 5-12 days, after which they were fixed in methanol and stained with crystal violet (2%). Wells containing surviving colonies were scanned and colonies with more than 50 cells were counted with the guidance of ImageJ software (NIH, Bethesda, MD). The number of surviving colonies per well was calculated for each treatment condition and normalized to that of mock-treated cells from the same experiment to calculate % colony counts. For the radiosensitivity assays, average surviving colony counts were normalized to those of mock-treated cells of each radiation dose from the same experiment to calculate surviving fractions. *Log10* of surviving fractions were plotted. All treatments were carried out in triplicates.

Annexin-V assays

Annexin-V staining was performed in accordance with the manufacturer's guidelines (BD Biosciences). Briefly, 2.5-7.5 X 10^5 cells were seeded in 6cm dishes and allowed to adhere overnight. The next day, cells were treated as indicated. All treatments were carried out in triplicates. 24 hour after treatments, media was collected from the dishes

and set aside to keep any floating cells. Adherent cells were harvested with trypsin and added to the previously collected media. The cells were then centrifuged, washed once in cold Phosphate Buffered Saline (PBS) and stained with Annexin-V APC (BD Biosciences) and 1μmol/L SytoxBlue (ThermoFisher) in Annexin-V binding buffer. Samples were mixed gently and incubated at room temperature for 30min after which they were subjected to flow cytometry analysis. Flow data were analyzed using FlowJo software.

Western blotting

2.5-7.5 X 10^5 HNSCC cells were seeded in 6cm dishes and allowed to adhere overnight. The next day, cells were treated as indicated. For radiosensitization studies, cells were exposed to 6Gy radiation. 24 hour after treatments, cells were washed once with cold PBS. Standard <u>r</u>adio<u>i</u>mmuno<u>p</u>recipitation <u>a</u>ssay (RIPA) buffer (containing 20 mM Tris [pH 7.5], 150 mM NaCl, 1 mM EDTA, 2.5 mM sodium pyrophosphate, 1 mM, 1 mM sodium orthovanadate, 1 mM phenylmethylsulfonyl fluoride [PMSF] and a cocktail of protease inhibitors [Roche]) was then added to each dish/plate followed by incubation of the dishes/plates on ice briefly. Cell lysates were then obtained with use of a plastic cell scraper and centrifuged at 14,000 rpm at 4°C for 25 minutes. The supernatant was removed, and total protein concentration was measured using Bio-Rad Protein Assay (Bio-Rad). Protein samples were prepared using 5% β-<u>m</u>ercapto<u>e</u>thanol (β-ME). Equal amounts of protein samples were then loaded onto 4-20% sodium dodecyl sulfate (SDS) gradient gels (Mini-PROTEAN TGX Stain-Free Precast Gels, BioRad) and subjected to polyacrylamide gel electrophoresis and transferred to <u>p</u>oly<u>v</u>inylidene <u>di</u>fluoride (PVDF) membranes using Trans-Blot Turbo Transfer System (ThermoFisher)

following manufacturer's instructions. After transfer, the membrane was blocked using 5% milk solution prepared in TBS-T buffer (containing 50mM Tris, 150mM sodium chloride and 0.1% Tween-20) for 1 hour on an agitator. Following the blocking step, the membrane was incubated with the primary antibody (5% milk in TBS-T) at a previously determined optimal dilution overnight at 4^0C on an agitator. After incubation, the membrane was washed for 10 min with TBS-T buffer about 3 times and incubated with an appropriate horseradish peroxidase (HRP)-conjugated secondary antibody (5% milk in TBS-T) at a previously determined optimal dilution for 1h at room temperature on an agitator. Protein signals were developed using Pierce™ ECL Western Blotting Substrate (Thermo Scientific) on an X-ray film. The list of WB antibodies used in the study can be found in **Table-5**.

No.	Antibody name	Catalog number	Source	Company	Dilution
1	human CASP8	551242	mouse	BD Biosciences	1:1000
2	human/mouse CASP8	AF1650	rabbit	R&D Systems	1:400
3	RIP1	610458	mouse	BD Biosciences	1:1000
4	human RIP3 (E1Z1D)	13526	rabbit	Cell Signaling	1:1000
5	mouse RIP3 (D4G2A)	95702	rabbit	Cell Signaling	1:1000
6	MLKL (D216N)	14993	rabbit	Cell Signaling	1:1000
7	MLKL (mouse specific)	28640	rabbit	Cell Signaling	1:1000
8	phospho-RIP1 (S166)	31122	rabbit	Cell Signaling	1:1000
9	phospho-MLKL (S358) (D6H3V)	91689	rabbit	Cell Signaling	1:1000
10	PARP	9542	rabbit	Cell Signaling	1:1000
11	Anti-HA	H3663	mouse	Sigma-Aldrich	1:2000
12	β-actin	A1978	mouse	Sigma-Aldrich	1:10000
13	Anti-rabbit IgG	1706515	goat	BioRad	1:5000
14	Anti-mouse IgG	1706516	goat	BioRad	1:5000

Table-5: List of antibodies used for western blotting in the study.

In vivo xenograft model

All *in vivo* experiments were carried out with approval of the Institutional Animal Care and Use Committee (IACUC) at MD Anderson. 2×10^6 MOC1 cells transduced with an inducible shRNA against *CASP8* were injected into the right flank of WT female C57BL/6 mice obtained from Envigo/Harlan Labs in the presence of Matrigel (Corning). 3 days after inoculation, mice were randomized and placed on control (Global 18% Protein Rodent Diet) or DOX diet (doxycycline hyclate added at 625 mg/kg) obtained from Envigo to induce knockdown of *CASP8 in vivo.* Control and shCASP8 mice were randomized into 4 treatment groups (***n*=7-10** mice/each) 27 days after injection of cells, when the average tumor volume reached ~150 mm^3. Treatments included Birinapant (15mg/kg Birinapant, every 3 days for 4 weeks, IP), radiation (5 X 2Gy, Monday to Friday for 1 week) or the combination (A detailed *in vivo* treatment schema is available in **Figure-13**). Tumor measurements were taken three times a week, and mice were euthanized when tumor burden has reached >1.5cm in any dimension. Tumor samples were collected from a subset of control and shCASP8 mice that were not recruited in the drug treatment study. These tumor samples were minced and cultured in medium for 48 hours. Cells shed from the tumors that have attached to culture dishes were collected, lysed and subjected to WB analysis for *CASP8*.
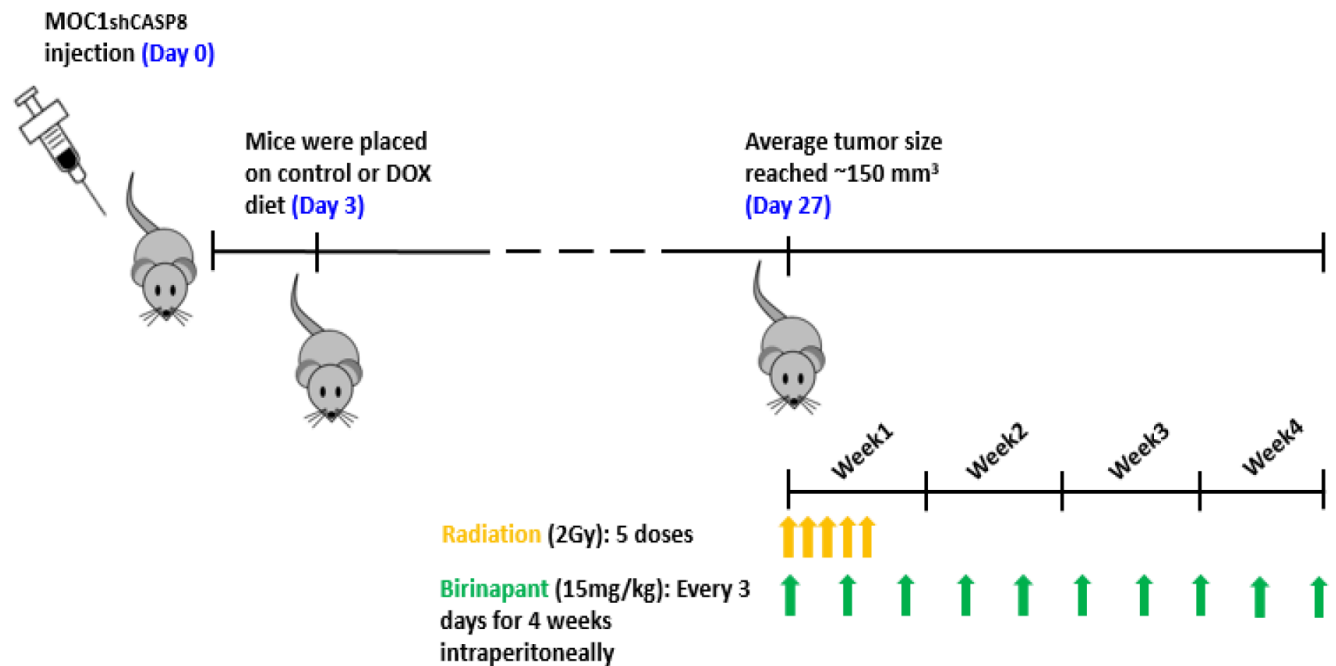
Figure-13: Treatment schema for *in vivo* experiments

Statistical Analysis

Kaplan-Meier method was used to calculate overall survival for the patient population. *P* values used to compare gene expression levels for necroptosis markers between different patient cohorts were computed using the Mann-Whitney U test. Student *t* tests were conducted to analyze *in vitro* data. For the *in vivo* studies, a two-way ANOVA test was used to make tumor volume comparisons between animal cohorts. Differences in survival rates between groups were compared using the log-rank (Mantel–Cox) test. All data were presented as mean±SD unless otherwise noted. *P* values < 0.05 were considered statistically significant.

CHAPTER-III : CASPASE-8 MUTATIONS ARE ASSOCITED WITH POOR PROGNOSIS IN HNSCC.

CHAPTER-3: Caspase-8 mutations are associated with poor prognosis in HNSCC

3.1 Caspase-8 mutations are associated with poor overall survival in HNSCC

Integrative genomic analysis of HNSCC has uncovered that Caspase-8 (*CASP8*) is one of the most frequently mutated genes in HNSCC, with somatic mutations detected in ~10% of cases (60, 74). Analysis of **t**he **C**ancer **G**enome **A**tlas (TCGA) dataset (340) revealed that CASP8 mutations are associated poor overall survival in HNSCC (**Figure-14**).
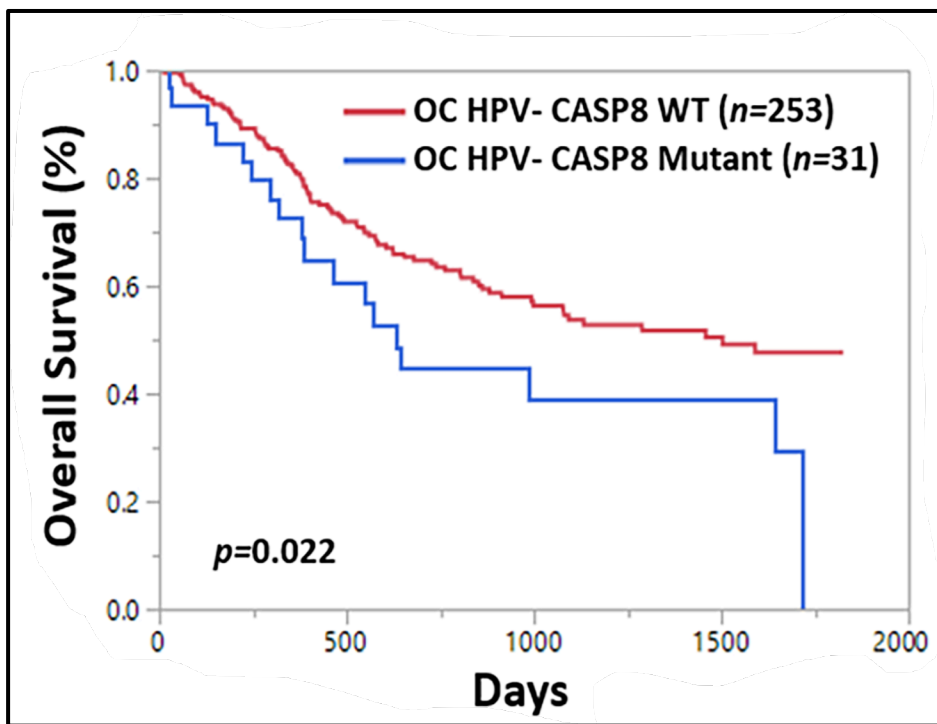
Figure-14: Caspase-8 mutations are associated with poor survival outcomes in HNSCC.

Kaplan-Meier survival plots showing overall survival for 284 HPV-negative oral cavity (OC) HNSCCs in TCGA by CASP8 mutation status. *P* value was computed using log-rank test.

3.2 Caspase-8 mutations are associated with radioresistance in HNSCC

Emerging data have linked CASP8 mutations to a gain-of-function (GOF) phenotype in which mutant CASP8 robustly activates NF-κB signaling independent of the catalytic activity of CASP8 (344). WT CASP8 is also able to activate NF-κB signaling, although at a reduced level (344). It is known that NF-κB activation is directly associated with radioresistance. Chemical inhibitors of NF-κB, as well as overexpression of IκB can radiosensitize tumor cells (345–347) and conversely, overexpression of NF-κB leads to radioresistance (348). Clinically, NFκB activity is associated with poor outcome following definitive radiotherapy in HNSCC (349, 350). Therefore, we next set out to determine whether poor overall survival outcomes might be linked to radioresistance in CASP8 mutant HNSCCs. Analysis of the TCGA HNSCC dataset showed that CASP8 mutant patients treated with ionizing radiation (XRT) show significantly higher locoreginal recurrence (LRR) rates and worse prognosis when compared to WT patients (**Figure-15**). To corroborate our observations in a pre-clinical setting, we selected a panel of 46 HNSCC cell lines with known CASP8 status (351). Next, we examined the sensitivity of these cell lines to increasing doses of radiation using a standard clonogenic survival assay (352) and determined the level of radiosensitivity using survival fraction at the 2Gy dose (SF2), since 2Gy is the dose typically used in clinical practice to treat HNSCC patients.
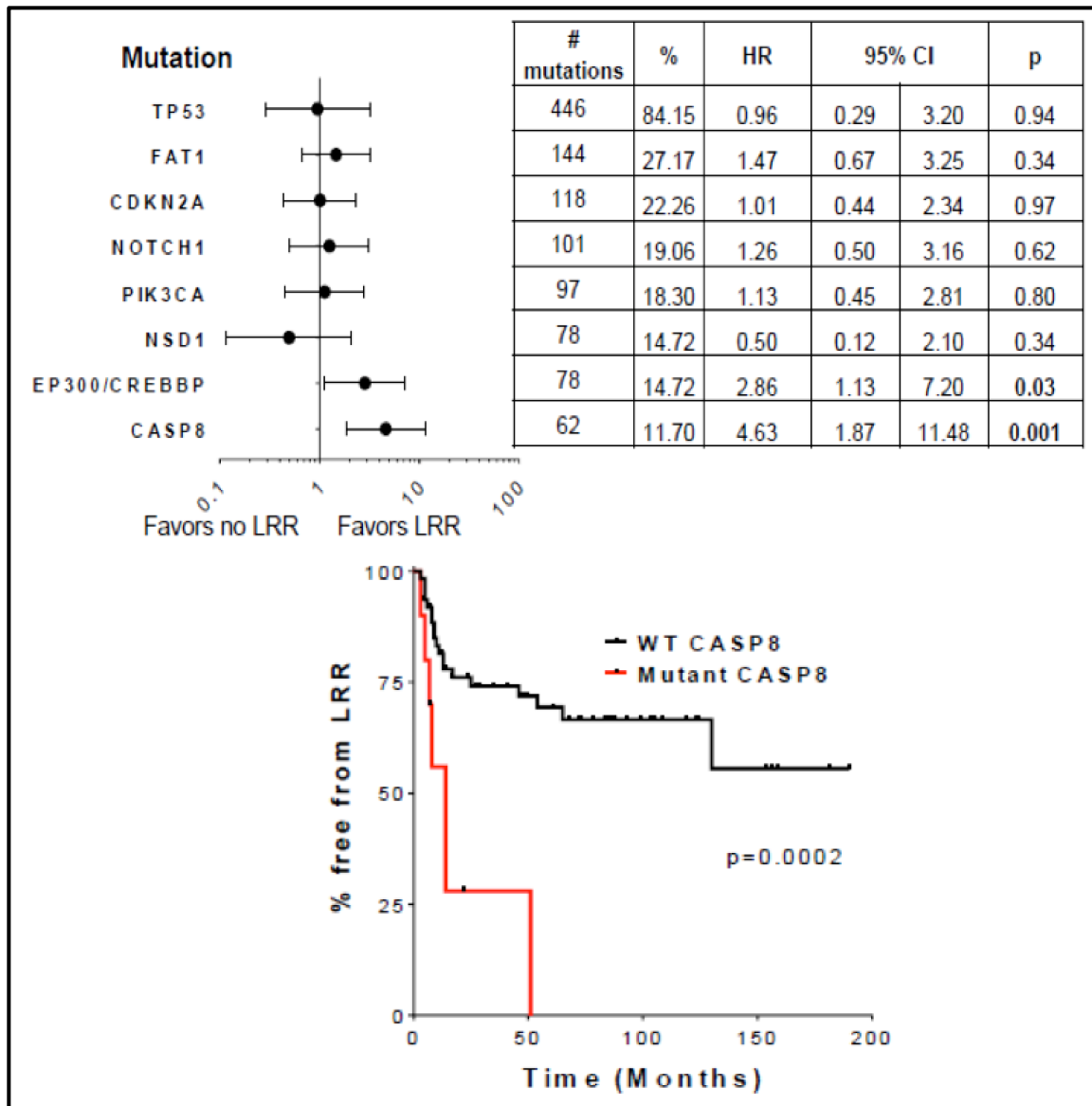
Figure-15: Caspase-8 mutations are associated with enhanced locoregional recurrence (LRR; see *Top Panel*) and worse prognosis (*Bottom Panel*) following ionizing radiation treatment in HNSCC

(Published with permission from **Dr. Heath Devin Skinner; University of Pennsylvania, Hillman Cancer Center**)

Interestingly, we found that CASP8 mutant HSNCC cell lines were significantly more radioresistant than those with WT CASP8 (**Figure-16**).
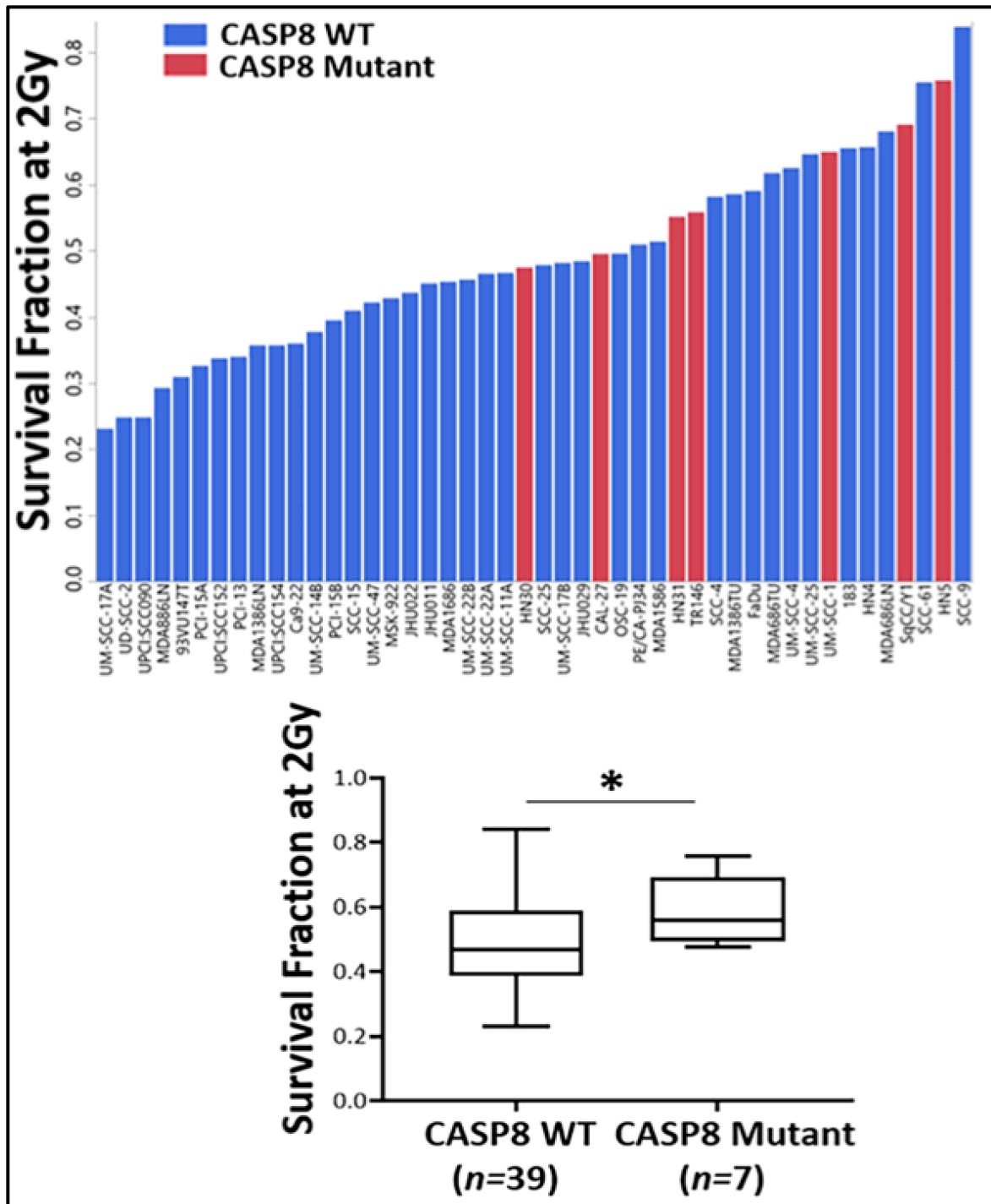
Figure-16: Caspase-8 mutations are associated with radioresistance in HNSCC. A panel of 46 HNSCC cell lines were sequenced for CASP8 and evaluated for sensitivity to radiation using clonogenic survival assays. Surviving fraction following 2Gy of XRT was used to determine radiosensitivity. (Cell lines with CASP8 mutation were marked in red). Cell lines were then grouped for CASP8 status and the average clonogenic survival data were shown for each group. Student t test was used for statistics. *p<0.05

3.3 Necroptosis emerges as a potential pathway to target in Caspase-8 mutant HNSCCs

Since CASP8 is known to regulate necroptosis and necroptosis can be induced by radiation in a variety of cancers (353, 354) we next aimed to understand if necroptosis can be exploited to radiosensitize CASP8 mutant HNSCCs to radiation. We first explored whether necroptosis-related genes are differentially expressed between CASP8 mutant and WT tumors in TCGA. Our analysis revealed that the top differentially expressed genes between the two groups (CASP8 mutant vs. WT) include at least 3 necroptosis-related genes: *MLKL* (**m**ixed **l**ineage **k**inase domain-**l**ike, p=3.39x10^{-10}), *FASLG* (Fas ligand, p=1.97x10^{-9}), and *TNFRSF10A* (**TNF** **R**eceptor **S**uper**f**amily Member **10A**, also known as TRAIL receptor-1, also called DR4, p=2.63x10^{-7}) showed higher expression in *CASP8* mutant HPV-negative oral cancers (OCs) than their WT counterparts, suggesting that necroptosis might be a potential pathway to target in *CASP8* mutant HNSCCs (**Figure-17).**
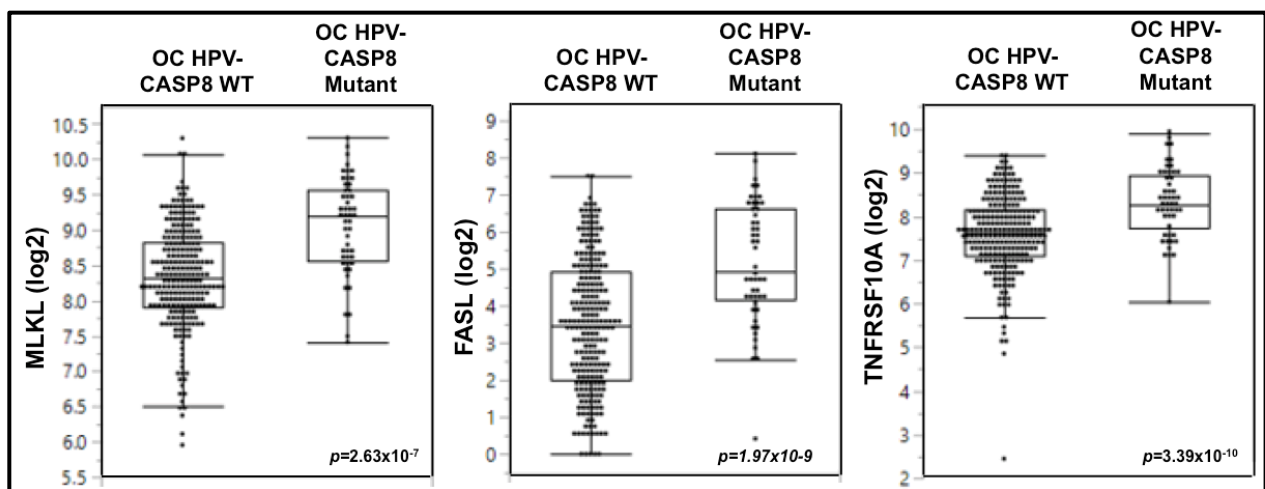
Figure-17: Caspase-8 mutations are associated with upregulation of necroptosis-related genes in HNSCC. Scatter plots show gene expression for MLKL, FASL and TNFRSF10A (TRAIL receptor) by *CASP8* status in TCGA HPV- oral cancer samples. Mean values are shown by the bar. P values were computed using Mann-Whitney test.

CHAPTER-IV : LOSS OF CASPASE-8

PREDISPOSES HNSCCs TO NECROPTOSIS

CHAPTER-4: Loss of Caspase-8 predisposes HNSCCs to necroptosis

4.1 Knockdown of Caspase-8 enhances reduction in cell viability in HNSCCs by Birinapant and zVAD-FMK through induction of necroptosis.

Inhibition or mutation of *CASP8* predisposes a wide variety of cancers to necroptosis (355). In an effort to understand how inactivating mutations of *CASP8* that result in loss of protein function impact necroptosis sensitivity in HNSCC, we stably knocked down CASP8 using a short hairpin RNA (shRNA) in two CASP8 WT HNSCC cell lines, namely the human-derived UMSCC-17A cells and mouse-derived syngeneic oral cancer MOC1 HNSCCs (339).
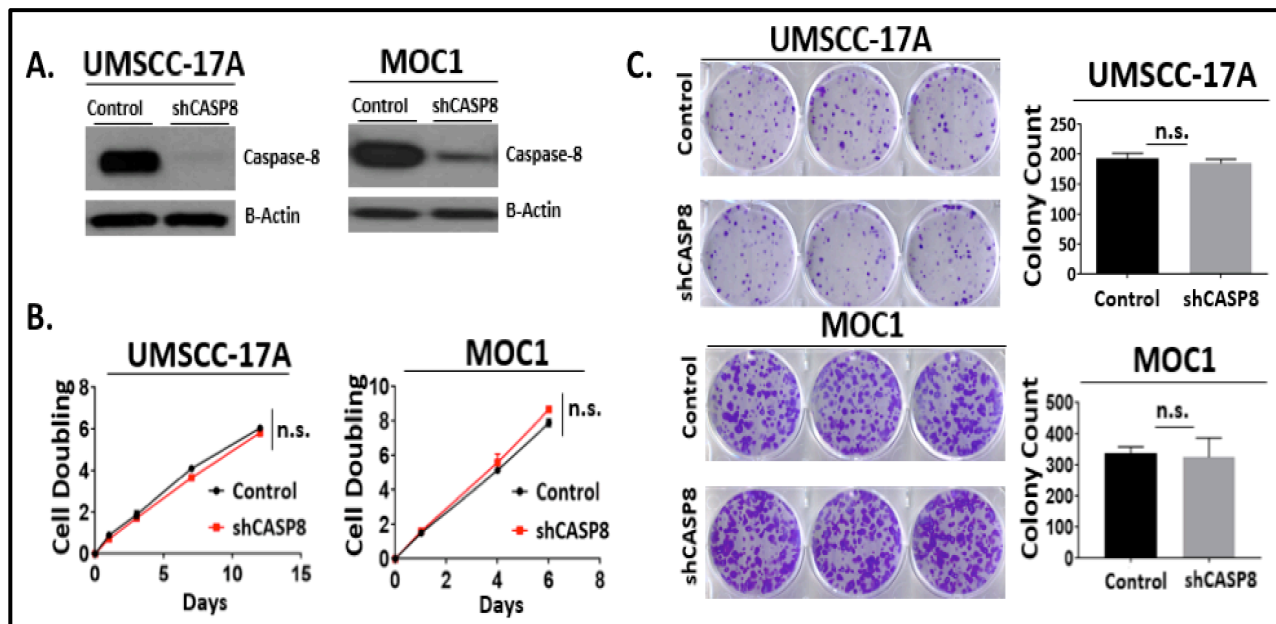
Figure-18: Effects of knockdown of Caspase-8 on *in vitro* cell proliferation and clonogenicity in HNSCCs. A. CASP8 was knocked down using shRNA in UMSCC-17A and MOC1 HNSCC cell lines. WB was performed for the validation of CASP8 knockdown. β-Actin was used as loading control. B. Control and shCASP8 UMSCC-17A and MOC1 cell lines were subjected to cell proliferation analysis by CellTiter-Glo. Luminescence reads were taken at the indicated time points and normalized to Day 0 reads to calculate cell doubling. Samples were run in triplicates. Student *t* test was used for statistics. C. Control and shCASP8 UMSCC-17A and MOC1 cells were subjected to clonogenic survival analysis. Colony counts were used to assess baseline clonogenicity. Samples were run in triplicates. Student *t* test was used for statistics.

Knockdown of *CASP8* alone did not significantly affect proliferative or colony-forming abilities of the cell lines (**Figure-18**). The UMSCC-17A and MOC1 CASP8 knockdown and scrambled shRNA control cells were treated with the SMAC mimetic Birinapant alone or in combination with the pan-caspase inhibitor zVAD-FMK at concentrations previously shown to be active (335). This combination is a standard method to experimentally induce necroptotic death (356). Cell survival was assessed by cell viability assay following treatments (**Figure-19**).
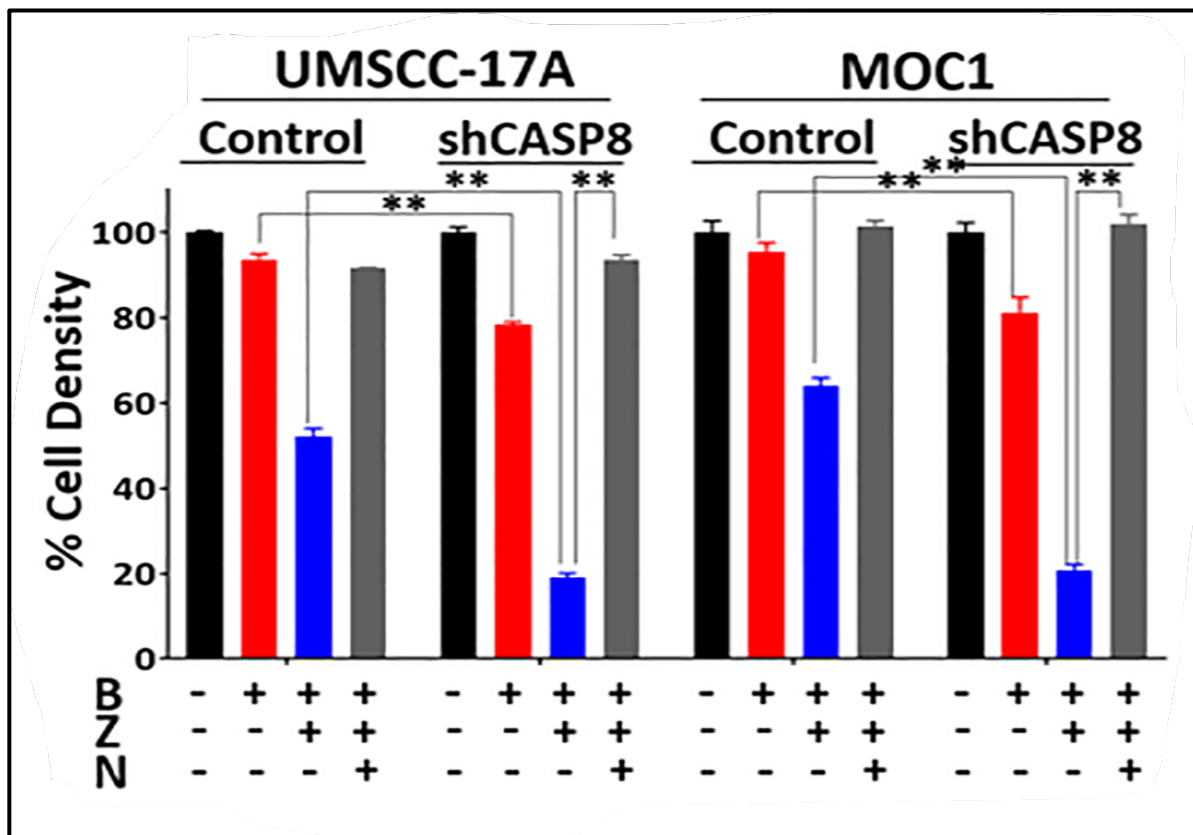
Figure-19: Knockdown of Caspase-8 enhances reduction in cell viability in HNSCCs by Birinapant and zVAD-FMK through induction of necroptosis. UMSCC-17A and MOC1 control and shCASP8 cells were treated with Birinapant (B [200nmol/L for UMSCC-17A; 1μmol/L for the MOC1]), zVAD-FMK (Z [5μmol/L for both the cell lines]), Necrostatin-1s (N [10μmol/L for both the cell lines]) or the combinations as indicated for 24 hours. Cell viability was assessed using CellTiter-Glo. Values normalized to nontreated cells from the same experiment to calculate % cell density. All treatments were carried out in triplicates. Student *t* test was used for statistics. *, P<0.05; **, P<0.001 for the indicated pairwise comparisons.

Knockdown of CASP8 significantly increased the sensitivity of UMSCC-17A and MOC1 cells to single agent Birinapant and Birinapant in combination with zVAD-FMK. To confirm that this was a necroptotic death the RIP1 inhibitor, Necrostatin-1s was used. Importantly, reduction in cell viability was abrogated by Necrostatin-1s, indicating that the observed mode of cell death was necroptosis not apoptosis.

4.2 Inhibition of clonogenic survival by Birinapant and zVAD-FMK is enhanced by knockdown of Caspase-8 in HNSCCs.

Next, we tested the effect of Birinapant and zVAD-FMK on clonogenic survival in control and CASP8 knockdown UMSCC-17A and MOC1 cells, using standard clonogenic assay (**Figure-20**). Consistent with our CellTiter Glo cell viability findings, Birinapant and zVAD-FMK combination reduced clonogenic survival in both the UMSCC-17A and MOC1 cells. Reduction in clonogenicty induced by the given combination treatment was enhanced under knockdown of CASP8 in both the cell lines. The fact that the inhibition in clonogenic survival was reversed upon addition of Necrostatin-1s to the Birinapant/zVAD-FMK combination confirmed that necroptosis was the underlying mode of cell death. Further indication that this was not an apoptotic death is the inclusion of zVAD-FMK treatment, a pan-caspase inhibitor that blocks apoptosis, which enhanced cell death rather than prevented it when combined with the SMAC mimetic Birinapant, consistent with necroptosis.
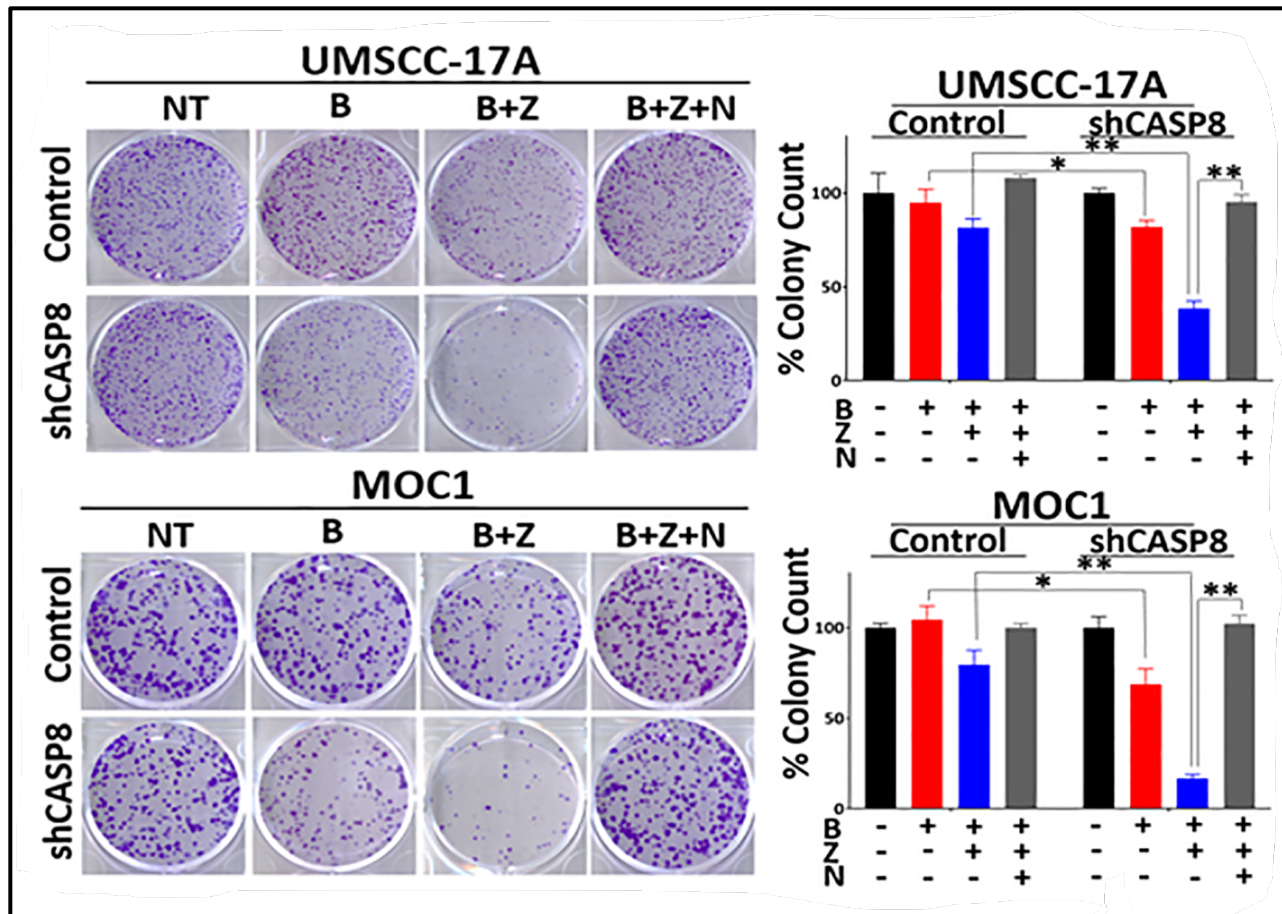
Figure-20: Inhibition of clonogenic survival by Birinapant and zVAD-FMK is enhanced by knockdown of Caspase-8 in HNSCCs. Representative images of clonogenic survival assays. 24 hour after treatments (Birinapant doses reduced to 50nmol/L and 250nmol/L for the UMSCC-17A and MOC1 cells respectively, for this assay. Other drugs used at the same concentrations as stated above), drug dilutions were washed out, colonies were allowed to form for 5-12 days, after which they were stained and counted. Surviving colonies were normalized to nontreated cells from the same experiment to calculate % colony count. All treatments were carried out in triplicates. *, $P<0.05$; **, $P<0.001$ for the indicated pairwise comparisons.

4.3. Knockdown of Caspase-8 sensitizes HNSCCs to necroptotic death by Birinapant and zVAD-FMK.

Enhanced necroptotic cell death observed under knockdown of CASP8 was further evaluated with Annexin-V staining (**Figure-21**). While Annexin-V staining is a method

conventionally used to detect apoptotic cells by its ability to bind to **p**hosphatidyl**s**erine (PS), (exposure of PS on the outer plasma membrane is a hallmark of apoptosis), recent evidence has suggested that necroptotic cells also expose PS on their plasma membrane and therefore are detectable by Annexin-V (357).
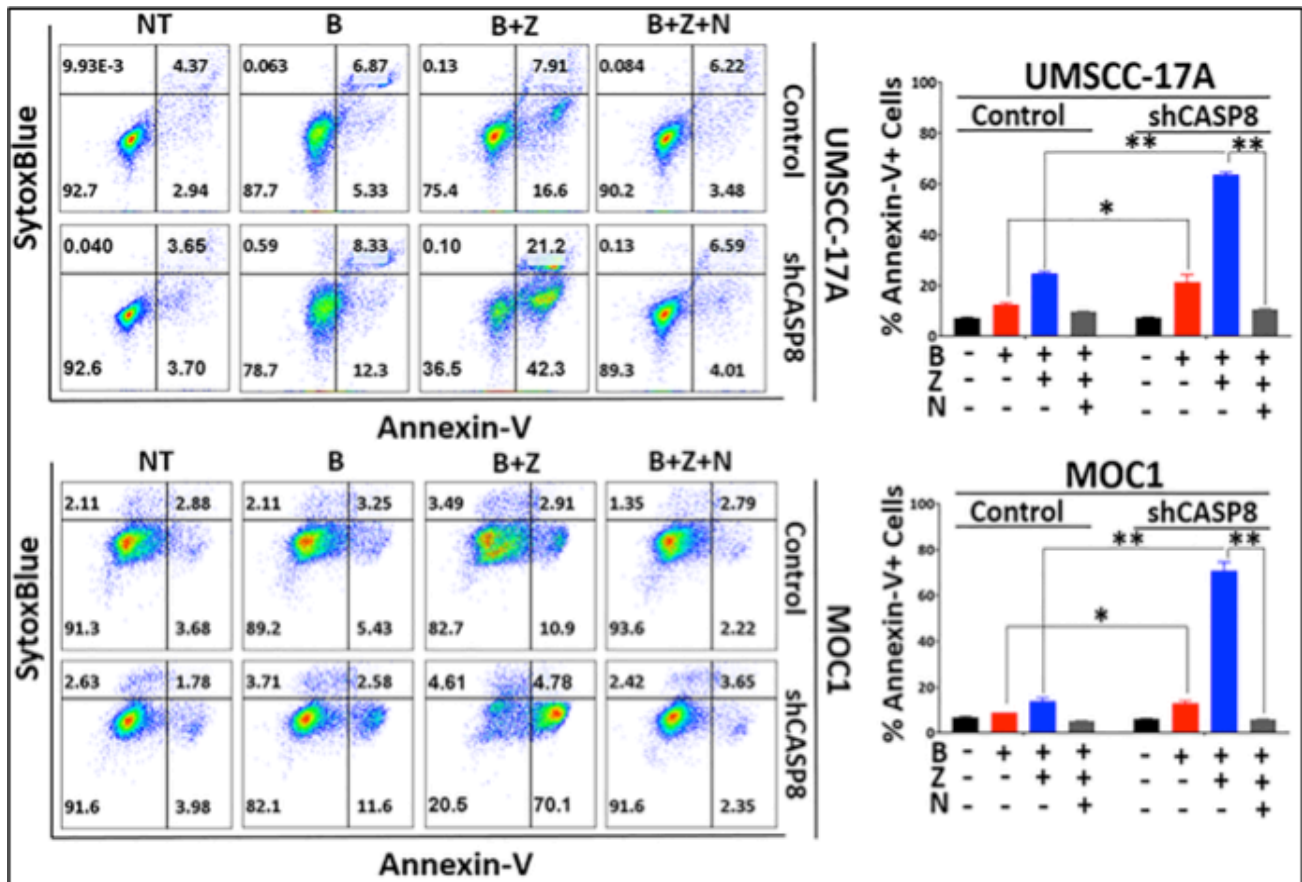
Figure-21: Knockdown of Caspase-8 sensitizes HNSCCs to necroptotic death by Birinapant and zVAD-FMK. UMSCC-17A and MOC1 control and shCASP8 cells were treated with Birinapant (B [200nmol/L for the UMSCC-17A cells; 1µmol/L for the MOC1 cells]), zVAD-FMK (Z [5µmol/L for both the cell lines]), Necrostatin-1s (N [10µmol/L for both the cell lines]) or the combinations as indicated for 24 hours. AnnexinV-APC/SytoxBlue staining was performed 24 hour after treatments. % Annexin-V positivity was used as a measure to assess cell death. All treatments were carried out in triplicates. *, $P<0.05$; **, $P<0.001$ for the indicated pairwise comparisons.

Knockdown of CASP8 led to a significant increase in Annexin-V positive staining following treatment of UMSCC-17A and MOC1 cells with Birinapant alone and

Birinapant in combination with zVAD-FMK. Necrostatin-1s reversed positive Annexin-V staining induced by Birinapant in combination with zVAD-FMK in both the cell lines, suggesting the predominant occurrence of RIP1-mediated necroptotic cell death.

4.4 Knockdown of Caspase-8 enhances the expression of necroptotic cell death markers induced by Birinapant and zVAD-FMK in HNSCCs.

Next, we evaluated the expression of key cell death pathway markers in UMSCC-17A and MOC1 cells following Birinapant alone and Birinapant/zVAD-FMK combination treatments in the absence or presence of Necrostatin-1s by WB (**Figure-22**).
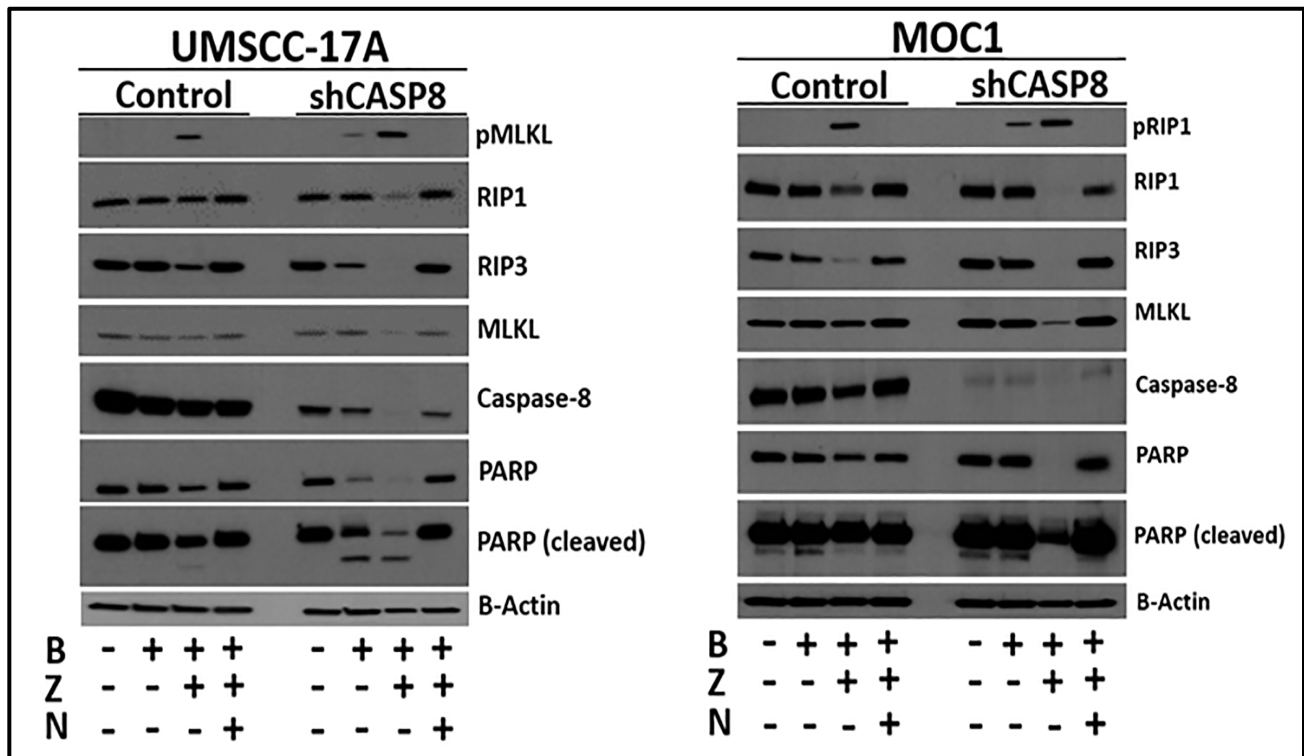
Figure-22: Knockdown of Caspase-8 enhances the expression of necroptotic cell death markers induced by Birinapant and zVAD-FMK in HNSCCs. UMSCC-17A and MOC1 control and shCASP8 cells were treated with Birinapant (B [200nmol/L for the UMSCC-17A cells; 1μmol/L for the MOC1 cells]), zVAD-FMK (Z [5μmol/L for both the cell lines]), Necrostatin-1s (N [10μmol/L for both the cell lines]) or the combinations as indicated for 24 hours. Whole cell lysates were collected 24 hour after treatments and subjected to Western blot analysis for the indicated key cell death markers. β-Actin was used as loading control.

Knockdown of CASP8 was associated with a significant increase in the protein levels of phospho-MLKL and phopsho-RIP1 following Birinapant alone and Birinapant/zVAD-FMK combination treatments in the UMSCC-17A and MOC1 cells, respectively. The increase in phosphorylation of the given markers was accompanied by a significant reduction in the total protein levels of RIP1, RIP3 and MLKL due to their proteosomal degradation at this 24 hour time point (260). Necrostatin-1s reversed the effects of Birinapant alone and the Birinapant/zVAD-FMK combination. Taken together, these data clearly demonstrate that loss of CASP8 sensitizes HNSCCs to Birinapant and Birinapant plus zVAD-FMK induced necroptotic cell death *in vitro*.

CHAPTER-V : LOSS OF CASPASE-8 RADIOSENSITIZES HNSCCs THROUGH INDUCTION OF NECROPTOSIS

CHAPTER-5: Loss of Caspase-8 radiosensitizes HNSCCs through induction of necroptosis

5.1 Knockdown of Caspase-8 enhances the radiosensitizing effects of Birinapant and zVAD-FMK through induction of necroptosis.

The combination of SMAC mimetic Birinapant and radiation has been shown to be effective in HNSCCs with alterations in cell death pathway (335). Given CASP8 mutant HNSCC cell lines are more radioresistant than their WT counterparts and CASP8 mutant HNSCCs show alterations in the necroptosis pathway, we sought to understand whether necroptosis could be exploited therapeutically to treat HNSCCs with compromised CASP8 status. To test this, CASP8 knockdown and scrambled shRNA control MOC1 cells were treated with increasing doses of radiation in combination with Birinapant and/or zVAD-FMK in the absence or presence of Necrostatin-1s, and assessed for clonogenic survival (**Figure-23**). Contrary to what we had hypothesized (that shRNA knockdown-mediated loss of CASP8 should render HNSCCs resistant to ionizing radiation) knockdown of CASP8 alone did not significantly impact radiosensitivity. Interestingly, single agent Birinapant and the Birinapant plus Z-VAD-FMK combination rendered control cells more radiosensitive. Additionally, the radiosensitizing effects of Birinapant and Birinapant plus Z-VAD-FMK were significantly enhanced under knockdown of CASP8. The addition of Necrostatin-1s returned all colony counts to comparable levels to those treated with radiation alone, indicating that necroptosis is the underlying mechanism through which the cells were sensitized.
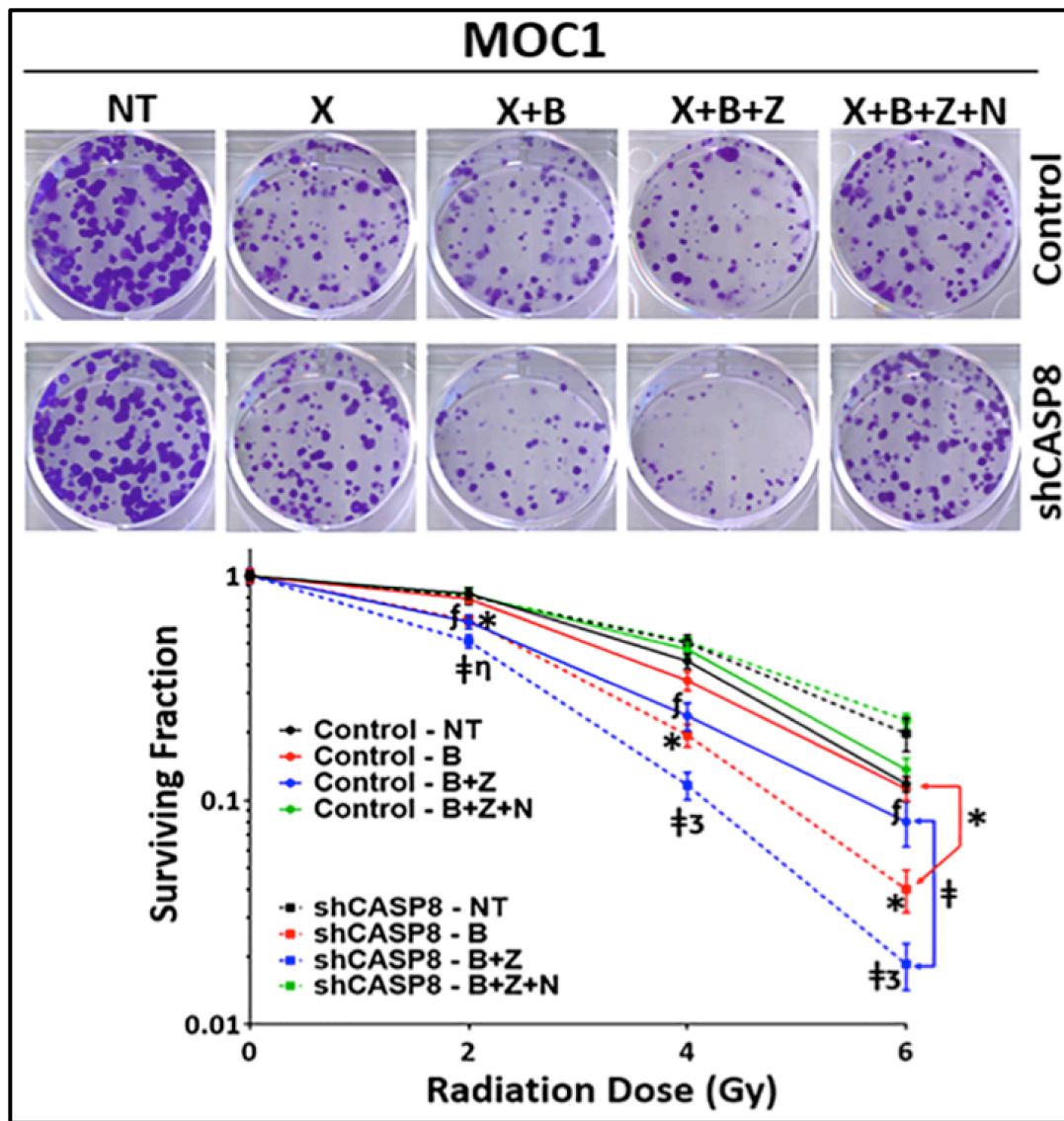
Figure-23: Knockdown of Caspase-8 enhances the radiosensitizing effects of Birinapant and zVAD-FMK through induction of necroptosis. MOC1 control and shCASP8 cells were treated with radiation (X [2,4 and 6 Gy]), Birinapant (B [125nmol/L]), zVAD-FMK (Z [5µmol/L]), Necrostatin-1s (N [10µmol/L]) or combinations as indicated for 24 hours. Representative images of clonogenic survival assays for the X(4Gy) conditions. Surviving colony counts were normalized to nontreated cells (cells treated with no drugs) of each radiation dose from the same experiment. *log10* of surviving fractions were plotted. All treatments were carried out in triplicates. Student *t* test was used for statistics. *, P<0.05; when comparing surviving fractions following X+B treatments between control and shCASP8 cells. ǂ, P<0.05; when comparing surviving fractions following X+B+Z treatments between control and shCASP8 cells. ƒ, P<0.05; when showing reversal of death upon addition of N to X+B+Z for the control cells. η, P<0.05; when showing reversal of death upon addition of N to X+B+Z for the shCASP8 cells. ʒ, P<0.001; when showing reversal of death upon addition of N to X+B+Z for the shCASP8 cells. Symbols are placed at the radiation doses they refer to.

These results were further confirmed with assays for Annexin-V (**Figure-24**) and cell viability (**Figure-25**) that demonstrated similar necroptotic radiosensitization.
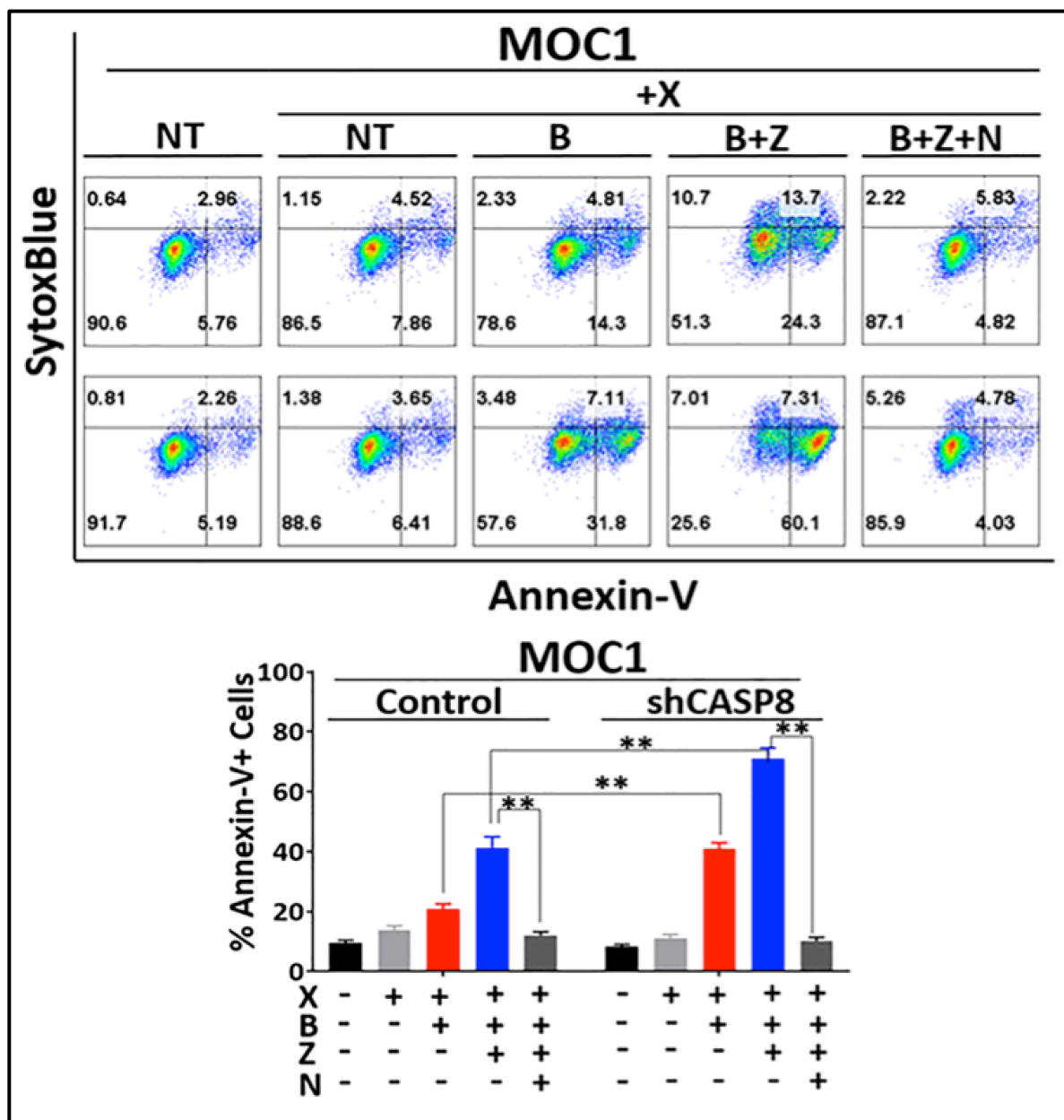
Figure-24: Knockdown of Caspase-8 enhances the radiosensitizing effects of Birinapant and zVAD-FMK through induction of necroptosis. MOC1 control and shCASP8 cells were treated with radiation (X [2, 4 and 6 Gy]), Birinapant (B [250nmol/L]), zVAD-FMK (Z [5μmol/L]), Necrostatin-1s (N [10μmol/L]) or the combinations as indicated. AnnexinV-APC/SytoxBlue staining was performed 24 hour after treatments. % Annexin-V positivity was used as a measure to assess cell death. All treatments were carried out in triplicates. Student *t* test was used for statistics *, P<0.05; **, P<0.001 for the indicated pairwise comparisons.
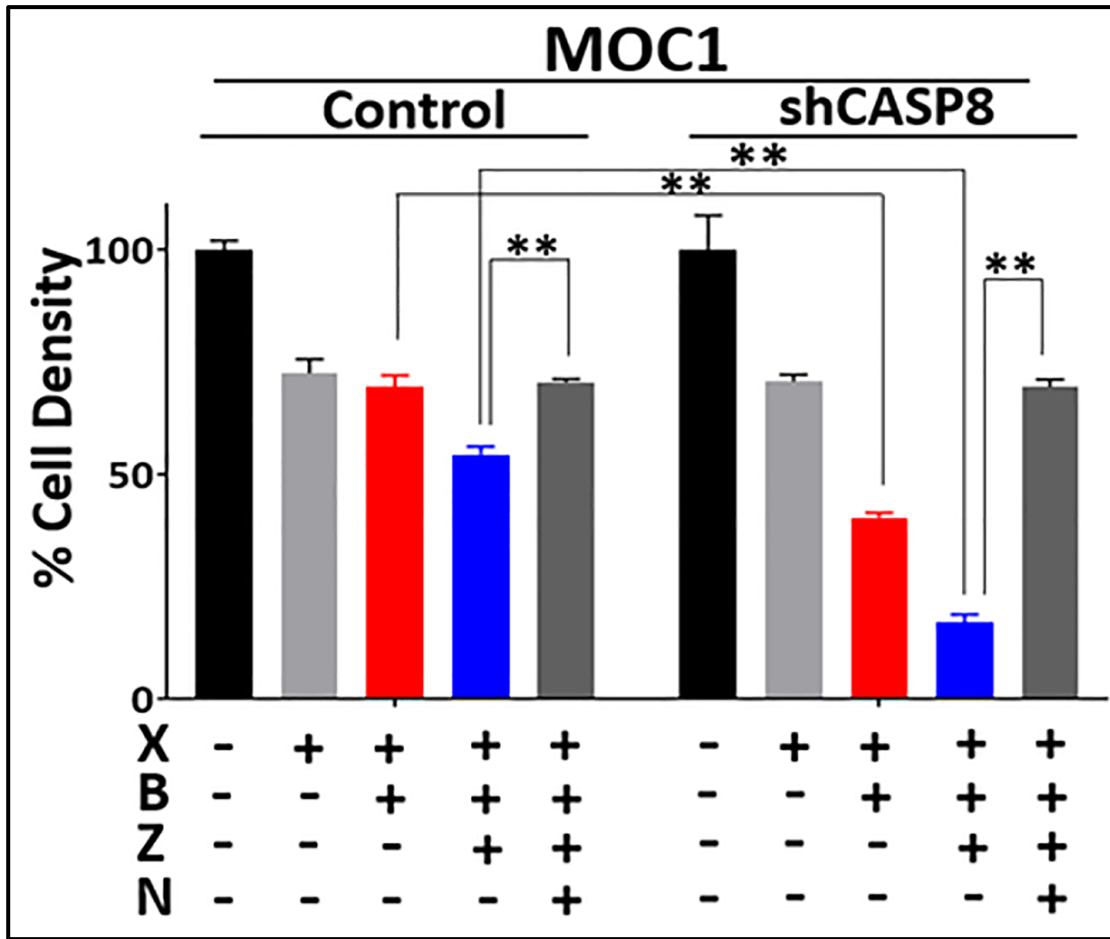
Figure-25: Knockdown of Caspase-8 enhances the radiosensitizing effects of Birinapant and zVAD-FMK through induction of necroptosis. MOC1 control and shCASP8 cells were treated with radiation (X [2, 4 and 6 Gy]), Birinapant (B [250nmol/L]), zVAD-FMK (Z [5μmol/L]), Necrostatin-1s (N [10μmol/L]) or the combinations as indicated. After 24 hours, cell viability was assessed using Cell-Titer Glo. Values normalized to nontreated cells from the same experiment to calculate % cell density. All treatments were carried out in triplicates. Student t test was used for statistics *, P<0.05; **, P<0.001 for the indicated pairwise comparisons.

5.2 Knockdown of Caspase-8 potentiates radiation killing by Birinapant and zVAD-FMK through induction of necroptosis leading to increased expression of necroptotic cell death markers.

To further elaborate on the mechanism(s) that lead to cell death, we assayed the levels of key cell death proteins by western blot following radiation treatment (**Figure-26**).
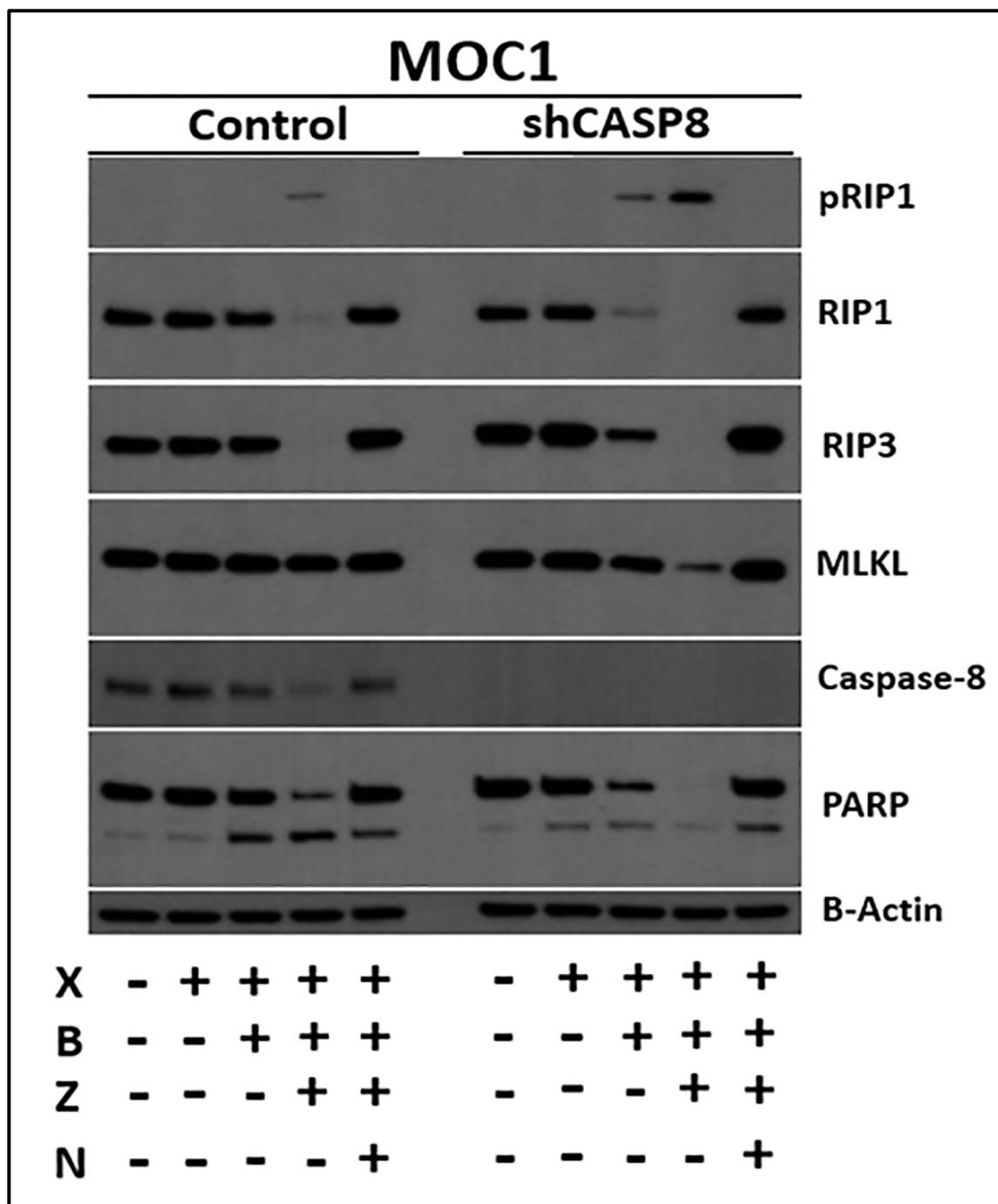
Figure-26: Knockdown of Caspase-8 potentiates radiation killing by Birinapant and zVAD-FMK through induction of necroptosis, leading to increased expression of necroptotic cell death markers. MOC1 control and shCASP8 cells were treated with radiation (X [2, 4 and 6 Gy]), Birinapant (B [250nmol/L]), zVAD-FMK (Z [5µmol/L]), Necrostatin-1s (N [10µmol/L]) or the combinations as indicated. Whole cell lysates were collected 24 hour after treatments and subjected to Western blot analysis for the indicated key cell death markers. β-Actin was used as loading control.

Birinapant when combined with radiation led to phosphorylation of RIP1 in CASP8 knockdown but not scrambled shRNA control MOC1 cells, a phenomenon which was accompanied by reduction in the protein levels of RIP1, RIP3 and MLKL, indicating activation of the necroptosis pathway. This phenotype was further enhanced by addition of zVAD-FMK to the treatment and reversed by the RIP1 kinase inhibitor Necrostatin-1s, indicating that the radiosensitizing effects of Birinapant and Birinapant plus zVAD-FMK manifest themselves through induction of necroptosis.

CHAPTER-VI : SUSCEPTIBILITY TO NECROPTOSIS IS DETERMINED BY RIP3 EXPRESSION IN HNSCCs.

CHAPTER-6: Susceptibility to necroptosis is determined by RIP3 expression in HNSCCs.

6.1 Knockout of Caspase-8 is not always associated with enhancement of necroptosis sensitivity in HNSCCs.

The observation that zVAD-FMK enhances Birinapant-induced necroptotic killing under knockdown of CASP8 might indicate inhibition of residual CASP8 activity. To further study how loss of CASP8 impacts necroptosis sensitivity, we genetically deleted CASP8 in MOC1 cells using CRISPR-Cas9. To rule out clone specific off-target effects, we designed two different single guide RNAs (sgRNA) against CASP8 to generate multiple independent CASP8 knockout clones. Matching CASP8 WT clones were created using a non-targeting sgRNA. The MOC1 CRISPR clones were then subjected to Western blotting to confirm efficient knockout of CASP8 (**Figure-27**).
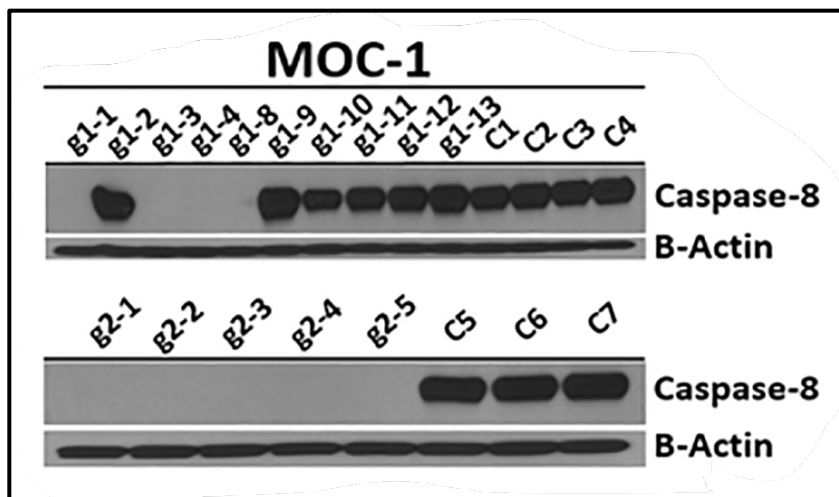
Figure-27: Knockout of Caspase-8 in the MOC1 cell line using CRISPR-Cas9
CRISPR/Cas9 was used to knock out Casp8 in the mouse-derived MOC1 cell line. Specifically, MOC1 parental cells were transiently transfected with two different small guide RNAs (sgRNA) designed against mouse *Casp8* (sgRNA-mCASP8 #1 and sgRNA-mCASP8 #2) or a non-targeting sgRNA after which clonal selection/expansion was performed. Engineered clones were subjected to a Western blot screen to identify CASP8WT and CASP8 knockout (CASP8KO) MOC1 clones.

Next, necroptosis sensitivity was tested in 4 independent CASP8 WT and CASP8 knockout clones following treatment with Birinapant or Birinapant in combination with zVAD-FMK in the absence or presence of Necrostatin-1s (**Figure-28**).
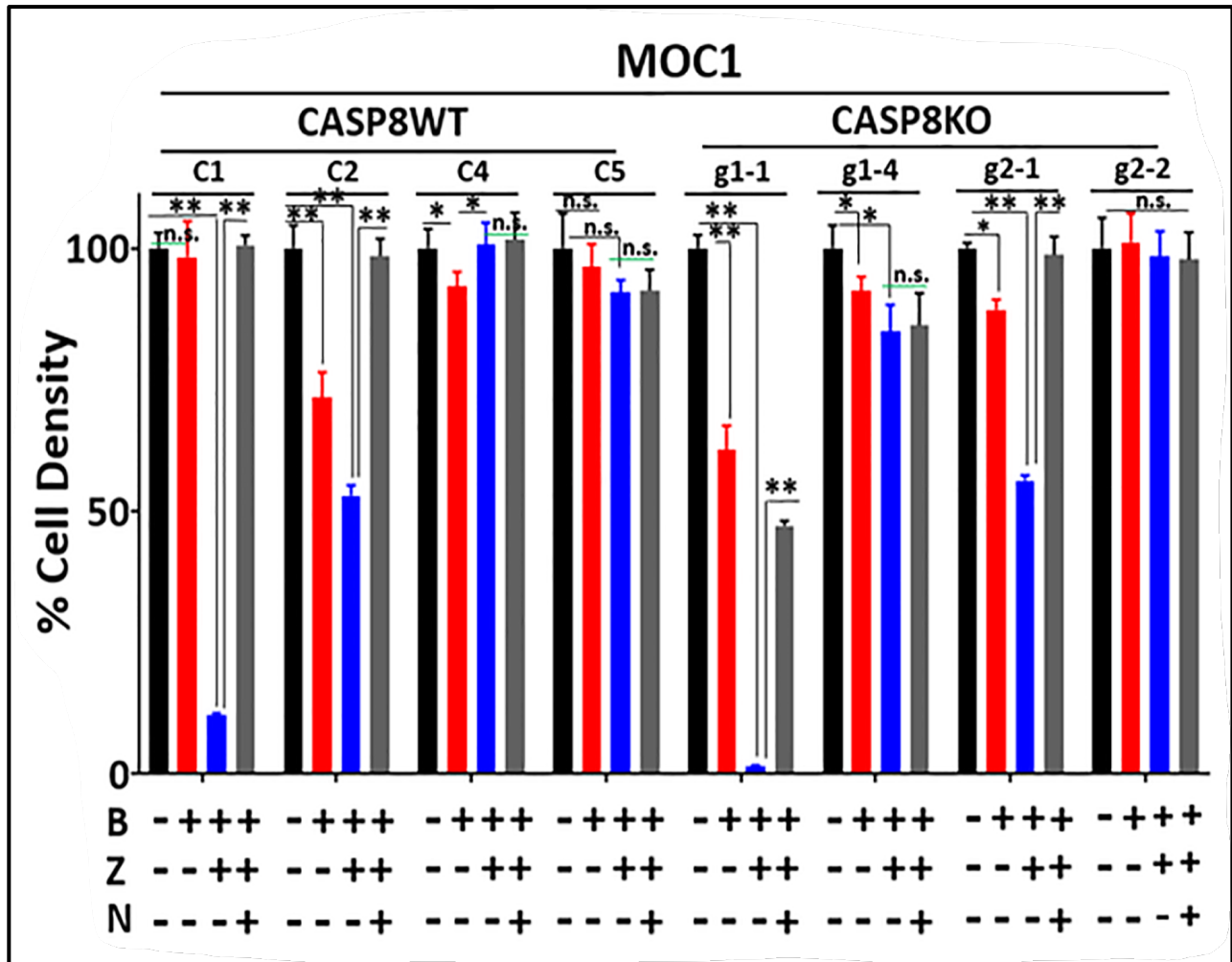
Figure-28: Knockout of Caspase-8 is not always associated with enhancement of necroptosis sensitivity in HNSCCs. Indicated CASP8WT and CASP8KO MOC1 clones were treated with Birinapant (B [1µmol/L]), Z-VAD-FMK (Z [5µmol/L]), Necrostatin-1s (N [10µmol/L]) or the combinations for 24 hours. Cell viability was assessed using CellTiter-Glo. Values normalized to nontreated cells from the same experiment to calculate % cell density. All treatments were carried out in triplicates. Student t test was used for statistical analysis. *, $P<0.05$; **, $P<0.001$ for the indicated pairwise comparisons.

Across the clones tested, two CASP8 WT clones (C1 and C2) and two CASP8 knockout clones (g1-1 and g2-1) showed sensitivity to Birinapant plus zVAD-FMK with Necrostatin-1s restoring cell density, indicating a predominantly RIP1-mediated necroptotic cell death. Intriguingly, however, among the CASP8 knockout clones, clone g2-2 showed complete resistance to Birinapant and Birinapant plus zVAD-FMK, and clone g1-4 demonstrated low sensitivity which was not reversed by Necrostatin-1s. Therefore, we concluded that these two clonal cell lines exhibit necroptosis resistance despite complete loss of protein expression of CASP8. Additionally, two control clones (C4 and C5) also demonstrated necroptotic resistance, while one clone (C1) had enhanced sensitivity to necroptosis.

6.2 Resistance to necroptosis is associated with lack of protein expression of RIP3 in HNSCCs.

In an effort to understand the underlying mechanism for the observed differences in necroptosis sensitivity among the clones tested, we queried the expression of necroptosis proteins in them. Western blot analysis of the whole-cell lysates obtained from the MOC1 clones and the parental cell line at baseline revealed considerable levels of RIP1 and MLKL for all the cells, but the clones with reduced sensitivity to necroptosis demonstrated lack of protein expression of RIP3 irrespective of CASP8 status. Intriguingly, RIP1 and MLKL were detected in all the clones (they were rather uniformly expressed across clones) independently of the necroptosis sensitivity they displayed, suggesting that expression of RIP3 might be the determining factor for necroptosis sensitivity in HNSCCs (**Figure-29**).
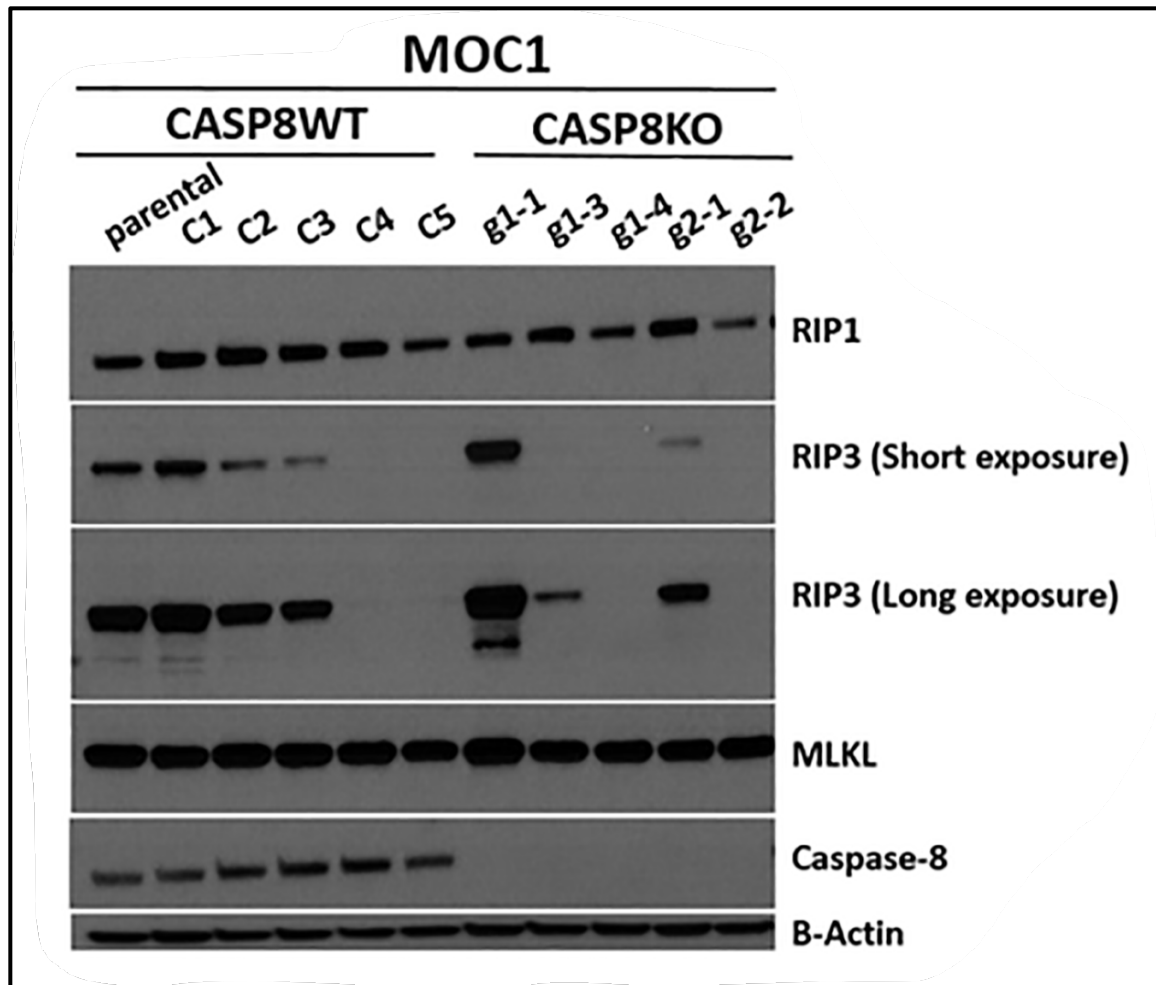
Figure-29: Resistance to necroptosis is associated with lack of protein expression of RIP3 in HNSCCs. Indicated CASP8WT and CASP8KO MOC1 clones were subjected to Western blot analysis for necroptosis markers, RIP1, RIP3 and MLKL along with Caspase-8. β-Actin was used as loading control.

6.3 Loss of RIP3 expression renders HNSCCs resistant to necroptosis.

Next, we conducted knockdown and overexpression studies to further validate the role of RIP3 in determining necroptosis sensitivity in HNSCCs. shRNA knockdown of RIP3 in two necroptosis sensitive MOC1 clones, namely a CASP8 WT C2 and a CASP8 knockout g2-1 clone resulted in acquisition of resistance to Birinapant plus zVAD-FMK induced necroptotic cell death (**Figure-30A, -B**)
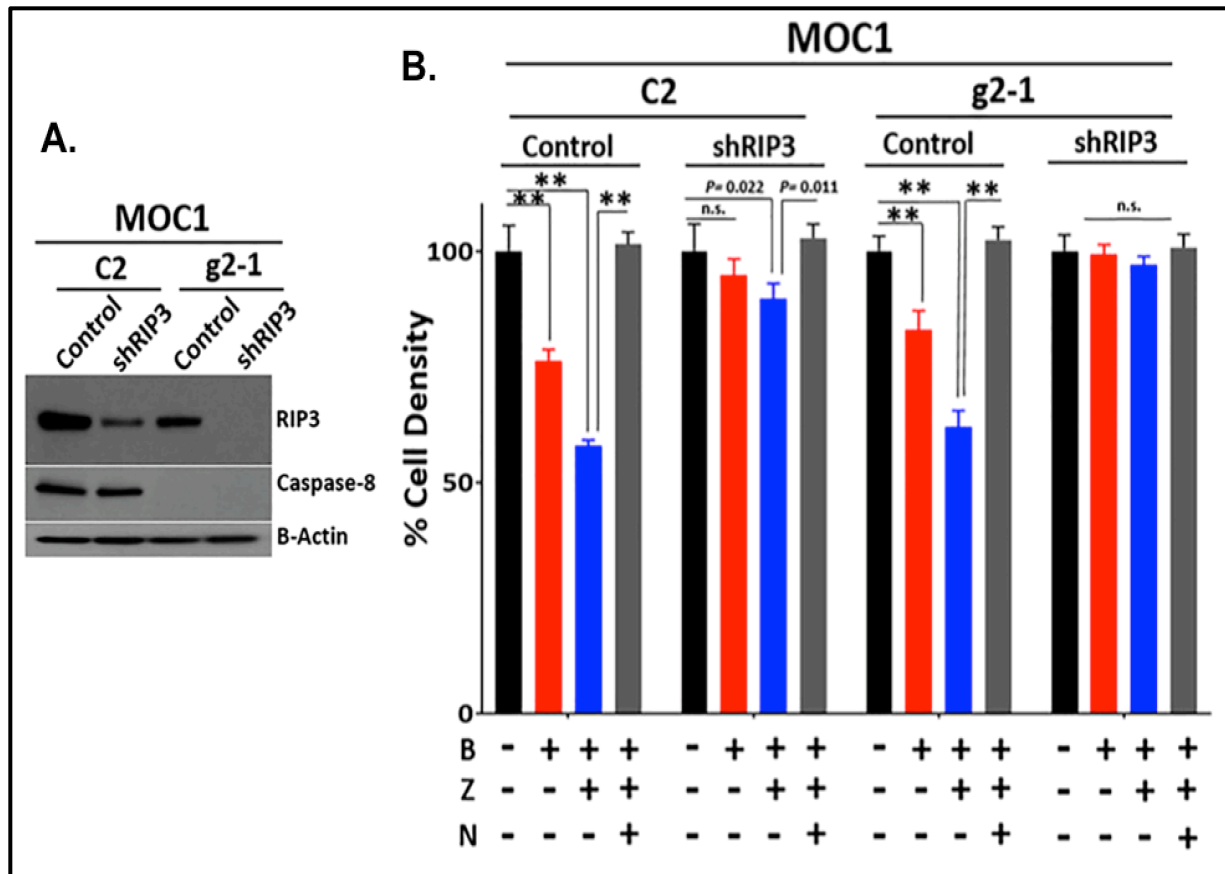
Figure-30: Loss of RIP3 expression renders HNSCCs resistant to necroptosis. A. RIP3 was knocked down using shRNA in two Necroptosis sensitive MOC1 clones: the CASP8WT C2 and CASP8KO g2-1 clones. Scrambled shRNA control and shRIP3 cells were subjected to WB for the validation of RIP3 knockdown. β-Actin was used as loading control. **B.** Control and shRIP3 C2 (CASP8WT) and g2-1 (CASP8KO) MOC1 clones were treated with Birinapant (B [1µmol/L]), zVAD-FMK (Z [5µmol/L]), Necrostatin-1s (N [10µmol/L]) or the combinations for 24 hours. Cell viability was assessed by Cell-Titer Glo. Values normalized to nontreated cells from the same experiment to calculate % cell density. All treatments were carried out in triplicates. Student *t* test was used for statistical analysis. *, P<0.05; **, P<0.001 for the indicated pairwise comparisons.

6.4 Expression of WT but not a kinase-dead mutant RIP3-D143N restores necroptosis sensitivity in HNSCCs.

Inducible expression of WT but not a kinase dead (D143N) mutant of RIP3 in two

necroptosis resistant MOC1 clones, namely a CASP8 WT C4 and a CASP8 knockout
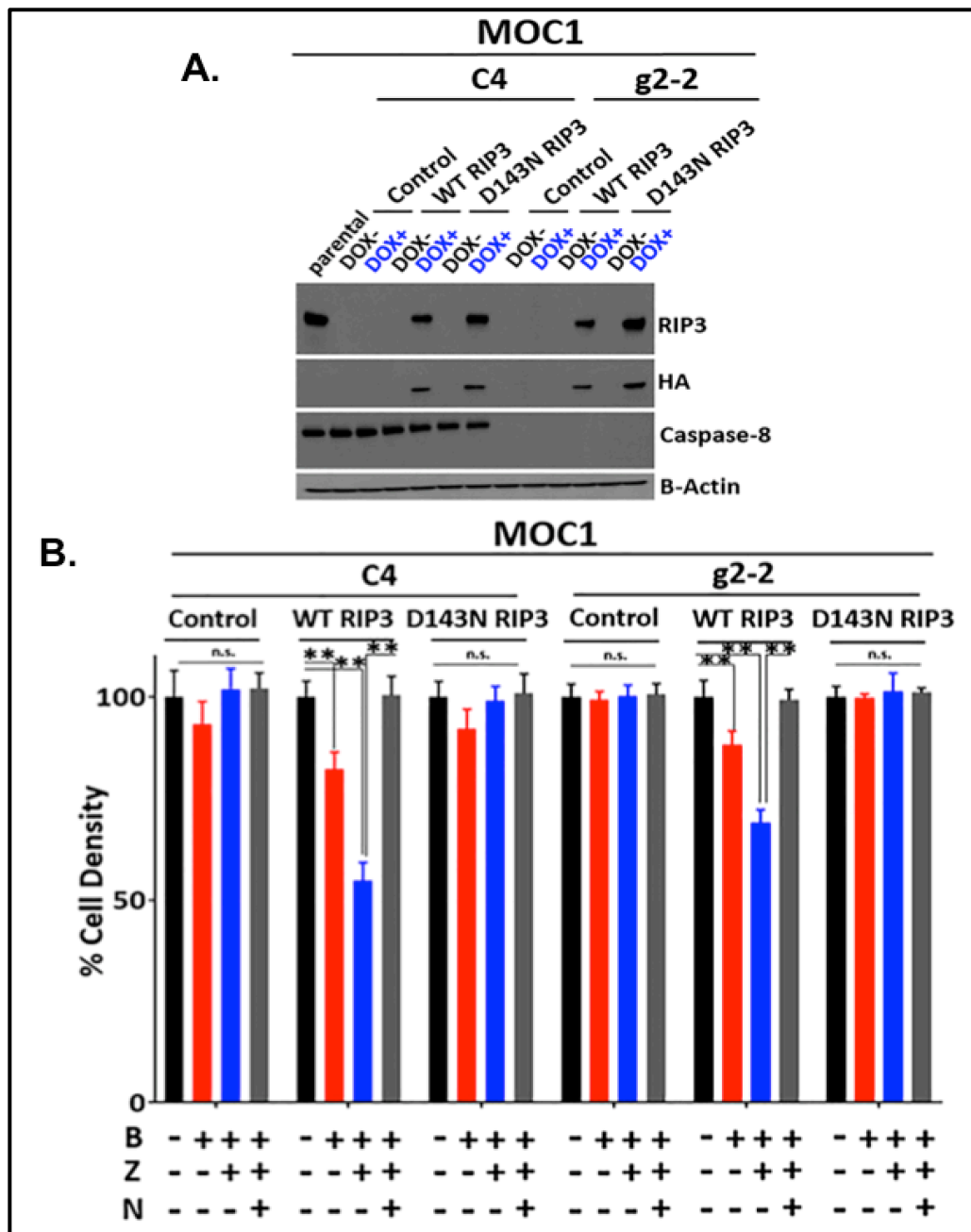
Figure-31: Expression of WT but not a kinase-dead mutant RIP3-D143N restores necroptosis sensitivity in HNSCCs. A. Necroptosis resistant C4 (CASP8WT) and g2-2 (CASP8KO) MOC1 clones were transduced with control, HA-tagged WT RIP3 or HA-tagged D143N RIP3 inducible expression constructs. RIP3 expression was induced with a 48h Doxycycline (50ng/ml) treatment. Western blot analysis was performed to validate expression of WT or D143N RIP3 in the indicated clones. β-Actin was used as loading control. **B.** Cells engineered in the previous step were treated with Birinapant (B [1μmol/L]), zVAD-FMK (Z [5μmol/L]), Necrostatin-1s (N [10μmol/L]) or the combinations for 24 hours. Cell viability was assessed by Cell-Titer Glo. Student t test was used for statistical analysis. *, P<0.05; **, P<0.001 for the indicated pairwise comparisons.

g2-2 clone rendered the cells sensitive to Birinapant plus zVAD-FMK induced

necroptotic cell death (**Figure-31A, -B**). Taken together, these data suggest that the

presence of functional RIP3 is required for susceptibility to necroptosis in HNSCCs.

CHAPTER-VII : RIP3 IS SILENCED IN MANY HNSCC CELL LINES, WHEREAS PATIENT TUMORS SHOW CONSIDERABLE EXPRESSION

CHAPTER-7: RIP3 is silenced in many HNSCC cell lines, whereas patient tumors show considerable expression.

7.1 Many HNSCC cell lines show loss of protein expression of RIP3.

The observation that MOC1 clones lacking functional RIP3 protein show necroptosis resistance led us to test whether RIP3 levels determine necroptosis sensitivity in other HNSCC cell lines. To test that, we took a panel of 5 CASP8 WT and 4 CASP8 mutant HNSCC cell lines in which we evaluated the baseline expression for key necroptosis proteins by Western blotting (**Figure-32**).
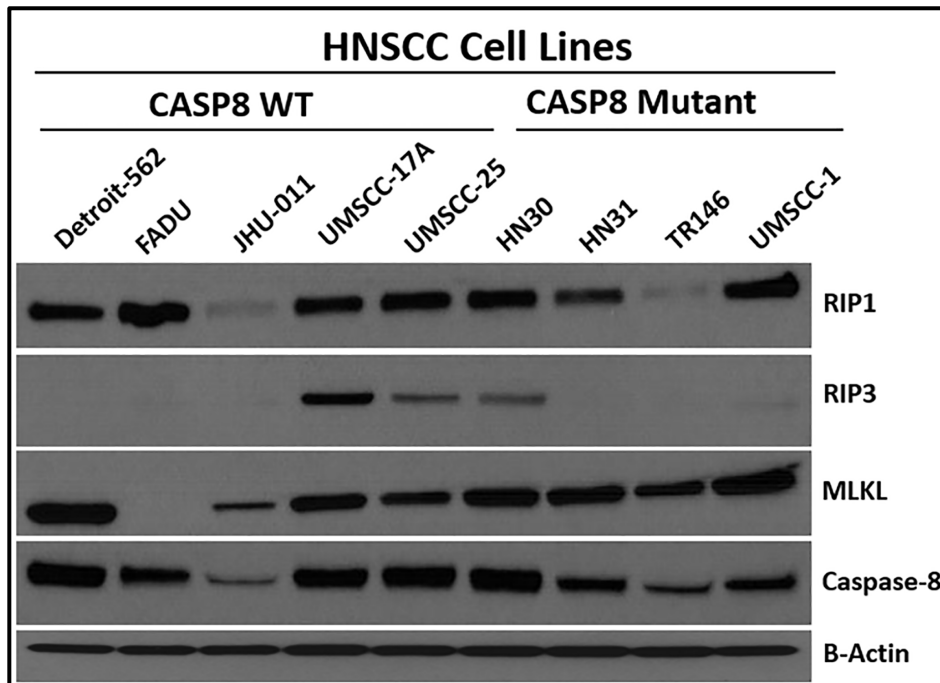
Figure-32: Many HNSCC cell lines show loss of protein expression of RIP3. Cell lysates obtained from a panel of 5 CASP8WT and 4 CASP8mutant human-derived HNSCC cell lines were subjected to Western blot analysis for Caspase-8 and key necroptosis markers. β-Actin was used as loading control.

Among the cell lines tested, only two CASP8WT cell lines, namely UMSCC-17A and UMSCC-25 and one CASP8 mutant cell line, namely HN30 showed considerable RIP3

levels. RIP3 expression was lost in the rest of the cell lines, indicating that silencing of

RIP3 might be common mechanism to evade necroptosis in HNSCCs.

7.2 Loss of RIP3 is associated with unresponsiveness to necroptotic stimuli in HNSCCs.

In an effort to understand if RIP3 levels correlate with necroptosis sensitivity in

HNSCCs, we measured inducibility of necroptotic death in those cell lines **(Figure-33)**.
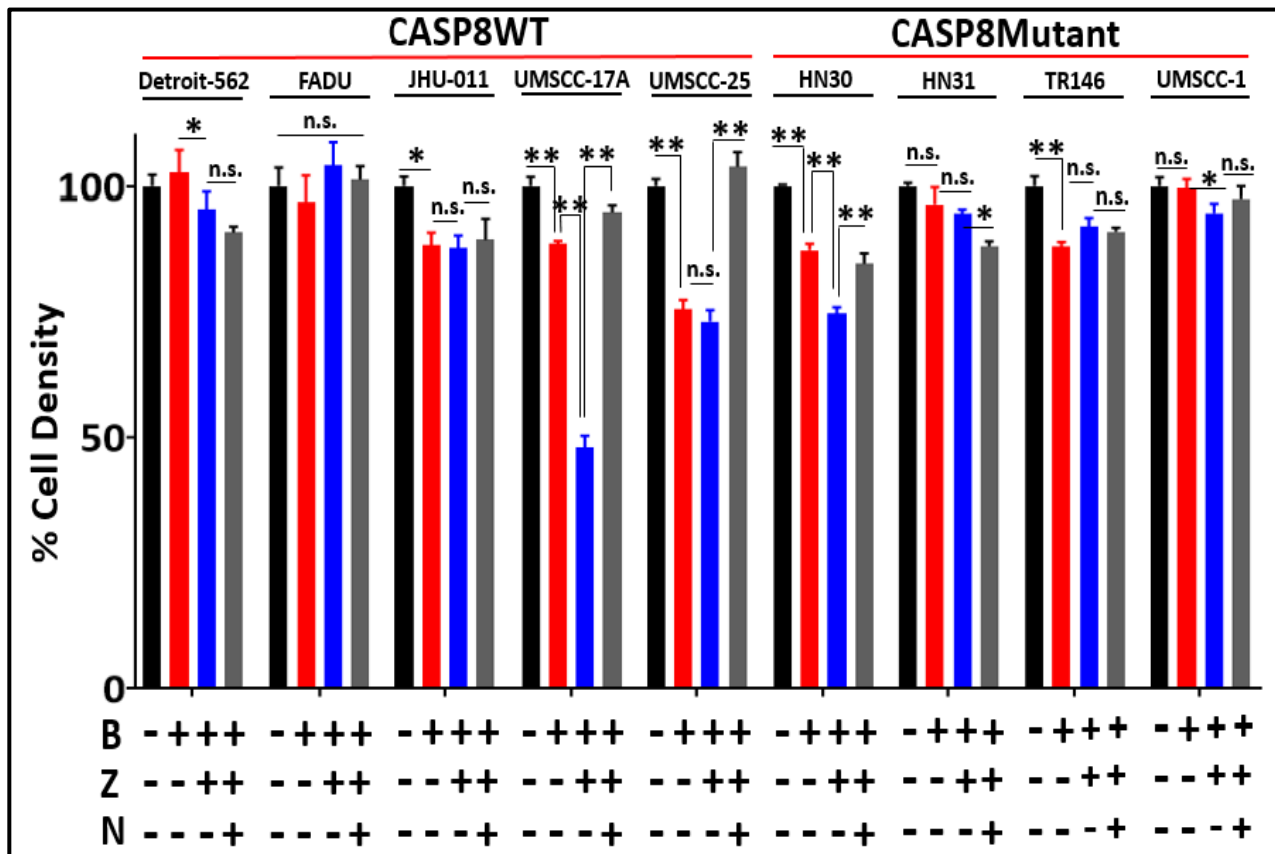
Figure-33: Loss of RIP3 is associated with unresponsiveness to necroptotic stimuli in HNSCCs. A panel of 9 human-derived HNSCC cell lines, 5 CASP8WT (Detroit-562, FADU, JHU-011, UMSCC-17A and UMSCC-25) and 4 CASP8 mutant (HN30, HN31, TR146 and UMSCC-1) were treated with Birinapant (B [1µmol/L]), zVAD-FMK (Z [5µmol/L]), Necrostatin-1s (N [10µmol/L]) or the combinations. 24 hour after treatments, cell viability was assessed by CellTiter Glo. Values normalized to nontreated cells from the same experiment to calculate % cell density. All treatments were carried out in triplicates. Student t test was used for statistics. *, P<0.05; **, P<0.001 for the indicated pairwise comparisons.

Consistent with our previous findings, across all the cell lines tested only the 3 cell lines that demonstrated considerable baseline protein levels of RIP3, the CASP8WT UMSCC-17A and UMSCC-25 cell lines and the CASP8 mutant HN30 cell line, showed sensitivity to Birinapant plus zVAD-FMK which was reversed by Necrostatin-1s, indicating that loss of RIP3 might render HNSCCs refractory to necroptotic stimuli.

7.3 RIP3 is silenced in many HNSCC cell lines, whereas patient tumors show considerable mRNA expression of RIP3.

We next evaluated RIP3 gene expression in HNSCC cell lines by using RNA sequencing (**Figure-34A**). Interestingly, mRNA expression of RIP3 correlated with RIP3 protein levels in cell lines, and majority of the cell lines demonstrated low RIP3 expression, suggesting that many HNSCC cell lines may be resistant to necroptosis, due to low levels of RIP3.
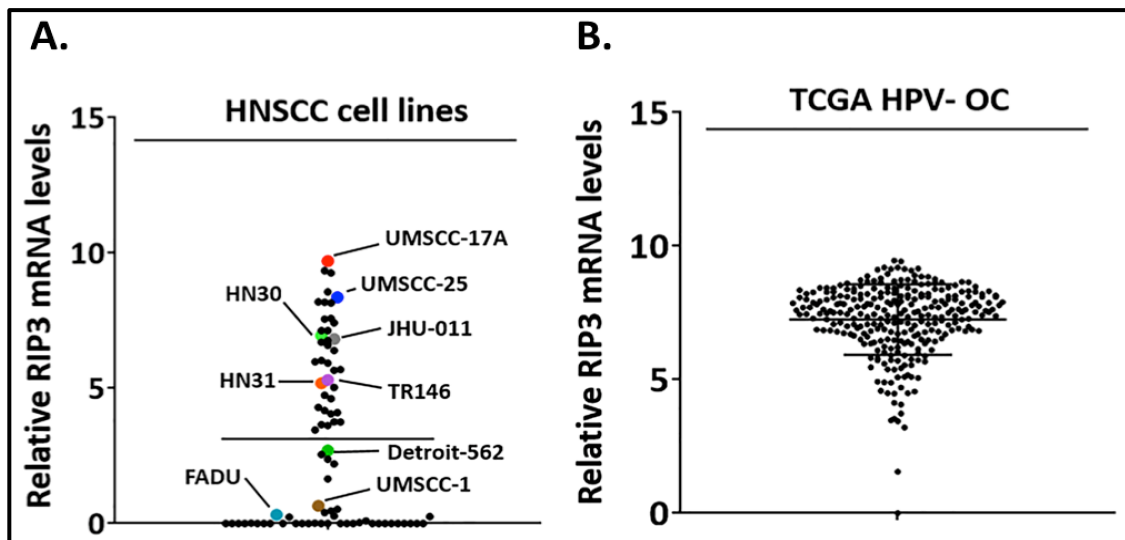
Figure-34: RIP3 is silenced in many HNSCC cell lines, whereas patient tumors show considerable mRNA expression of RIP3. A. Scatter plot shows gene expression for RIP3 in a panel of 80 human-derived HNSCC cell lines. Mean values are shown by the bar. Cell lines used for the Western Blot analysis were highlighted. **B.** RIP3 gene expression in TCGA HPV-negative oral cancer (OC) samples. Mean values are shown by the bar.

Given our interest in the use of necroptosis as a therapeutic target in HNSCCs, we assessed RIP3 gene expression in HNSCC tumors using the publicly available The Cancer Genome Atlas (TCGA) HNSCC dataset (**Figure-34B**). Analysis of TCGA tumors confirmed high levels of RIP3 in most tumors, providing justification for therapeutic use of necroptosis in HNSCC. We hypothesize that the loss of RIP3 expression in many cell lines may be due to promoter DNA methylation that occurs *in vitro* (358, 359).

CHAPTER-VIII : LOSS OF CASPASE-8 IN COMBINATION WITH SMAC MIMETIC TREATMENT SENSITIZES HNSCC TO RADIATION

CHAPTER-8: Loss of Caspase-8 in combination with SMAC mimetic treatment sensitizes HNSCC to radiation.

8.1 Loss of Caspase-8 increases sensitivity to single agent Birinapant and Birinapant plus radiation *in vivo*, improving survival outcomes.

On the basis of our *in vitro* observations that loss of CASP8 increases Birinapant sensitivity and enhances the radiosensitizing effects of Birinapant in MOC1 cells, we sought to assess the therapeutic efficacy of Birinapant alone or in combination with radiation in the absence or presence of CASP8 knockdown using the syngeneic MOC1 model *in vivo*. To test this, we generated a MOC1 cell subline transduced with a doxycycline-inducible lentiviral CASP8 shRNA vector (343). Treatment of the CASP8 shRNA-MOC1 cells with doxycycline, but not vehicle control, led to efficient knockdown of CASP8 *in vitro* (**Figure-35**).
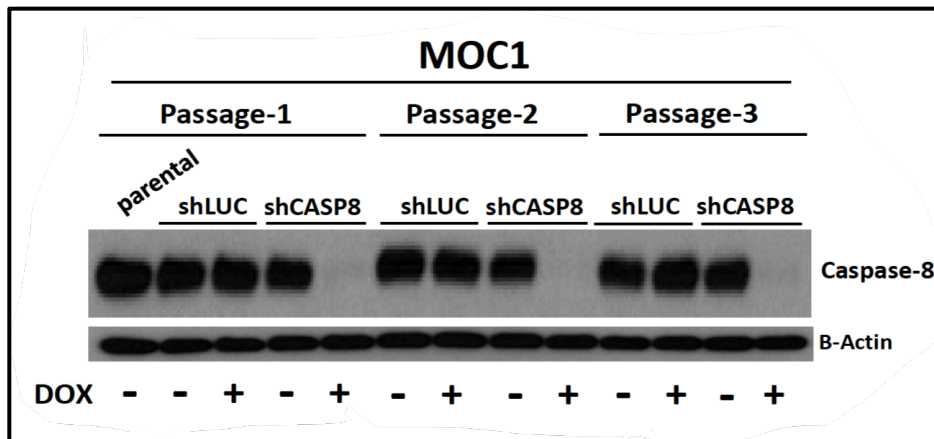
Figure-35: Validation of *in vitro* Caspase-8 knockdown using Tetracycline-Regulated Inducible RNA interference (RNAi) system. MOC1 cells were transduced with lentiviral constructs designed against Luciferase (shLUC) or CASP8 (shCASP8) (343). The engineered shLUC and shCASP8 cells were cultured in the absence or presence of Doxycycline (50ng/ml). 72 hours after treatment, cells were passaged and cell lysates were obtained. This cycle was repeated 3 times. Cell lysates obtained from each cycle along with that from MOC1 parental cells were subjected to WB analysis for Caspase-8 . β-Actin was used as loading control.

The CASP8 shRNA-MOC1 cells were injected subcutaneously into the upper leg of syngeneic C57BL/6 mice and knockdown of CASP8 was achieved *in vivo* by feeding the animals doxycycline containing food or matching control diet throughout the study (**Figure-36**).
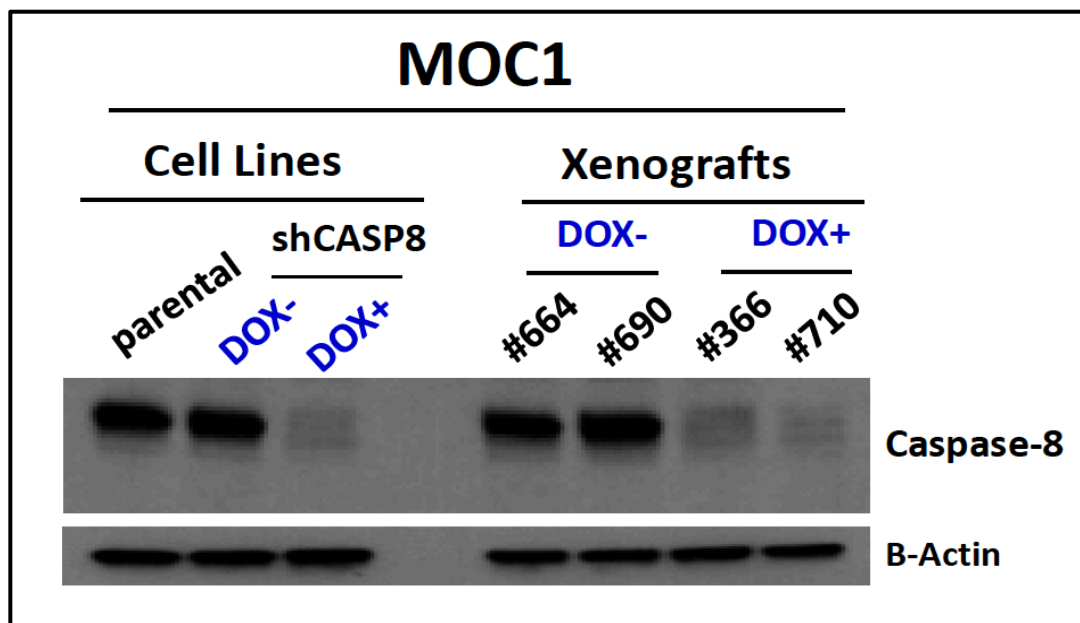
Figure-36: Validation of *in vivo* Caspase-8 knockdown using Tetracycline-Regulated Inducible RNA interference (RNAi) system. 2×10^6 MOC1 cells transduced with an inducible shRNA against Caspase-8 were injected into the right flank of WT female C57BL/6 mice obtained from Envigo/Harlan Labs in the presence of Matrigel (Corning). 3 days after inoculation, mice were randomized and placed on control (Global 18% Protein Rodent Diet) or DOX diet (doxycycline hyclate added at 625 mg/kg) obtained from Envigo to induce knockdown of Caspase-8 *in vivo*. Tumor samples were collected from a subset of control (#664, #690) and shCASP8 mice (#366, #710) that were not recruited in the drug treatment study. These tumor samples were minced and cultured in medium for 48 hours. Cells shed from the tumors that have attached to culture dishes were collected, lysed and subjected to WB analysis for Caspase-8. β-Actin was used as loading control.

Mouse cohorts with control and CASP8 knockdown MOC1 flank tumors were treated with Birinapant (15mg/kg intraperitoneally) every 3 days for 4 weeks, radiation (2 Gy) daily Monday to Friday for 1 week, or the combination when the tumors reached 150 mm^3 (335). The schema of *in vivo* treatments is included in the **Materials and Methods**

section. Treatment with radiation alone significantly inhibited *in vivo* tumor growth (**Figure-37**, **Table-6**) and improved survival (**Figure-38**, **Table-7**) in both the control and CASP8 knockdown animal cohorts.
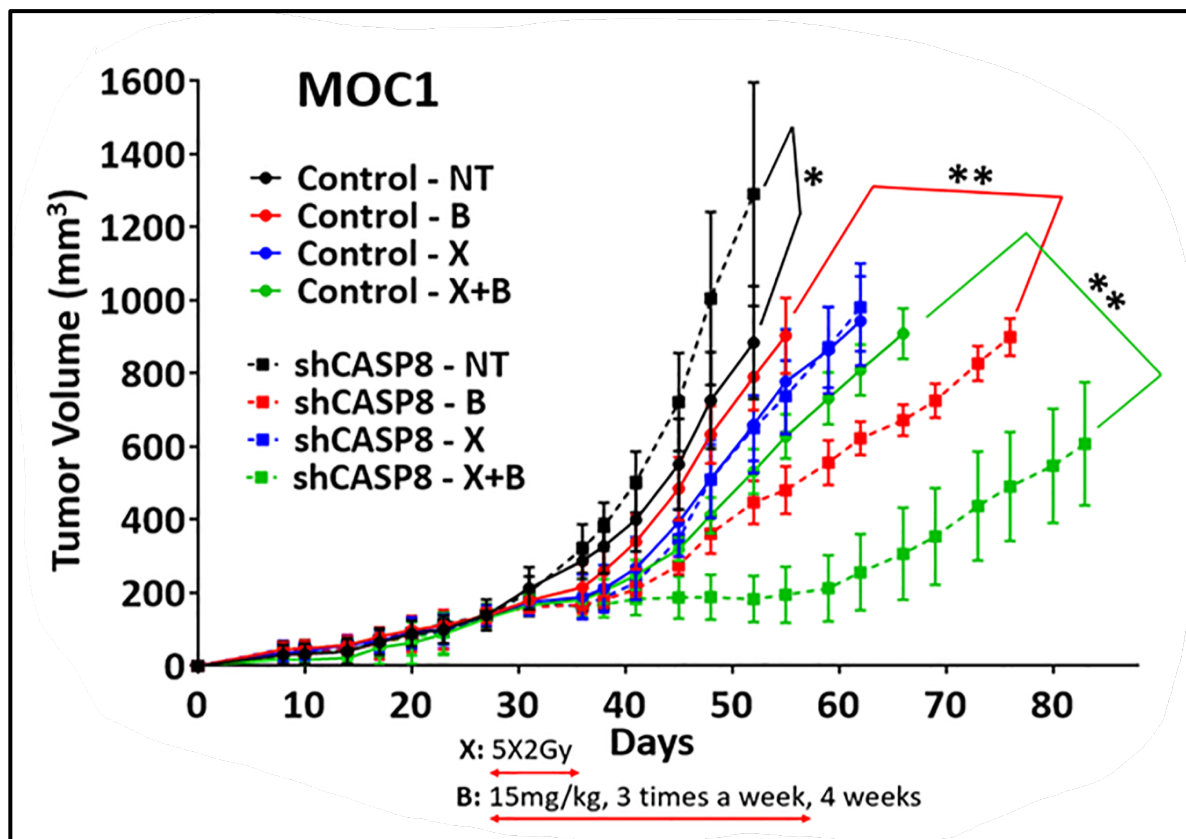
Figure-37: Loss of Caspase-8 increases sensitivity to single agent Birinapant and Birinapant plus radiation *in vivo*. 2×10^6 MOC1 cells transduced with an inducible shRNA against Caspase-8 were injected into the right flank of WT female C57BL/6 mice. Mice were randomized and placed on control or DOX diet (doxycycline hyclate added at 625 mg/kg) 3 days post injection to induce knockdown (KD) of Caspase-8 *in vivo* (Please refer to Figure-36 for the WB images). Control and Caspase-8 KD mice were randomized into 4 treatment groups (vehicle control, 15mg/kg Birinapant, 5X2Gy radiation or combination, n=7-10/each) 27 days post inoculation when the average tumor volume reached ~150 mm^3. Solid and dashed lines were used to represent control and Caspase-8 KD mice respectively for the indicated treatment groups. Radiation (X) started on Day 27: 2Gy of radiation given Monday to Friday for 1 week (Solid and dashed blue lines). Birinapant (B) started on Day 27: 15mg/kg Birinapant given intraperitoneally every 3 days for 4 weeks (Solid and dashed red lines). Black and green lines show vehicle control (NT) and combo (X+B) groups respectively. A more detailed treatment schema is available in the Materials and Methods section. Error bars represent standard deviation. 2-way ANOVA was used for statistical analysis. *p < 0.05, **p < 0.001 for the indicated pairwise comparisons.
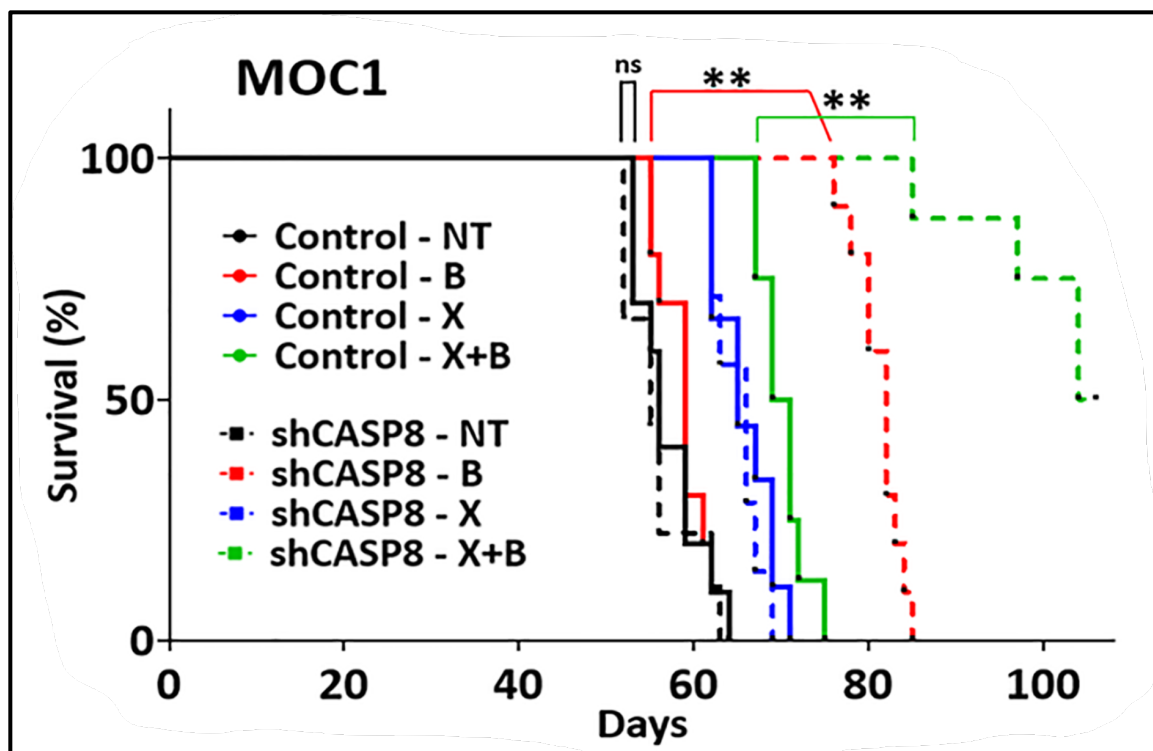
Figure-38: Enhancement of *in vivo* sensitivity to single agent Birinapant and Birinapant plus radiation observed under Caspase-8 knockdown is associated with improved survival outcomes in mice. Kaplan-Meier survival curves representing each treatment group. Log-rank (Mantel-Cox) test was used for statistical analysis. *p < 0.05, **p < 0.001 for the indicated pairwise comparisons.

However, single agent Birinapant proved effective in delaying tumor growth only when combined with CASP8 knockdown (**Figure-37**, **Table-6**), a phenomenon which was accompanied by a significant survival benefit (**Figure-38**, **Table-7**). The radiation plus Birinapant combination further reduced *in vivo* tumor growth (**Figure-37**, **Table-6**), and provided survival benefit in both the control and CASP8 knockdown animal cohorts (**Figure-38**, **Table-7**). However, mice bearing CASP8 knockdown MOC1 tumors demonstrated a significant increase in tumor growth delay (**Figure-37**, **Table-6**), and a significantly improved survival (**Figure-38**, **Table-7**) when compared to those bearing matching control tumors.

Compared Animal Cohorts		p value
Cohort#1	**Cohort#2**	
Control-NT	Control-B	0.7628
Control-NT	Control-X	0.0093
Control-NT	Control-X+B	<0.001
Control-B	Control-X	0.0795
Control-B	Control-X+B	<0.001
Control-X	Control-X+B	0.1357
shCASP8-NT	shCASP8-B	<0.001
shCASP8-NT	shCASP8-X	<0.001
shCASP8-NT	shCASP8-X+B	<0.001
shCASP8-B	shCASP8-X	<0.001
shCASP8-B	shCASP8-X+B	<0.001
shCASP8-X	shCASP8-X+B	<0.001
Control-NT	shCASP8-NT	<0.001
Control-B	shCASP8-B	<0.001
Control-X	shCASP8-X	0.9714
Control-X+B	shCASP8-X+B	<0.001

Table-6: *p* values for key pairwise comparisons in tumor growth analysis

Compared Animal Cohorts		p value
Cohort#1	**Cohort#2**	
Control-NT	Control-B	0.4345
Control-NT	Control-X	<0.001
Control-NT	Control-X+B	<0.001
Control-B	Control-X	<0.001
Control-B	Control-X+B	<0.001
Control-X	Control-X+B	0.0206
shCASP8-NT	shCASP8-B	<0.001
shCASP8-NT	shCASP8-X	<0.001
shCASP8-NT	shCASP8-X+B	<0.001
shCASP8-B	shCASP8-X	<0.001
shCASP8-B	shCASP8-X+B	<0.001
shCASP8-X	shCASP8-X+B	<0.001
Control-NT	shCASP8-NT	0.4846
Control-B	shCASP8-B	<0.001
Control-X	shCASP8-X	0.4747
Control-X+B	shCASP8-X+B	<0.001

Table-7: *p* values for key pairwise comparisons in survival analysis

Taken together, our results suggest that loss of CASP8 sensitizes HNSCCs to Birinapant and potentiates its radiosensitizing effects *in vivo*.

CHAPTER-IX: PHARMACOLOGICAL INHIBITION OF CASPASE-8 SENSITIZES HNSCC TO THE SMAC MIMETIC-RADIATION COMBINATION

CHAPTER-9: Pharmacological inhibition of Caspase-8 sensitizes HNSCC to the SMAC mimetic radiation combination

9.1 Chemical inhibition of Caspase-8 with emricasan sensitizes HNSCCs to radiation killing by Birinapant through induction of necroptosis

Since only a subset of HNSCC contain inactivation of CASP8 by mutation, we sought to determine whether chemical inhibition of CASP8 could mimic knockdown of CASP8 for necroptotic radiosensitization. emricasan (IDN-655) is a potent pan-caspase inhibitor that was found to be clinically well-tolerated when it was tested to reduce liver toxicity in patients with chronic liver diseases (360). To test our hypothesis, we treated UMSCC-17A and MOC1 parental cell lines with increasing doses of radiation in combination with Birinapant and/or emricasan in the absence or presence of Necrostatin-1s, after which we assessed cell viability by CellTiter-Glo (**Figure-39**). We found that emricasan enhanced the sensitivity of CASP8 WT UMSCC-17A and MOC1 cells to the radiation Birinapant combination *in vitro*. The increase in radiosensitizing effects of Birinapant achieved with the chemical (pharmacological) inhibition of Caspase-8 was reversed by the RIP1 inhibitor Necrostatin-1s, indicating that induction of necroptotic cell death was the underlying mechanism for radiosensitization.
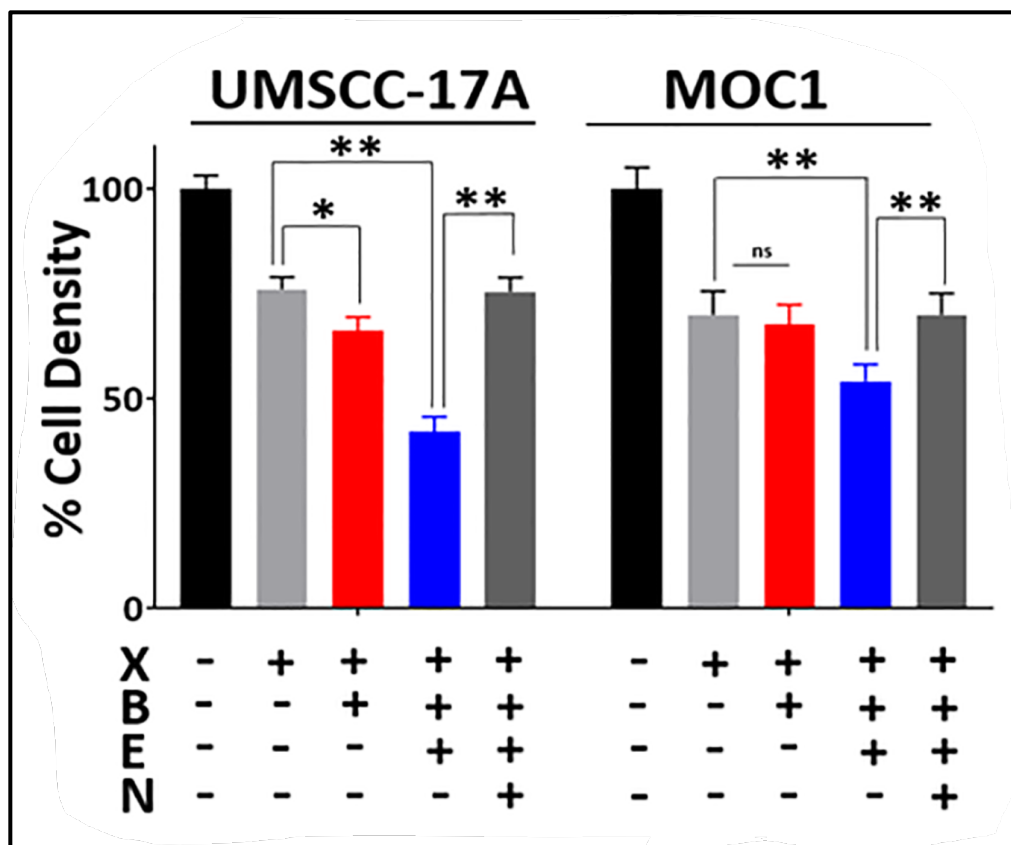
Figure-39: Chemical inhibition of Caspase-8 with emricasan sensitizes HNSCCs to radiation killing by Birinapant through induction of necroptosis. UMSCC-17A and MOC1 parental cells were treated with radiation (X [2, 4 and 6 Gy]), Birinapant (B [50nmol/L for the UMSCC-17A cells; 250nmol/L for the MOC1 cells]), emricasan (E [1µmol/L for both the cell lines]), Necrostatin-1s (N [10µmol/L for both the cell lines]) or the combinations as indicated for 24 hours. Cell viability was assessed using CellTiter-Glo. Values normalized to nontreated cells from the same experiment to calculate % cell density. All treatments were carried out in triplicates. Student *t* test was used for statistics. *, P<0.05; **, P<0.001 for the indicated pairwise comparisons.

9.2   Chemical inhibition of Caspase-8 with emricasan potentiates reduction in clonogenic survival induced by Birinapant and radiation in HNSCCs.

To corroborate our findings, we performed clonogenic survival assay following treatment of UMSCC-17A and MOC1 parental cells with radiation in combination with Birinapant and emricasan in the absence or presence, Necrostatin-1s as detailed above (**Figure-40**).
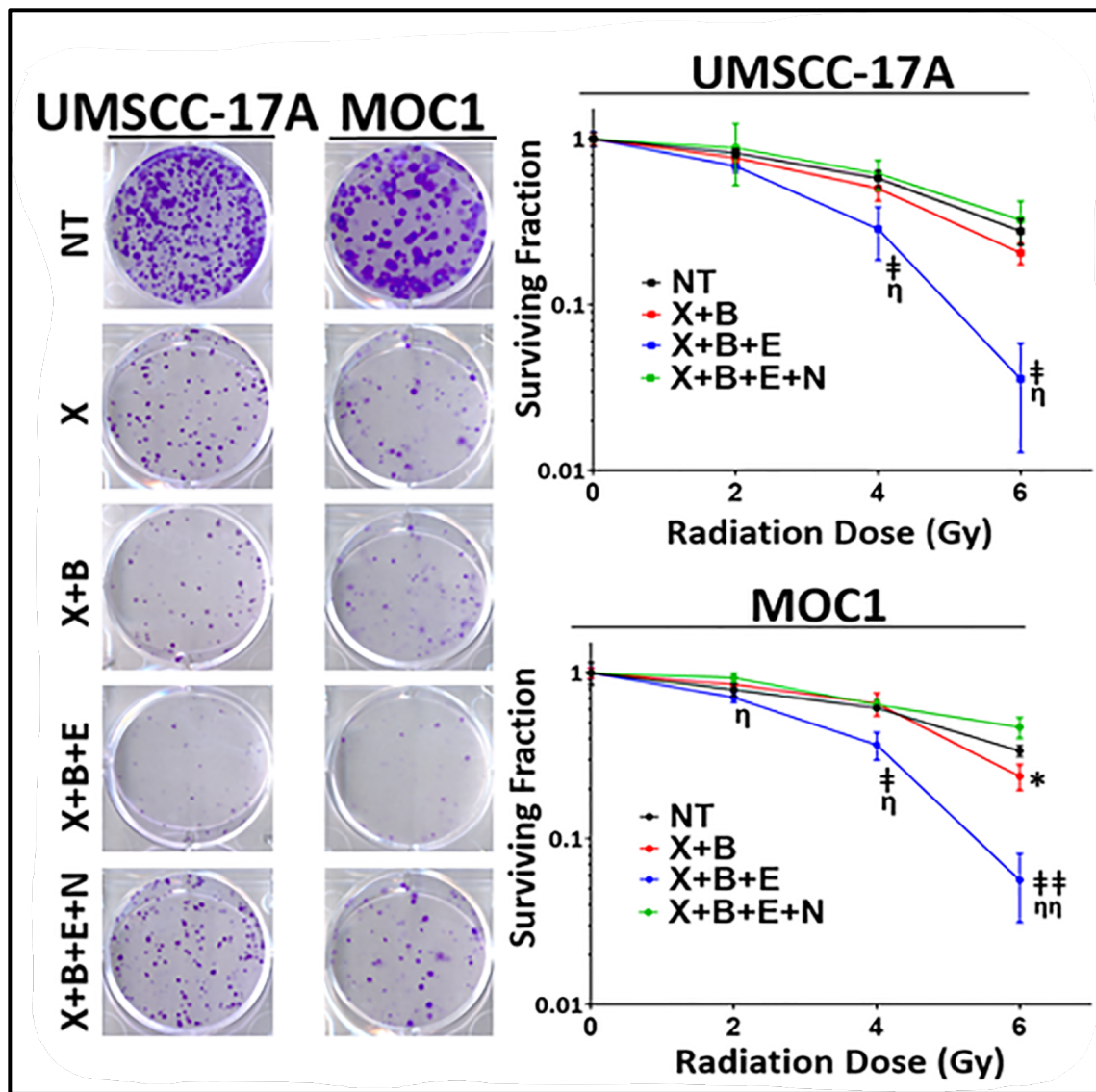
Figure-40: Chemical inhibition of Caspase-8 with emricasan potentiates reduction in clonogenic survival induced by Birinapant and radiation in HNSCCs. UMSCC-17A and MOC1 parental cells were treated with radiation (X [2, 4 and 6 Gy]), Birinapant (B [25nmol/L for the UMSCC-17A cells; 125nmol/L for the MOC1 cells]), emricasan (E [1μmol/L for both the cell lines]), Necrostatin-1s (N [10μmol/L for both the cell lines]) or the combinations as indicated for 24 hours. Representative images of clonogenic survival assays for the X(6Gy) conditions. 24 hour after treatments drug dilutions were washed out, colonies were allowed to form for 5-12 days, after which they were stained and counted. Surviving colony counts were normalized to nontreated cells (cells treated with no drugs) of each radiation dose from the same experiment. *log10* of surviving fractions were plotted. All treatments were carried out in triplicates. Student *t* test was used for statistics. *, P<0.05; when comparing X+B to X alone for the indicated radiation dose. ‡, P<0.05 and ‡‡, P<0.001; when comparing X+B+E to X alone for the indicated radiation doses. η, P<0.05 and ηη, P<0.001; when comparing X+B+E to X+B+E+N for the indicated radiation doses.

Chemical inhibition of CASP8 with emricasan potentiated radiation killing by Birinapant in both the UMSCC-17A and MOC1 cell lines through induction of necroptosis. Taken together, our results suggest that targeting the necroptosis pathway through pharmacological inhibition of CASP8 (with a clinically well-tolerated caspase inhibitor like emricasan) could be a viable therapeutic strategy to radiosensitize HNSCCs.

CHAPTER-X: DISCUSSION

CHAPTER-10: DISCUSSION

In this study, we found that CASP8 status regulates necroptotic death in HNSCC, and SMAC mimetic treatment may be useful to exploit this pathway for therapeutic benefit. SMAC mimetics have shown therapeutic potential in a variety of cancers, including HNSCC, through induction of cancer cell death directly or via synergistic interaction with other cytotoxic therapies such as chemotherapy, radiotherapy or immunotherapies (218, 329–334). Previous studies of HNSCC have reported that SMAC mimetics, including Birinapant, might synergize with radiation to delay tumor growth in various xenograft models (335–337). We show for the first time that inhibition of CASP8 function can lead to enhanced radiosensitization by Birinapant through induction of necroptotic death (**Chapter-5; Figures 23-26**). Since CASP8 mutant HNSCCs might be more radioresistant than their WT counterparts (**Chapter-3; Figure-16**), combining SMAC mimetics with radiation is a potentially promising therapeutic strategy to improve radiation response in HNSCCs with compromised CASP8 status, and this combination should be further investigated in future studies.

While previous reports have demonstrated that SMAC mimetics alone or in combination with radiation can suppress tumor cell growth in CASP8 WT HNSCC through induction of apoptosis (335, 337) we did not identify a large apoptotic component in most of the cell lines we analyzed. Rather, the apoptotic inhibitor zVAD-FMK enhanced cell death in our studies. This discrepancy may be due to the use of different HNSCC cell lines that reflect the genomic diversity of HNSCC. However, it may also indicate the broad therapeutic potential of these treatment combinations. It is likely that many HNSCC may

be sensitive to some type of cell death induced by a SMAC mimetic alone or in combination with radiation. The CASP8 status and other genomic alterations (FADD/BIRC2/BIRC3 amplification, RIP3 expression) may determine whether the death is necroptotic or apoptotic, but many genotypes will be sensitive. Additionally, we found that the mode of cell death for CASP8 WT cells can be pushed toward necroptosis by adding treatment with a caspase inhibitor, such as emricasan. The ability to tailor the mode of cell death could facilitate therapeutic synergy with other treatment agents, including immunotherapy.

Immunotherapy is an exciting new treatment modality for HNSCC and many other tumor types, however, only a minority of patients respond. Some tumors seems to have an immunologically cold microenvironment that prevents an immunologic response (361). It has been argued, and recently demonstrated (362) that activation of necroptotic death can potentiate antitumor immunity. Rapid permeabilization of cellular membranes is the underlying mechanism for necroptosis, a phenomenon that is characterized by the release of cytoplasmic cellular content into the extracellular space leading to exposure of **d**amage-**a**ssociated **m**olecular **p**atterns (DAMPs) such as Calreticulin (CRT), ATP and **H**igh **m**obility **g**roup **b**ox-1 protein (HMGB1) as well as cytokines and chemokines. Release of these molecules as part of necroptotic cell death mechanism underlies the immunogenic nature of necroptosis, which could be detrimental to healthy tissues but may be useful as a treatment for cancer through induction of secondary anti-tumor immune responses (368). DAMPs, when released from the dying tumor cells (e.g. cells that have undergone necroptosis) attract **a**ntigen **p**resenting **c**ells (APCs; e.g. dendritic cells and macrophages) in the tumor microenvironment and induce APC maturation

119

through engagement with their surface **P**attern **R**ecognition **R**eceptors (PRRs; e.g. **L**ow density lipoprotein **r**eceptor-related **p**rotein-1 [LRP-1, which recognizes CRT], **P**urinergic **R**eceptor **P$_2$X$_7$** [P$_2$RX$_7$, which recognizes ATP] and **T**oll-**l**ike **r**eceptor-4 [TLR4, which recognizes HMGB1]), leading to their activation and induction of anti-tumor immune responses (369). Consistent with this, in a study by Aaes *et. al*., inducible expression of Rip3 triggered necroptosis in a CT26 murine-derived colorectal carcinoma cell line, a phenomenon that was accompanied by release of ATP and HMGB1 from the dying tumor cells in *vitro* (370). In co-culture conditions, release of these DAMPs from the dying tumor cells stimulated *in vitro* maturation of bone marrow-derived dendritic cells (DCs). When necroptotic cells were used in a tumor vaccination model in immunocompetent BALB/c mice, they prevented tumor growth *in vivo*, a phenomenon that was associated with enhanced cross-priming, proliferation and IFN-γ production of CD8+ T cells obtained from the draining inguinal lymph nodes of mice (370). Moreover, cells that undergo necroptosis can release pro-inflammatory cytokines such as IL-1α and IL-6 (369). In a study by Schmidt *et. al*., treatment of the C4-I human-derived cervical carcinoma cell line with a **d**ouble-**s**tranded **RNA** (dsRNA) analog, **P**oly**i**nosinic-poly**c**ytidylic acid (poly(I:C)) induced necroptosis and RIP3-dependent IL-1α release from the dying tumor cells *in vitro*. Intriguingly, release of IL-1α from the necroptotic C4-I tumor cells was associated with enhanced IL-12 production by DCs in co-culture conditions (371). Taken together, these results highlight the immunogenic potential of necroptosis. It is, therefore, attractive to speculate that the treatments we have investigated could enhance responses to immunotherapy by inducing an immunogenic necroptotic death, a concept that is to be tested in future

studies using the syngeneic mouse oral cancer (MOC1) model. In light of the literature and our findings discussed in the previous chapters of this thesis, we hypothesize that inhibition and/or loss of CASP8 sensitizes HNSCCs to SMAC mimetic- or SMAC mimetic plus radiation-induced necroptosis leading to enhanced anti-tumor immune response *in vivo* (through mechanisms discussed above), characterized by enhanced APC maturation and cross-priming, proliferation and inflammatory cytokine production by cytotoxic CD8+ T cells, immunological events that predispose HNSCCs to immunotherapy such as immune checkpoint blockade (e.g. PD1 inhibitors such as nivolumab and pembrolizumab).

Caspase inhibition has generally not been thought of as a useful therapeutic approach for cancer because the goal is to promote cell death rather than block it. However, a previous report showed that the caspase inhibitor emricasan renders clinically relevant models of acute myeloid leukemia (AML) susceptible to Birinapant induced necroptosis *in vitro* and *in vivo* (363). In our study, emricasan significantly enhanced the radiosensitizing effects of Birinapant in two preclinical models of HNSCC, through induction of necroptosis (**Chapter-9; Figures 39-40**). Emricasan is well tolerated in patients and is being tested in humans for the treatment of liver diseases characterized by hepatic inflammation and fibrosis (364). It is interesting to propose the combination of Birinapant (or other SMAC mimetics such as ASTX660 or LCL161) and radiation with emricasan to inhibit apoptotic death but promote necroptotic death, thereby using caspase inhibition for cancer therapy.

Presence of RIP3 has been shown to be pivotal in determining the sensitivity of a variety of cancer types to necroptosis (356). In that study, the cancer cell lines that

showed lack of RIP3 expression were found to be resistant to the combination of TNFα, zVAD-FMK and the SMAC mimetic SM-164. Similarly, in another study where 8 colon cancer cell lines were tested for sensitivity to a TNFα, SMAC mimetic and zVAD-FMK combination, only those that were devoid of RIP3 at the mRNA and protein levels failed to undergo necroptosis (365). Consistent with these results, our data suggest that RIP3 loss can be an underlying mechanism by which HNSCCs become resistant to necroptotic death stimulated with Birinapant and zVAD-FMK (**Chapter-6; Figures 27-31**). Loss of protein expression of RIP3 in necroptosis-resistant HNSCCs coincided with low mRNA levels of *Rip3* (**Chapter-7; Figures 32-34**)*,* indicating a likely transcriptional regulation of RIP3. Intriguingly, in a study where mechanisms of RIP3 loss were investigated in various cancer cell lines, treatment of RIP3 lacking cells with the hypomethylating agent 5-aza-2′-deoxycytidine but not the proteosome inhibitor MG132 restored RIP3 expression. Further analyses conducted by the authors revealed that RIP3 loss in those cells was associated with methylation of 4 CpG islands located downstream of the transcription start site (TSS) of *Rip3* (358). Therefore, it is likely that DNA methylation is the underlying mechanism for loss of RIP3 in the preclinical models of HNSCC that we employed in our studies. Since cell lines grown in 2D culture are prone to increased DNA methylation (359) we evaluated RIP3 gene expression in HNSCC tumors using TCGA HNSCC dataset (**Chapter-7; Figure-34**). Analysis of TCGA tumors revealed that patient tumors show high levels of *Rip3*, providing justification for exploitation of necroptosis therapeutically in HNSCC, and suggesting that the silencing of RIP3 in some cell lines may be an artifact of 2D culture.

In conclusion, here we demonstrate that inhibition of CASP8 function enhances sensitivity of HNSCCs to Birinapant and Birinapant plus radiation through induction of necroptosis *in vitro* and *in vivo,* on the condition that RIP3 function is maintained. These results provide a strong clinical relevance for the combination of SMAC mimetics like Birinapant and radiation in CASP8 mutant HNSCCs, a therapeutic approach that might potentially be effective even in CASP8 wild-type patients with the use of a clinically tolerable caspase inhibitor, such as emricasan. Further studies to identify optimal and effective combination dose of emricasan with Birinapant and/or radiation *in vivo* are warranted as are combinations with immunotherapy.

REFERENCES

1. Ferlay, J., Colombet, M., Soerjomataram, I., Mathers, C., Parkin, D. M., Piñeros, M., Znaor, A., and Bray, F. (2019) Estimating the global cancer incidence and mortality in 2018: GLOBOCAN sources and methods. *Int. J. cancer*. **144**, 1941–1953

2. McDermott, J. D., and Bowles, D. W. (2019) Epidemiology of Head and Neck Squamous Cell Carcinomas: Impact on Staging and Prevention Strategies. *Curr. Treat. Options Oncol.* **20**, 43

3. Siegel, R. L., Miller, K. D., and Jemal, A. (2019) Cancer statistics, 2019. *CA. Cancer J. Clin.* **69**, 7–34

4. Chow, L. Q. M. (2020) Head and Neck Cancer. *N. Engl. J. Med.* **382**, 60–72

5. Kato, I., and Nomura, A. M. (1994) Alcohol in the aetiology of upper aerodigestive tract cancer. *Eur. J. Cancer. B. Oral Oncol.* **30B**, 75–81

6. Andre, K., Schraub, S., Mercier, M., and Bontemps, P. (1995) Role of alcohol and tobacco in the aetiology of head and neck cancer: a case-control study in the Doubs region of France. *Eur. J. Cancer. B. Oral Oncol.* **31B**, 301–9

7. Murata, M., Takayama, K., Choi, B. C., and Pak, A. W. (1996) A nested case-control study on alcohol drinking, tobacco smoking, and cancer. *Cancer Detect. Prev.* **20**, 557–65

8.   Hashibe, M., Brennan, P., Benhamou, S., Castellsague, X., Chen, C., Curado, M. P., Dal Maso, L., Daudt, A. W., Fabianova, E., Fernandez, L., Wünsch-Filho, V., Franceschi, S., Hayes, R. B., Herrero, R., Koifman, S., La Vecchia, C., Lazarus, P., Levi, F., Mates, D., Matos, E., Menezes, A., Muscat, J., Eluf-Neto, J., Olshan, A. F., Rudnai, P., Schwartz, S. M., Smith, E., Sturgis, E. M., Szeszenia-Dabrowska, N., Talamini, R., Wei, Q., Winn, D. M., Zaridze, D., Zatonski, W., Zhang, Z.-F., Berthiller, J., and Boffetta, P. (2007) Alcohol drinking in never users of tobacco, cigarette smoking in never drinkers, and the risk of head and neck cancer: pooled analysis in the International Head and Neck Cancer Epidemiology Consortium. *J. Natl. Cancer Inst.* **99**, 777–89

9.   Park, S., Bae, J., Nam, B.-H., and Yoo, K.-Y. Aetiology of cancer in Asia. *Asian Pac. J. Cancer Prev.* **9**, 371–80

10.   Trizna, Z., and Schantz, S. P. (1992) Hereditary and environmental factors associated with risk and progression of head and neck cancer. *Otolaryngol. Clin. North Am.* **25**, 1089–103

11.   Foulkes, W. D., Brunet, J. S., Sieh, W., Black, M. J., Shenouda, G., and Narod, S. A. (1996) Familial risks of squamous cell carcinoma of the head and neck: retrospective case-control study. *BMJ.* **313**, 716–21

12.   Cloos, J., Spitz, M. R., Schantz, S. P., Hsu, T. C., Zhang, Z. F., Tobi, H., Braakhuis, B. J., and Snow, G. B. (1996) Genetic susceptibility to head and neck squamous cell carcinoma. *J. Natl. Cancer Inst.* **88**, 530–5

13.   Kutler, D. I., Auerbach, A. D., Satagopan, J., Giampietro, P. F., Batish, S. D.,

Huvos, A. G., Goberdhan, A., Shah, J. P., and Singh, B. (2003) High incidence of head and neck squamous cell carcinoma in patients with Fanconi anemia. *Arch. Otolaryngol. Head. Neck Surg.* **129**, 106–12

14.   D'Souza, G., Kreimer, A. R., Viscidi, R., Pawlita, M., Fakhry, C., Koch, W. M., Westra, W. H., and Gillison, M. L. (2007) Case-control study of human papillomavirus and oropharyngeal cancer. *N. Engl. J. Med.* **356**, 1944–56

15.   Chaturvedi, A. K., Engels, E. A., Pfeiffer, R. M., Hernandez, B. Y., Xiao, W., Kim, E., Jiang, B., Goodman, M. T., Sibug-Saber, M., Cozen, W., Liu, L., Lynch, C. F., Wentzensen, N., Jordan, R. C., Altekruse, S., Anderson, W. F., Rosenberg, P. S., and Gillison, M. L. (2011) Human papillomavirus and rising oropharyngeal cancer incidence in the United States. *J. Clin. Oncol.* **29**, 4294–301

16.   Castellsagué, X., Alemany, L., Quer, M., Halec, G., Quirós, B., Tous, S., Clavero, O., Alòs, L., Biegner, T., Szafarowski, T., Alejo, M., Holzinger, D., Cadena, E., Claros, E., Hall, G., Laco, J., Poljak, M., Benevolo, M., Kasamatsu, E., Mehanna, H., Ndiaye, C., Guimerà, N., Lloveras, B., León, X., Ruiz-Cabezas, J. C., Alvarado-Cabrero, I., Kang, C.-S., Oh, J.-K., Garcia-Rojo, M., Iljazovic, E., Ajayi, O. F., Duarte, F., Nessa, A., Tinoco, L., Duran-Padilla, M. A., Pirog, E. C., Viarheichyk, H., Morales, H., Costes, V., Félix, A., Germar, M. J. V, Mena, M., Ruacan, A., Jain, A., Mehrotra, R., Goodman, M. T., Lombardi, L. E., Ferrera, A., Malami, S., Albanesi, E. I., Dabed, P., Molina, C., López-Revilla, R., Mandys, V., González, M. E., Velasco, J., Bravo, I. G., Quint, W., Pawlita, M., Muñoz, N., de Sanjosé, S., Xavier Bosch, F., and ICO International HPV in Head and Neck Cancer Study Group (2016) HPV Involvement in Head and Neck Cancers:

Comprehensive Assessment of Biomarkers in 3680 Patients. *J. Natl. Cancer Inst.* **108**, djv403

17.   Crosbie, E. J., Einstein, M. H., Franceschi, S., and Kitchener, H. C. (2013) Human papillomavirus and cervical cancer. *Lancet (London, England)*. **382**, 889–99

18.   Dyson, N., Howley, P. M., Münger, K., and Harlow, E. (1989) The human papilloma virus-16 E7 oncoprotein is able to bind to the retinoblastoma gene product. *Science*. **243**, 934–7

19.   Crook, T., Tidy, J. A., and Vousden, K. H. (1991) Degradation of p53 can be targeted by HPV E6 sequences distinct from those required for p53 binding and trans-activation. *Cell*. **67**, 547–56

20.   Chung, C. H., and Gillison, M. L. (2009) Human papillomavirus in head and neck cancer: its role in pathogenesis and clinical implications. *Clin. Cancer Res.* **15**, 6758–62

21.   Braakhuis, B. J. M., Snijders, P. J. F., Keune, W.-J. H., Meijer, C. J. L. M., Ruijter-Schippers, H. J., Leemans, C. R., and Brakenhoff, R. H. (2004) Genetic patterns in head and neck cancers that contain or lack transcriptionally active human papillomavirus. *J. Natl. Cancer Inst.* **96**, 998–1006

22.   Smeets, S. J., Braakhuis, B. J. M., Abbas, S., Snijders, P. J. F., Ylstra, B., van de Wiel, M. A., Meijer, G. A., Leemans, C. R., and Brakenhoff, R. H. (2006) Genome-wide DNA copy number alterations in head and neck squamous cell carcinomas with or without oncogene-expressing human papillomavirus. *Oncogene*. **25**, 2558–64

23. Slebos, R. J. C., Yi, Y., Ely, K., Carter, J., Evjen, A., Zhang, X., Shyr, Y., Murphy, B. M., Cmelak, A. J., Burkey, B. B., Netterville, J. L., Levy, S., Yarbrough, W. G., and Chung, C. H. (2006) Gene expression differences associated with human papillomavirus status in head and neck squamous cell carcinoma. *Clin. Cancer Res.* **12**, 701–9

24. Ang, K. K., Harris, J., Wheeler, R., Weber, R., Rosenthal, D. I., Nguyen-Tân, P. F., Westra, W. H., Chung, C. H., Jordan, R. C., Lu, C., Kim, H., Axelrod, R., Silverman, C. C., Redmond, K. P., and Gillison, M. L. (2010) Human papillomavirus and survival of patients with oropharyngeal cancer. *N. Engl. J. Med.* **363**, 24–35

25. Fakhry, C., Westra, W. H., Li, S., Cmelak, A., Ridge, J. A., Pinto, H., Forastiere, A., and Gillison, M. L. (2008) Improved survival of patients with human papillomavirus-positive head and neck squamous cell carcinoma in a prospective clinical trial. *J. Natl. Cancer Inst.* **100**, 261–9

26. Amin, M. B., Greene, F. L., Edge, S. B., Compton, C. C., Gershenwald, J. E., Brookland, R. K., Meyer, L., Gress, D. M., Byrd, D. R., and Winchester, D. P. (2017) The Eighth Edition AJCC Cancer Staging Manual: Continuing to build a bridge from a population-based to a more "personalized" approach to cancer staging. *CA. Cancer J. Clin.* **67**, 93–99

27. Lydiatt, W. M., Patel, S. G., O'Sullivan, B., Brandwein, M. S., Ridge, J. A., Migliacci, J. C., Loomis, A. M., and Shah, J. P. (2017) Head and Neck cancers-major changes in the American Joint Committee on cancer eighth edition cancer

staging manual. *CA. Cancer J. Clin.* **67**, 122–137

28.   Mirghani, H., and Blanchard, P. (2018) Treatment de-escalation for HPV-driven oropharyngeal cancer: Where do we stand? *Clin. Transl. Radiat. Oncol.* **8**, 4–11

29.   Brana, I., and Siu, L. L. (2012) Locally advanced head and neck squamous cell cancer: treatment choice based on risk factors and optimizing drug prescription. *Ann. Oncol. Off. J. Eur. Soc. Med. Oncol.* **23 Suppl 1**, x178-85

30.   Pignon, J.-P., le Maître, A., Maillard, E., Bourhis, J., and MACH-NC Collaborative Group (2009) Meta-analysis of chemotherapy in head and neck cancer (MACH-NC): an update on 93 randomised trials and 17,346 patients. *Radiother. Oncol.* **92**, 4–14

31.   Guan, J., Li, Q., Zhang, Y., Xiao, N., Chen, M., Zhang, Y., Li, L., and Chen, L. (2016) A meta-analysis comparing cisplatin-based to carboplatin-based chemotherapy in moderate to advanced squamous cell carcinoma of head and neck (SCCHN). *Oncotarget.* **7**, 7110–9

32.   Bonner, J. A., Harari, P. M., Giralt, J., Azarnia, N., Shin, D. M., Cohen, R. B., Jones, C. U., Sur, R., Raben, D., Jassem, J., Ove, R., Kies, M. S., Baselga, J., Youssoufian, H., Amellal, N., Rowinsky, E. K., and Ang, K. K. (2006) Radiotherapy plus cetuximab for squamous-cell carcinoma of the head and neck. *N. Engl. J. Med.* **354**, 567–78

33.   Ferris, R. L., Blumenschein, G., Fayette, J., Guigay, J., Colevas, A. D., Licitra, L., Harrington, K. J., Kasper, S., Vokes, E. E., Even, C., Worden, F., Saba, N. F., Docampo, L. C. I., Haddad, R., Rordorf, T., Kiyota, N., Tahara, M., Lynch, M.,

Jayaprakash, V., Li, L., and Gillison, M. L. (2018) Nivolumab vs investigator's choice in recurrent or metastatic squamous cell carcinoma of the head and neck: 2-year long-term survival update of CheckMate 141 with analyses by tumor PD-L1 expression. *Oral Oncol.* **81**, 45–51

34. Bronstein, D., and Akil, H. (1990) Effects of electrical stimulation in the periaqueductal gray on POMC peptides and mRNA in the rat brain. *Prog. Clin. Biol. Res.* **328**, 219–22

35. Leemans, C. R., Snijders, P. J. F., and Brakenhoff, R. H. (2018) The molecular landscape of head and neck cancer. *Nat. Rev. Cancer.* **18**, 269–282

36. Califano, J., van der Riet, P., Westra, W., Nawroz, H., Clayman, G., Piantadosi, S., Corio, R., Lee, D., Greenberg, B., Koch, W., and Sidransky, D. (1996) Genetic progression model for head and neck cancer: implications for field cancerization. *Cancer Res.* **56**, 2488–92

37. Villa, A., and Woo, S. Bin (2017) Leukoplakia-A Diagnostic and Management Algorithm. *J. Oral Maxillofac. Surg.* **75**, 723–734

38. Napier, S. S., and Speight, P. M. (2008) Natural history of potentially malignant oral lesions and conditions: an overview of the literature. *J. Oral Pathol. Med.* **37**, 1–10

39. SLAUGHTER, D. P., SOUTHWICK, H. W., and SMEJKAL, W. (1953) Field cancerization in oral stratified squamous epithelium; clinical implications of multicentric origin. *Cancer.* **6**, 963–8

40. Curtius, K., Wright, N. A., and Graham, T. A. (2018) An evolutionary perspective on field cancerization. *Nat. Rev. Cancer*. **18**, 19–32

41. Ryser, M. D., Lee, W. T., Ready, N. E., Leder, K. Z., and Foo, J. (2016) Quantifying the Dynamics of Field Cancerization in Tobacco-Related Head and Neck Cancer: A Multiscale Modeling Approach. *Cancer Res.* **76**, 7078–7088

42. Sabharwal, R., Mahendra, A., Moon, N. J., Gupta, P., Jain, A., and Gupta, S. (2014) Genetically altered fields in head and neck cancer and second field tumor. *South Asian J. cancer*. **3**, 151–3

43. Leemans, C. R., Braakhuis, B. J. M., and Brakenhoff, R. H. (2011) The molecular biology of head and neck cancer. *Nat. Rev. Cancer*. **11**, 9–22

44. Jonason, A. S., Kunala, S., Price, G. J., Restifo, R. J., Spinelli, H. M., Persing, J. A., Leffell, D. J., Tarone, R. E., and Brash, D. E. (1996) Frequent clones of p53-mutated keratinocytes in normal human skin. *Proc. Natl. Acad. Sci. U. S. A.* **93**, 14025–9

45. van Houten, V. M. M., Tabor, M. P., van den Brekel, M. W. M., Kummer, J. A., Denkers, F., Dijkstra, J., Leemans, R., van der Waal, I., Snow, G. B., and Brakenhoff, R. H. (2002) Mutated p53 as a molecular marker for the diagnosis of head and neck cancer. *J. Pathol.* **198**, 476–86

46. van der Riet, P., Nawroz, H., Hruban, R. H., Corio, R., Tokino, K., Koch, W., and Sidransky, D. (1994) Frequent loss of chromosome 9p21-22 early in head and neck cancer progression. *Cancer Res.* **54**, 1156–8

47. Reed, A. L., Califano, J., Cairns, P., Westra, W. H., Jones, R. M., Koch, W., Ahrendt, S., Eby, Y., Sewell, D., Nawroz, H., Bartek, J., and Sidransky, D. (1996) High frequency of p16 (CDKN2/MTS-1/INK4A) inactivation in head and neck squamous cell carcinoma. *Cancer Res.* **56**, 3630–3

48. Lee, J. W., Soung, Y. H., Kim, S. Y., Nam, H. K., Park, W. S., Nam, S. W., Kim, M. S., Sun, D. II, Lee, Y. S., Jang, J. J., Lee, J. Y., Yoo, N. J., and Lee, S. H. (2005) Somatic mutations of EGFR gene in squamous cell carcinoma of the head and neck. *Clin. Cancer Res.* **11**, 2879–82

49. Sheu, J. J.-C., Hua, C.-H., Wan, L., Lin, Y.-J., Lai, M.-T., Tseng, H.-C., Jinawath, N., Tsai, M.-H., Chang, N.-W., Lin, C.-F., Lin, C.-C., Hsieh, L.-J., Wang, T.-L., Shih, I.-M., and Tsai, F.-J. (2009) Functional genomic analysis identified epidermal growth factor receptor activation as the most common genetic event in oral squamous cell carcinoma. *Cancer Res.* **69**, 2568–76

50. Seiwert, T. Y., Jagadeeswaran, R., Faoro, L., Janamanchi, V., Nallasura, V., El Dinali, M., Yala, S., Kanteti, R., Cohen, E. E. W., Lingen, M. W., Martin, L., Krishnaswamy, S., Klein-Szanto, A., Christensen, J. G., Vokes, E. E., and Salgia, R. (2009) The MET receptor tyrosine kinase is a potential novel therapeutic target for head and neck squamous cell carcinoma. *Cancer Res.* **69**, 3021–31

51. Kozaki, K., Imoto, I., Pimkhaokham, A., Hasegawa, S., Tsuda, H., Omura, K., and Inazawa, J. (2006) PIK3CA mutation is an oncogenic aberration at advanced stages of oral squamous cell carcinoma. *Cancer Sci.* **97**, 1351–8

52. Qiu, W., Schönleben, F., Li, X., Ho, D. J., Close, L. G., Manolidis, S., Bennett, B.

P., and Su, G. H. (2006) PIK3CA mutations in head and neck squamous cell carcinoma. *Clin. Cancer Res.* **12**, 1441–6

53. Okami, K., Wu, L., Riggins, G., Cairns, P., Goggins, M., Evron, E., Halachmi, N., Ahrendt, S. A., Reed, A. L., Hilgers, W., Kern, S. E., Koch, W. M., Sidransky, D., and Jen, J. (1998) Analysis of PTEN/MMAC1 alterations in aerodigestive tract tumors. *Cancer Res.* **58**, 509–11

54. Hermsen, M., Guervós, M. A., Meijer, G., Baak, J., van Diest, P., Marcos, C. A., and Sampedro, A. (2001) New chromosomal regions with high-level amplifications in squamous cell carcinomas of the larynx and pharynx, identified by comparative genomic hybridization. *J. Pathol.* **194**, 177–82

55. Jin, C., Jin, Y., Wennerberg, J., Annertz, K., Enoksson, J., and Mertens, F. (2006) Cytogenetic abnormalities in 106 oral squamous cell carcinomas. *Cancer Genet. Cytogenet.* **164**, 44–53

56. Kastan, M. B., and Bartek, J. (2004) Cell-cycle checkpoints and cancer. *Nature.* **432**, 316–23

57. Poeta, M. L., Manola, J., Goldwasser, M. A., Forastiere, A., Benoit, N., Califano, J. A., Ridge, J. A., Goodwin, J., Kenady, D., Saunders, J., Westra, W., Sidransky, D., and Koch, W. M. (2007) TP53 mutations and survival in squamous-cell carcinoma of the head and neck. *N. Engl. J. Med.* **357**, 2552–61

58. Balz, V., Scheckenbach, K., Götte, K., Bockmühl, U., Petersen, I., and Bier, H. (2003) Is the p53 inactivation frequency in squamous cell carcinomas of the head and neck underestimated? Analysis of p53 exons 2-11 and human papillomavirus

16/18 E6 transcripts in 123 unselected tumor specimens. *Cancer Res.* **63**, 1188–91

59. Opitz, O. G., Suliman, Y., Hahn, W. C., Harada, H., Blum, H. E., and Rustgi, A. K. (2001) Cyclin D1 overexpression and p53 inactivation immortalize primary oral keratinocytes by a telomerase-independent mechanism. *J. Clin. Invest.* **108**, 725–32

60. Agrawal, N., Frederick, M. J., Pickering, C. R., Bettegowda, C., Chang, K., Li, R. J., Fakhry, C., Xie, T.-X., Zhang, J., Wang, J., Zhang, N., El-Naggar, A. K., Jasser, S. A., Weinstein, J. N., Treviño, L., Drummond, J. A., Muzny, D. M., Wu, Y., Wood, L. D., Hruban, R. H., Westra, W. H., Koch, W. M., Califano, J. A., Gibbs, R. A., Sidransky, D., Vogelstein, B., Velculescu, V. E., Papadopoulos, N., Wheeler, D. A., Kinzler, K. W., and Myers, J. N. (2011) Exome sequencing of head and neck squamous cell carcinoma reveals inactivating mutations in NOTCH1. *Science.* **333**, 1154–7

61. Stransky, N., Egloff, A. M., Tward, A. D., Kostic, A. D., Cibulskis, K., Sivachenko, A., Kryukov, G. V, Lawrence, M. S., Sougnez, C., McKenna, A., Shefler, E., Ramos, A. H., Stojanov, P., Carter, S. L., Voet, D., Cortés, M. L., Auclair, D., Berger, M. F., Saksena, G., Guiducci, C., Onofrio, R. C., Parkin, M., Romkes, M., Weissfeld, J. L., Seethala, R. R., Wang, L., Rangel-Escareño, C., Fernandez-Lopez, J. C., Hidalgo-Miranda, A., Melendez-Zajgla, J., Winckler, W., Ardlie, K., Gabriel, S. B., Meyerson, M., Lander, E. S., Getz, G., Golub, T. R., Garraway, L. A., and Grandis, J. R. (2011) The mutational landscape of head and neck squamous cell carcinoma. *Science.* **333**, 1157–60

62. Cancer Genome Atlas Network (2015) Comprehensive genomic characterization of head and neck squamous cell carcinomas. *Nature*. **517**, 576–82

63. Moody, C. A., and Laimins, L. A. (2010) Human papillomavirus oncoproteins: pathways to transformation. *Nat. Rev. Cancer*. **10**, 550–60

64. Gross, A. M., Orosco, R. K., Shen, J. P., Egloff, A. M., Carter, H., Hofree, M., Choueiri, M., Coffey, C. S., Lippman, S. M., Hayes, D. N., Cohen, E. E., Grandis, J. R., Nguyen, Q. T., and Ideker, T. (2014) Multi-tiered genomic analysis of head and neck cancer ties TP53 mutation to 3p loss. *Nat. Genet.* **46**, 939–43

65. Stupack, D. G. (2013) Caspase-8 as a therapeutic target in cancer. *Cancer Lett.* **332**, 133–40

66. Hopkins-Donaldson, S., Bodmer, J. L., Bourloud, K. B., Brognara, C. B., Tschopp, J., and Gross, N. (2000) Loss of caspase-8 expression in highly malignant human neuroblastoma cells correlates with resistance to tumor necrosis factor-related apoptosis-inducing ligand-induced apoptosis. *Cancer Res.* **60**, 4315–9

67. Teitz, T., Lahti, J. M., and Kidd, V. J. (2001) Aggressive childhood neuroblastomas do not express caspase-8: an important component of programmed cell death. *J. Mol. Med. (Berl).* **79**, 428–36

68. Ebinger, M., Senf, L., Wachowski, O., and Scheurlen, W. (2004) Promoter methylation pattern of caspase-8, P16INK4A, MGMT, TIMP-3, and E-cadherin in medulloblastoma. *Pathol. Oncol. Res.* **10**, 17–21

69. Martinez, R., Setien, F., Voelter, C., Casado, S., Quesada, M. P., Schackert, G.,

and Esteller, M. (2007) CpG island promoter hypermethylation of the pro-apoptotic gene caspase-8 is a common hallmark of relapsed glioblastoma multiforme. *Carcinogenesis*. **28**, 1264–8

70.   Grotzer, M. A., Eggert, A., Zuzak, T. J., Janss, A. J., Marwaha, S., Wiewrodt, B. R., Ikegaki, N., Brodeur, G. M., and Phillips, P. C. (2000) Resistance to TRAIL-induced apoptosis in primitive neuroectodermal brain tumor cells correlates with a loss of caspase-8 expression. *Oncogene*. **19**, 4604–10

71.   Shivapurkar, N., Toyooka, S., Eby, M. T., Huang, C. X., Sathyanarayana, U. G., Cunningham, H. T., Reddy, J. L., Brambilla, E., Takahashi, T., Minna, J. D., Chaudhary, P. M., and Gazdar, A. F. Differential inactivation of caspase-8 in lung cancers. *Cancer Biol. Ther.* **1**, 65–9

72.   Kim, H. S., Lee, J. W., Soung, Y. H., Park, W. S., Kim, S. Y., Lee, J. H., Park, J. Y., Cho, Y. G., Kim, C. J., Jeong, S. W., Nam, S. W., Kim, S. H., Lee, J. Y., Yoo, N. J., and Lee, S. H. (2003) Inactivating mutations of caspase-8 gene in colorectal carcinomas. *Gastroenterology*. **125**, 708–15

73.   Soung, Y. H., Lee, J. W., Kim, S. Y., Jang, J., Park, Y. G., Park, W. S., Nam, S. W., Lee, J. Y., Yoo, N. J., and Lee, S. H. (2005) CASPASE-8 gene is inactivated by somatic mutations in gastric carcinomas. *Cancer Res.* **65**, 815–21

74.   Pickering, C. R., Zhang, J., Yoo, S. Y., Bengtsson, L., Moorthy, S., Neskey, D. M., Zhao, M., Ortega Alves, M. V, Chang, K., Drummond, J., Cortez, E., Xie, T.-X., Zhang, D., Chung, W., Issa, J.-P. J., Zweidler-McKay, P. A., Wu, X., El-Naggar, A. K., Weinstein, J. N., Wang, J., Muzny, D. M., Gibbs, R. A., Wheeler, D. A., Myers,

J. N., and Frederick, M. J. (2013) Integrative genomic characterization of oral squamous cell carcinoma identifies frequent somatic drivers. *Cancer Discov.* **3**, 770–81

75. Kesavardhana, S., Malireddi, R. K. S., and Kanneganti, T.-D. (2020) Caspases in Cell Death, Inflammation, and Gasdermin-Induced Pyroptosis. *Annu. Rev. Immunol.* 10.1146/annurev-immunol-073119-095439

76. Kantari, C., and Walczak, H. (2011) Caspase-8 and bid: caught in the act between death receptors and mitochondria. *Biochim. Biophys. Acta*. **1813**, 558–63

77. Alnemri, E. S., Livingston, D. J., Nicholson, D. W., Salvesen, G., Thornberry, N. A., Wong, W. W., and Yuan, J. (1996) Human ICE/CED-3 protease nomenclature. *Cell*. **87**, 171

78. Man, S. M., and Kanneganti, T.-D. (2016) Converging roles of caspases in inflammasome activation, cell death and innate immunity. *Nat. Rev. Immunol.* **16**, 7–21

79. Ramirez, M. L. G., and Salvesen, G. S. (2018) A primer on caspase mechanisms. *Semin. Cell Dev. Biol.* **82**, 79–85

80. Galluzzi, L., López-Soto, A., Kumar, S., and Kroemer, G. (2016) Caspases Connect Cell-Death Signaling to Organismal Homeostasis. *Immunity*. **44**, 221–31

81. Lamkanfi, M., Declercq, W., Kalai, M., Saelens, X., and Vandenabeele, P. (2002) Alice in caspase land. A phylogenetic analysis of caspases from worm to man.

Cell Death Differ. **9**, 358–61

82. Siegel, R. M. (2006) Caspases at the crossroads of immune-cell life and death. *Nat. Rev. Immunol.* **6**, 308–17

83. Martinon, F., Burns, K., and Tschopp, J. (2002) The inflammasome: a molecular platform triggering activation of inflammatory caspases and processing of proIL-beta. *Mol. Cell*. **10**, 417–26

84. Itoh, N., Yonehara, S., Ishii, A., Yonehara, M., Mizushima, S., Sameshima, M., Hase, A., Seto, Y., and Nagata, S. (1991) The polypeptide encoded by the cDNA for human cell surface antigen Fas can mediate apoptosis. *Cell*. **66**, 233–43

85. Oehm, A., Behrmann, I., Falk, W., Pawlita, M., Maier, G., Klas, C., Li-Weber, M., Richards, S., Dhein, J., and Trauth, B. C. (1992) Purification and molecular cloning of the APO-1 cell surface antigen, a member of the tumor necrosis factor/nerve growth factor receptor superfamily. Sequence identity with the Fas antigen. *J. Biol. Chem.* **267**, 10709–15

86. Schneider, P., Bodmer, J. L., Thome, M., Hofmann, K., Holler, N., and Tschopp, J. (1997) Characterization of two receptors for TRAIL. *FEBS Lett.* **416**, 329–34

87. Pan, G., O'Rourke, K., Chinnaiyan, A. M., Gentz, R., Ebner, R., Ni, J., and Dixit, V. M. (1997) The receptor for the cytotoxic ligand TRAIL. *Science*. **276**, 111–3

88. Screaton, G. R., Mongkolsapaya, J., Xu, X. N., Cowper, A. E., McMichael, A. J., and Bell, J. I. (1997) TRICK2, a new alternatively spliced receptor that transduces the cytotoxic signal from TRAIL. *Curr. Biol.* **7**, 693–6

89. Walczak, H., Degli-Esposti, M. A., Johnson, R. S., Smolak, P. J., Waugh, J. Y., Boiani, N., Timour, M. S., Gerhart, M. J., Schooley, K. A., Smith, C. A., Goodwin, R. G., and Rauch, C. T. (1997) TRAIL-R2: a novel apoptosis-mediating receptor for TRAIL. *EMBO J.* **16**, 5386–97

90. Sheridan, J. P., Marsters, S. A., Pitti, R. M., Gurney, A., Skubatch, M., Baldwin, D., Ramakrishnan, L., Gray, C. L., Baker, K., Wood, W. I., Goddard, A. D., Godowski, P., and Ashkenazi, A. (1997) Control of TRAIL-induced apoptosis by a family of signaling and decoy receptors. *Science*. **277**, 818–21

91. MacFarlane, M., Ahmad, M., Srinivasula, S. M., Fernandes-Alnemri, T., Cohen, G. M., and Alnemri, E. S. (1997) Identification and molecular cloning of two novel receptors for the cytotoxic ligand TRAIL. *J. Biol. Chem.* **272**, 25417–20

92. Loetscher, H., Pan, Y. C., Lahm, H. W., Gentz, R., Brockhaus, M., Tabuchi, H., and Lesslauer, W. (1990) Molecular cloning and expression of the human 55 kd tumor necrosis factor receptor. *Cell*. **61**, 351–9

93. Schall, T. J., Lewis, M., Koller, K. J., Lee, A., Rice, G. C., Wong, G. H., Gatanaga, T., Granger, G. A., Lentz, R., and Raab, H. (1990) Molecular cloning and expression of a receptor for human tumor necrosis factor. *Cell*. **61**, 361–70

94. Chinnaiyan, A. M., O'Rourke, K., Yu, G. L., Lyons, R. H., Garg, M., Duan, D. R., Xing, L., Gentz, R., Ni, J., and Dixit, V. M. (1996) Signal transduction by DR3, a death domain-containing receptor related to TNFR-1 and CD95. *Science*. **274**, 990–2

95. Bodmer, J. L., Burns, K., Schneider, P., Hofmann, K., Steiner, V., Thome, M.,

Bornand, T., Hahne, M., Schröter, M., Becker, K., Wilson, A., French, L. E., Browning, J. L., MacDonald, H. R., and Tschopp, J. (1997) TRAMP, a novel apoptosis-mediating receptor with sequence homology to tumor necrosis factor receptor 1 and Fas(Apo-1/CD95). *Immunity*. **6**, 79–88

96. Suda, T., Takahashi, T., Golstein, P., and Nagata, S. (1993) Molecular cloning and expression of the Fas ligand, a novel member of the tumor necrosis factor family. *Cell*. **75**, 1169–78

97. Pitti, R. M., Marsters, S. A., Ruppert, S., Donahue, C. J., Moore, A., and Ashkenazi, A. (1996) Induction of apoptosis by Apo-2 ligand, a new member of the tumor necrosis factor cytokine family. *J. Biol. Chem.* **271**, 12687–90

98. Wiley, S. R., Schooley, K., Smolak, P. J., Din, W. S., Huang, C. P., Nicholl, J. K., Sutherland, G. R., Smith, T. D., Rauch, C., and Smith, C. A. (1995) Identification and characterization of a new member of the TNF family that induces apoptosis. *Immunity*. **3**, 673–82

99. Carswell, E. A., Old, L. J., Kassel, R. L., Green, S., Fiore, N., and Williamson, B. (1975) An endotoxin-induced serum factor that causes necrosis of tumors. *Proc. Natl. Acad. Sci. U. S. A.* **72**, 3666–70

100. Migone, T. S., Zhang, J., Luo, X., Zhuang, L., Chen, C., Hu, B., Hong, J. S., Perry, J. W., Chen, S. F., Zhou, J. X. H., Cho, Y. H., Ullrich, S., Kanakaraj, P., Carrell, J., Boyd, E., Olsen, H. S., Hu, G., Pukac, L., Liu, D., Ni, J., Kim, S., Gentz, R., Feng, P., Moore, P. A., Ruben, S. M., and Wei, P. (2002) TL1A is a TNF-like ligand for DR3 and TR6/DcR3 and functions as a T cell costimulator. *Immunity*. **16**, 479–92

101. Deveraux, Q. L., Takahashi, R., Salvesen, G. S., and Reed, J. C. (1997) X-linked IAP is a direct inhibitor of cell-death proteases. *Nature*. **388**, 300–4

102. Blanchard, H., Donepudi, M., Tschopp, M., Kodandapani, L., Wu, J. C., and Grütter, M. G. (2000) Caspase-8 specificity probed at subsite S(4): crystal structure of the caspase-8-Z-DEVD-cho complex. *J. Mol. Biol.* **302**, 9–16

103. Blanchard, H., Kodandapani, L., Mittl, P. R., Marco, S. D., Krebs, J. F., Wu, J. C., Tomaselli, K. J., and Grütter, M. G. (1999) The three-dimensional structure of caspase-8: an initiator enzyme in apoptosis. *Structure*. **7**, 1125–33

104. Park, H. H., Lo, Y.-C., Lin, S.-C., Wang, L., Yang, J. K., and Wu, H. (2007) The death domain superfamily in intracellular signaling of apoptosis and inflammation. *Annu. Rev. Immunol.* **25**, 561–86

105. Henry, C. M., and Martin, S. J. (2017) Caspase-8 Acts in a Non-enzymatic Role as a Scaffold for Assembly of a Pro-inflammatory "FADDosome" Complex upon TRAIL Stimulation. *Mol. Cell*. **65**, 715-729.e5

106. Croft, M., and Siegel, R. M. (2017) Beyond TNF: TNF superfamily cytokines as targets for the treatment of rheumatic diseases. *Nat. Rev. Rheumatol.* **13**, 217–233

107. Silke, J., and Brink, R. (2010) Regulation of TNFRSF and innate immune signalling complexes by TRAFs and cIAPs. *Cell Death Differ.* **17**, 35–45

108. Karin, M., and Gallagher, E. (2009) TNFR signaling: ubiquitin-conjugated TRAFfic signals control stop-and-go for MAPK signaling complexes. *Immunol. Rev.* **228**,

225–40

109. Micheau, O., and Tschopp, J. (2003) Induction of TNF receptor I-mediated apoptosis via two sequential signaling complexes. *Cell*. **114**, 181–90

110. Mandal, R., Barrón, J. C., Kostova, I., Becker, S., and Strebhardt, K. (2020) Caspase-8: The double-edged sword. *Biochim. Biophys. acta. Rev. cancer*. **1873**, 188357

111. Shen, C., Pei, J., Guo, X., Zhou, L., Li, Q., and Quan, J. (2018) Structural basis for dimerization of the death effector domain of the F122A mutant of Caspase-8. *Sci. Rep.* **8**, 16723

112. Grönholm, M., Sainio, M., Zhao, F., Heiska, L., Vaheri, A., and Carpén, O. (1999) Homotypic and heterotypic interaction of the neurofibromatosis 2 tumor suppressor protein merlin and the ERM protein ezrin. *J. Cell Sci.* **112 (Pt 6**, 895–904

113. Hughes, M. A., Harper, N., Butterworth, M., Cain, K., Cohen, G. M., and MacFarlane, M. (2009) Reconstitution of the death-inducing signaling complex reveals a substrate switch that determines CD95-mediated death or survival. *Mol. Cell*. **35**, 265–79

114. Dickens, L. S., Boyd, R. S., Jukes-Jones, R., Hughes, M. A., Robinson, G. L., Fairall, L., Schwabe, J. W. R., Cain, K., and Macfarlane, M. (2012) A death effector domain chain DISC model reveals a crucial role for caspase-8 chain assembly in mediating apoptotic cell death. *Mol. Cell*. **47**, 291–305

115. Siegel, R. M., Martin, D. A., Zheng, L., Ng, S. Y., Bertin, J., Cohen, J., and Lenardo, M. J. (1998) Death-effector filaments: novel cytoplasmic structures that recruit caspases and trigger apoptosis. *J. Cell Biol.* **141**, 1243–53

116. Schleich, K., Warnken, U., Fricker, N., Oztürk, S., Richter, P., Kammerer, K., Schnölzer, M., Krammer, P. H., and Lavrik, I. N. (2012) Stoichiometry of the CD95 death-inducing signaling complex: experimental and modeling evidence for a death effector domain chain model. *Mol. Cell*. **47**, 306–19

117. Hoffmann, J. C., Pappa, A., Krammer, P. H., and Lavrik, I. N. (2009) A new C-terminal cleavage product of procaspase-8, p30, defines an alternative pathway of procaspase-8 activation. *Mol. Cell. Biol.* **29**, 4431–40

118. Shi, Y. (2004) Caspase activation: revisiting the induced proximity model. *Cell*. **117**, 855–8

119. Salvesen, G. S., and Dixit, V. M. (1999) Caspase activation: the induced-proximity model. *Proc. Natl. Acad. Sci. U. S. A.* **96**, 10964–7

120. Boatright, K. M., Renatus, M., Scott, F. L., Sperandio, S., Shin, H., Pedersen, I. M., Ricci, J. E., Edris, W. A., Sutherlin, D. P., Green, D. R., and Salvesen, G. S. (2003) A unified model for apical caspase activation. *Mol. Cell*. **11**, 529–41

121. Donepudi, M., Mac Sweeney, A., Briand, C., and Grütter, M. G. (2003) Insights into the regulatory mechanism for caspase-8 activation. *Mol. Cell*. **11**, 543–9

122. Zhao, Y., Sui, X., and Ren, H. (2010) From procaspase-8 to caspase-8: revisiting structural functions of caspase-8. *J. Cell. Physiol.* **225**, 316–20

123. Mandal, R., Raab, M., Matthess, Y., Becker, S., Knecht, R., and Strebhardt, K. (2014) pERK 1/2 inhibit Caspase-8 induced apoptosis in cancer cells by phosphorylating it in a cell cycle specific manner. *Mol. Oncol.* **8**, 232–49

124. Ozören, N., and El-Deiry, W. S. Defining characteristics of Types I and II apoptotic cells in response to TRAIL. *Neoplasia*. **4**, 551–7

125. Chang, D. W., Xing, Z., Capacio, V. L., Peter, M. E., and Yang, X. (2003) Interdimer processing mechanism of procaspase-8 activation. *EMBO J.* **22**, 4132–42

126. Medema, J. P., Scaffidi, C., Kischkel, F. C., Shevchenko, A., Mann, M., Krammer, P. H., and Peter, M. E. (1997) FLICE is activated by association with the CD95 death-inducing signaling complex (DISC). *EMBO J.* **16**, 2794–804

127. Chang, D. W., Xing, Z., Pan, Y., Algeciras-Schimnich, A., Barnhart, B. C., Yaish-Ohad, S., Peter, M. E., and Yang, X. (2002) c-FLIP(L) is a dual function regulator for caspase-8 activation and CD95-mediated apoptosis. *EMBO J.* **21**, 3704–14

128. Micheau, O., Thome, M., Schneider, P., Holler, N., Tschopp, J., Nicholson, D. W., Briand, C., and Grütter, M. G. (2002) The long form of FLIP is an activator of caspase-8 at the Fas death-inducing signaling complex. *J. Biol. Chem.* **277**, 45162–71

129. Oberst, A., Pop, C., Tremblay, A. G., Blais, V., Denault, J.-B., Salvesen, G. S., and Green, D. R. (2010) Inducible dimerization and inducible cleavage reveal a requirement for both processes in caspase-8 activation. *J. Biol. Chem.* **285**, 16632–42

130. Scaffidi, C., Schmitz, I., Krammer, P. H., and Peter, M. E. (1999) The role of c-FLIP in modulation of CD95-induced apoptosis. *J. Biol. Chem.* **274**, 1541–8

131. Tsuchiya, Y., Nakabayashi, O., and Nakano, H. (2015) FLIP the Switch: Regulation of Apoptosis and Necroptosis by cFLIP. *Int. J. Mol. Sci.* **16**, 30321–41

132. Ueffing, N., Singh, K. K., Christians, A., Thorns, C., Feller, A. C., Nagl, F., Fend, F., Heikaus, S., Marx, A., Zotz, R. B., Brade, J., Schulz, W. A., Schulze-Osthoff, K., Schmitz, I., and Schwerk, C. (2009) A single nucleotide polymorphism determines protein isoform production of the human c-FLIP protein. *Blood*. **114**, 572–9

133. Golks, A., Brenner, D., Fritsch, C., Krammer, P. H., and Lavrik, I. N. (2005) c-FLIPR, a new regulator of death receptor-induced apoptosis. *J. Biol. Chem.* **280**, 14507–13

134. Safa, A. R. (2012) c-FLIP, a master anti-apoptotic regulator. *Exp. Oncol.* **34**, 176–84

135. Boatright, K. M., Deis, C., Denault, J.-B., Sutherlin, D. P., and Salvesen, G. S. (2004) Activation of caspases-8 and -10 by FLIP(L). *Biochem. J.* **382**, 651–7

136. Yu, J. W., Jeffrey, P. D., and Shi, Y. (2009) Mechanism of procaspase-8 activation by c-FLIPL. *Proc. Natl. Acad. Sci. U. S. A.* **106**, 8169–74

137. Hughes, M. A., Powley, I. R., Jukes-Jones, R., Horn, S., Feoktistova, M., Fairall, L., Schwabe, J. W. R., Leverkus, M., Cain, K., and MacFarlane, M. (2016) Co-operative and Hierarchical Binding of c-FLIP and Caspase-8: A Unified Model

Defines How c-FLIP Isoforms Differentially Control Cell Fate. *Mol. Cell*. **61**, 834–49

138. Schleich, K., Buchbinder, J. H., Pietkiewicz, S., Kähne, T., Warnken, U., Öztürk, S., Schnölzer, M., Naumann, M., Krammer, P. H., and Lavrik, I. N. (2016) Molecular architecture of the DED chains at the DISC: regulation of procaspase-8 activation by short DED proteins c-FLIP and procaspase-8 prodomain. *Cell Death Differ.* **23**, 681–94

139. Tummers, B., and Green, D. R. (2017) Caspase-8: regulating life and death. *Immunol. Rev.* **277**, 76–89

140. Helmke, C., Raab, M., Rödel, F., Matthess, Y., Oellerich, T., Mandal, R., Sanhaji, M., Urlaub, H., Rödel, C., Becker, S., and Strebhardt, K. (2016) Ligand stimulation of CD95 induces activation of Plk3 followed by phosphorylation of caspase-8. *Cell Res.* **26**, 914–34

141. Matthess, Y., Raab, M., Knecht, R., Becker, S., and Strebhardt, K. (2014) Sequential Cdk1 and Plk1 phosphorylation of caspase-8 triggers apoptotic cell death during mitosis. *Mol. Oncol.* **8**, 596–608

142. Powley, I. R., Hughes, M. A., Cain, K., and MacFarlane, M. (2016) Caspase-8 tyrosine-380 phosphorylation inhibits CD95 DISC function by preventing procaspase-8 maturation and cycling within the complex. *Oncogene*. **35**, 5629–5640

143. Jin, Z., Li, Y., Pitti, R., Lawrence, D., Pham, V. C., Lill, J. R., and Ashkenazi, A. (2009) Cullin3-based polyubiquitination and p62-dependent aggregation of

caspase-8 mediate extrinsic apoptosis signaling. *Cell*. **137**, 721–35

144. Békés, M., and Salvesen, G. S. (2009) The CULt of caspase-8 ubiquitination. *Cell*. **137**, 604–6

145. Moscat, J., and Diaz-Meco, M. T. (2009) p62 at the crossroads of autophagy, apoptosis, and cancer. *Cell*. **137**, 1001–4

146. Walsh, J. G., Cullen, S. P., Sheridan, C., Lüthi, A. U., Gerner, C., and Martin, S. J. (2008) Executioner caspase-3 and caspase-7 are functionally distinct proteases. *Proc. Natl. Acad. Sci. U. S. A.* **105**, 12815–9

147. Lamkanfi, M., and Kanneganti, T.-D. (2010) Caspase-7: a protease involved in apoptosis and inflammation. *Int. J. Biochem. Cell Biol.* **42**, 21–4

148. Los, M., Mozoluk, M., Ferrari, D., Stepczynska, A., Stroh, C., Renz, A., Herceg, Z., Wang, Z.-Q., and Schulze-Osthoff, K. (2002) Activation and caspase-mediated inhibition of PARP: a molecular switch between fibroblast necrosis and apoptosis in death receptor signaling. *Mol. Biol. Cell*. **13**, 978–88

149. Chaitanya, G. V., Steven, A. J., and Babu, P. P. (2010) PARP-1 cleavage fragments: signatures of cell-death proteases in neurodegeneration. *Cell Commun. Signal.* **8**, 31

150. Zandy, A. J., Lakhani, S., Zheng, T., Flavell, R. A., and Bassnett, S. (2005) Role of the executioner caspases during lens development. *J. Biol. Chem.* **280**, 30263–72

151. Slee, E. A., Adrain, C., and Martin, S. J. (2001) Executioner caspase-3, -6, and -7

perform distinct, non-redundant roles during the demolition phase of apoptosis. *J. Biol. Chem.* **276**, 7320–6

152. Kaufmann, S. H., Desnoyers, S., Ottaviano, Y., Davidson, N. E., and Poirier, G. G. (1993) Specific proteolytic cleavage of poly(ADP-ribose) polymerase: an early marker of chemotherapy-induced apoptosis. *Cancer Res.* **53**, 3976–85

153. Tewari, M., Quan, L. T., O'Rourke, K., Desnoyers, S., Zeng, Z., Beidler, D. R., Poirier, G. G., Salvesen, G. S., and Dixit, V. M. (1995) Yama/CPP32 beta, a mammalian homolog of CED-3, is a CrmA-inhibitable protease that cleaves the death substrate poly(ADP-ribose) polymerase. *Cell*. **81**, 801–9

154. Soldani, C., Lazzè, M. C., Bottone, M. G., Tognon, G., Biggiogera, M., Pellicciari, C. E., and Scovassi, A. I. (2001) Poly(ADP-ribose) polymerase cleavage during apoptosis: when and where? *Exp. Cell Res.* **269**, 193–201

155. D'Amours, D., Sallmann, F. R., Dixit, V. M., and Poirier, G. G. (2001) Gain-of-function of poly(ADP-ribose) polymerase-1 upon cleavage by apoptotic proteases: implications for apoptosis. *J. Cell Sci.* **114**, 3771–8

156. Smulson, M. E., Pang, D., Jung, M., Dimtchev, A., Chasovskikh, S., Spoonde, A., Simbulan-Rosenthal, C., Rosenthal, D., Yakovlev, A., and Dritschilo, A. (1998) Irreversible binding of poly(ADP)ribose polymerase cleavage product to DNA ends revealed by atomic force microscopy: possible role in apoptosis. *Cancer Res.* **58**, 3495–8

157. Alvarez-Gonzalez, R., Spring, H., Müller, M., and Bürkle, A. (1999) Selective loss of poly(ADP-ribose) and the 85-kDa fragment of poly(ADP-ribose) polymerase in

nucleoli during alkylation-induced apoptosis of HeLa cells. *J. Biol. Chem.* **274**, 32122–6

158. Ouyang, L., Shi, Z., Zhao, S., Wang, F.-T., Zhou, T.-T., Liu, B., and Bao, J.-K. (2012) Programmed cell death pathways in cancer: a review of apoptosis, autophagy and programmed necrosis. *Cell Prolif.* **45**, 487–98

159. Coleman, M. L., Sahai, E. A., Yeo, M., Bosch, M., Dewar, A., and Olson, M. F. (2001) Membrane blebbing during apoptosis results from caspase-mediated activation of ROCK I. *Nat. Cell Biol.* **3**, 339–45

160. Jost, P. J., Grabow, S., Gray, D., McKenzie, M. D., Nachbur, U., Huang, D. C. S., Bouillet, P., Thomas, H. E., Borner, C., Silke, J., Strasser, A., and Kaufmann, T. (2009) XIAP discriminates between type I and type II FAS-induced apoptosis. *Nature*. **460**, 1035–9

161. Galluzzi, L., Vitale, I., Aaronson, S. A., Abrams, J. M., Adam, D., Agostinis, P., Alnemri, E. S., Altucci, L., Amelio, I., Andrews, D. W., Annicchiarico-Petruzzelli, M., Antonov, A. V, Arama, E., Baehrecke, E. H., Barlev, N. A., Bazan, N. G., Bernassola, F., Bertrand, M. J. M., Bianchi, K., Blagosklonny, M. V, Blomgren, K., Borner, C., Boya, P., Brenner, C., Campanella, M., Candi, E., Carmona-Gutierrez, D., Cecconi, F., Chan, F. K.-M., Chandel, N. S., Cheng, E. H., Chipuk, J. E., Cidlowski, J. A., Ciechanover, A., Cohen, G. M., Conrad, M., Cubillos-Ruiz, J. R., Czabotar, P. E., D'Angiolella, V., Dawson, T. M., Dawson, V. L., De Laurenzi, V., De Maria, R., Debatin, K.-M., DeBerardinis, R. J., Deshmukh, M., Di Daniele, N., Di Virgilio, F., Dixit, V. M., Dixon, S. J., Duckett, C. S., Dynlacht, B. D., El-Deiry,

W. S., Elrod, J. W., Fimia, G. M., Fulda, S., García-Sáez, A. J., Garg, A. D.,

Garrido, C., Gavathiotis, E., Golstein, P., Gottlieb, E., Green, D. R., Greene, L. A.,

Gronemeyer, H., Gross, A., Hajnoczky, G., Hardwick, J. M., Harris, I. S.,

Hengartner, M. O., Hetz, C., Ichijo, H., Jäättelä, M., Joseph, B., Jost, P. J., Juin,

P. P., Kaiser, W. J., Karin, M., Kaufmann, T., Kepp, O., Kimchi, A., Kitsis, R. N.,

Klionsky, D. J., Knight, R. A., Kumar, S., Lee, S. W., Lemasters, J. J., Levine, B.,

Linkermann, A., Lipton, S. A., Lockshin, R. A., López-Otín, C., Lowe, S. W.,

Luedde, T., Lugli, E., MacFarlane, M., Madeo, F., Malewicz, M., Malorni, W.,

Manic, G., Marine, J.-C., Martin, S. J., Martinou, J.-C., Medema, J. P., Mehlen, P.,

Meier, P., Melino, S., Miao, E. A., Molkentin, J. D., Moll, U. M., Muñoz-Pinedo, C.,

Nagata, S., Nuñez, G., Oberst, A., Oren, M., Overholtzer, M., Pagano, M.,

Panaretakis, T., Pasparakis, M., Penninger, J. M., Pereira, D. M., Pervaiz, S.,

Peter, M. E., Piacentini, M., Pinton, P., Prehn, J. H. M., Puthalakath, H.,

Rabinovich, G. A., Rehm, M., Rizzuto, R., Rodrigues, C. M. P., Rubinsztein, D. C.,

Rudel, T., Ryan, K. M., Sayan, E., Scorrano, L., Shao, F., Shi, Y., Silke, J., Simon,

H.-U., Sistigu, A., Stockwell, B. R., Strasser, A., Szabadkai, G., Tait, S. W. G.,

Tang, D., Tavernarakis, N., Thorburn, A., Tsujimoto, Y., Turk, B., Vanden Berghe,

T., Vandenabeele, P., Vander Heiden, M. G., Villunger, A., Virgin, H. W.,

Vousden, K. H., Vucic, D., Wagner, E. F., Walczak, H., Wallach, D., Wang, Y.,

Wells, J. A., Wood, W., Yuan, J., Zakeri, Z., Zhivotovsky, B., Zitvogel, L., Melino,

G., and Kroemer, G. (2018) Molecular mechanisms of cell death:

recommendations of the Nomenclature Committee on Cell Death 2018. *Cell

Death Differ.* **25**, 486–541

162. Luo, X., Budihardjo, I., Zou, H., Slaughter, C., and Wang, X. (1998) Bid, a Bcl2 interacting protein, mediates cytochrome c release from mitochondria in response to activation of cell surface death receptors. *Cell*. **94**, 481–90

163. Yin, X. M., Wang, K., Gross, A., Zhao, Y., Zinkel, S., Klocke, B., Roth, K. A., and Korsmeyer, S. J. (1999) Bid-deficient mice are resistant to Fas-induced hepatocellular apoptosis. *Nature*. **400**, 886–91

164. Li, H., Zhu, H., Xu, C. J., and Yuan, J. (1998) Cleavage of BID by caspase 8 mediates the mitochondrial damage in the Fas pathway of apoptosis. *Cell*. **94**, 491–501

165. Rich, T., Allen, R. L., and Wyllie, A. H. (2000) Defying death after DNA damage. *Nature*. **407**, 777–83

166. Brenner, D., and Mak, T. W. (2009) Mitochondrial cell death effectors. *Curr. Opin. Cell Biol.* **21**, 871–7

167. Tait, S. W. G., and Green, D. R. (2010) Mitochondria and cell death: outer membrane permeabilization and beyond. *Nat. Rev. Mol. Cell Biol.* **11**, 621–32

168. Galluzzi, L., Kepp, O., and Kroemer, G. (2016) Mitochondrial regulation of cell death: a phylogenetically conserved control. *Microb. cell (Graz, Austria)*. **3**, 101–108

169. Liu, X., Kim, C. N., Yang, J., Jemmerson, R., and Wang, X. (1996) Induction of apoptotic program in cell-free extracts: requirement for dATP and cytochrome c. *Cell*. **86**, 147–57

170. Li, K., Li, Y., Shelton, J. M., Richardson, J. A., Spencer, E., Chen, Z. J., Wang, X., and Williams, R. S. (2000) Cytochrome c deficiency causes embryonic lethality and attenuates stress-induced apoptosis. *Cell*. **101**, 389–99

171. Li, P., Nijhawan, D., Budihardjo, I., Srinivasula, S. M., Ahmad, M., Alnemri, E. S., and Wang, X. (1997) Cytochrome c and dATP-dependent formation of Apaf-1/caspase-9 complex initiates an apoptotic protease cascade. *Cell*. **91**, 479–89

172. Chai, J., Du, C., Wu, J. W., Kyin, S., Wang, X., and Shi, Y. (2000) Structural and biochemical basis of apoptotic activation by Smac/DIABLO. *Nature*. **406**, 855–62

173. Verhagen, A. M., Ekert, P. G., Pakusch, M., Silke, J., Connolly, L. M., Reid, G. E., Moritz, R. L., Simpson, R. J., and Vaux, D. L. (2000) Identification of DIABLO, a mammalian protein that promotes apoptosis by binding to and antagonizing IAP proteins. *Cell*. **102**, 43–53

174. Du, C., Fang, M., Li, Y., Li, L., and Wang, X. (2000) Smac, a mitochondrial protein that promotes cytochrome c-dependent caspase activation by eliminating IAP inhibition. *Cell*. **102**, 33–42

175. Zou, H., Li, Y., Liu, X., and Wang, X. (1999) An APAF-1.cytochrome c multimeric complex is a functional apoptosome that activates procaspase-9. *J. Biol. Chem.* **274**, 11549–56

176. Srinivasula, S. M., Ahmad, M., Fernandes-Alnemri, T., and Alnemri, E. S. (1998) Autoactivation of procaspase-9 by Apaf-1-mediated oligomerization. *Mol. Cell*. **1**, 949–57

177. Cheng, T. C., Hong, C., Akey, I. V, Yuan, S., and Akey, C. W. (2016) A near atomic structure of the active human apoptosome. *Elife*. 10.7554/eLife.17755

178. Hu, Q., Wu, D., Chen, W., Yan, Z., Yan, C., He, T., Liang, Q., and Shi, Y. (2014) Molecular determinants of caspase-9 activation by the Apaf-1 apoptosome. *Proc. Natl. Acad. Sci. U. S. A.* **111**, 16254–61

179. Li, Y., Zhou, M., Hu, Q., Bai, X.-C., Huang, W., Scheres, S. H. W., and Shi, Y. (2017) Mechanistic insights into caspase-9 activation by the structure of the apoptosome holoenzyme. *Proc. Natl. Acad. Sci. U. S. A.* **114**, 1542–1547

180. Wu, C.-C., Lee, S., Malladi, S., Chen, M.-D., Mastrandrea, N. J., Zhang, Z., and Bratton, S. B. (2016) The Apaf-1 apoptosome induces formation of caspase-9 homo- and heterodimers with distinct activities. *Nat. Commun.* **7**, 13565

181. Riedl, S. J., and Salvesen, G. S. (2007) The apoptosome: signalling platform of cell death. *Nat. Rev. Mol. Cell Biol.* **8**, 405–13

182. Fulda, S., and Debatin, K.-M. (2006) Extrinsic versus intrinsic apoptosis pathways in anticancer chemotherapy. *Oncogene*. **25**, 4798–811

183. Julien, O., and Wells, J. A. (2017) Caspases and their substrates. *Cell Death Differ*. **24**, 1380–1389

184. Czabotar, P. E., Lessene, G., Strasser, A., and Adams, J. M. (2014) Control of apoptosis by the BCL-2 protein family: implications for physiology and therapy. *Nat. Rev. Mol. Cell Biol.* **15**, 49–63

185. Shamas-Din, A., Brahmbhatt, H., Leber, B., and Andrews, D. W. (2011) BH3-only

proteins: Orchestrators of apoptosis. *Biochim. Biophys. Acta*. **1813**, 508–20

186. Sutton, V. R., Davis, J. E., Cancilla, M., Johnstone, R. W., Ruefli, A. A., Sedelies, K., Browne, K. A., and Trapani, J. A. (2000) Initiation of apoptosis by granzyme B requires direct cleavage of bid, but not direct granzyme B-mediated caspase activation. *J. Exp. Med.* **192**, 1403–14

187. Reiners, J. J., Caruso, J. A., Mathieu, P., Chelladurai, B., Yin, X.-M., and Kessel, D. (2002) Release of cytochrome c and activation of pro-caspase-9 following lysosomal photodamage involves Bid cleavage. *Cell Death Differ.* **9**, 934–44

188. Stoka, V., Turk, B., Schendel, S. L., Kim, T. H., Cirman, T., Snipas, S. J., Ellerby, L. M., Bredesen, D., Freeze, H., Abrahamson, M., Bromme, D., Krajewski, S., Reed, J. C., Yin, X. M., Turk, V., and Salvesen, G. S. (2001) Lysosomal protease pathways to apoptosis. Cleavage of bid, not pro-caspases, is the most likely route. *J. Biol. Chem.* **276**, 3149–57

189. Mandic, A., Viktorsson, K., Strandberg, L., Heiden, T., Hansson, J., Linder, S., and Shoshan, M. C. (2002) Calpain-mediated Bid cleavage and calpain-independent Bak modulation: two separate pathways in cisplatin-induced apoptosis. *Mol. Cell. Biol.* **22**, 3003–13

190. Lovell, J. F., Billen, L. P., Bindner, S., Shamas-Din, A., Fradin, C., Leber, B., and Andrews, D. W. (2008) Membrane binding by tBid initiates an ordered series of events culminating in membrane permeabilization by Bax. *Cell*. **135**, 1074–84

191. Raemy, E., Montessuit, S., Pierredon, S., van Kampen, A. H., Vaz, F. M., and Martinou, J.-C. (2016) Cardiolipin or MTCH2 can serve as tBID receptors during

apoptosis. *Cell Death Differ.* **23**, 1165–74

192. Pasparakis, M., and Vandenabeele, P. (2015) Necroptosis and its role in inflammation. *Nature*. **517**, 311–20

193. Vanden Berghe, T., Linkermann, A., Jouan-Lanhouet, S., Walczak, H., and Vandenabeele, P. (2014) Regulated necrosis: the expanding network of non-apoptotic cell death pathways. *Nat. Rev. Mol. Cell Biol.* **15**, 135–47

194. Schwarzer, R., Laurien, L., and Pasparakis, M. (2020) New insights into the regulation of apoptosis, necroptosis, and pyroptosis by receptor interacting protein kinase 1 and caspase-8. *Curr. Opin. Cell Biol.* **63**, 186–193

195. Kaczmarek, A., Vandenabeele, P., and Krysko, D. V (2013) Necroptosis: the release of damage-associated molecular patterns and its physiological relevance. *Immunity*. **38**, 209–23

196. Zhang, X., Fan, C., Zhang, H., Zhao, Q., Liu, Y., Xu, C., Xie, Q., Wu, X., Yu, X., Zhang, J., and Zhang, H. (2016) MLKL and FADD Are Critical for Suppressing Progressive Lymphoproliferative Disease and Activating the NLRP3 Inflammasome. *Cell Rep.* **16**, 3247–3259

197. Dara, L., Liu, Z.-X., and Kaplowitz, N. Questions and controversies: the role of necroptosis in liver disease. *Cell death Discov.* **2**, 16089

198. Liu, Y., Liu, T., Lei, T., Zhang, D., Du, S., Girani, L., Qi, D., Lin, C., Tong, R., and Wang, Y. (2019) RIP1/RIP3-regulated necroptosis as a target for multifaceted disease therapy (Review). *Int. J. Mol. Med.* **44**, 771–786

199. Weinlich, R., Oberst, A., Beere, H. M., and Green, D. R. (2017) Necroptosis in development, inflammation and disease. *Nat. Rev. Mol. Cell Biol.* **18**, 127–136

200. Feltham, R., Vince, J. E., and Lawlor, K. E. (2017) Caspase-8: not so silently deadly. *Clin. Transl. Immunol.* **6**, e124

201. Sedger, L. M., and McDermott, M. F. (2014) TNF and TNF-receptors: From mediators of cell death and inflammation to therapeutic giants - past, present and future. *Cytokine Growth Factor Rev.* **25**, 453–72

202. Pobezinskaya, Y. L., and Liu, Z. (2012) The role of TRADD in death receptor signaling. *Cell Cycle*. **11**, 871–6

203. Csomos, R. A., Brady, G. F., and Duckett, C. S. (2009) Enhanced cytoprotective effects of the inhibitor of apoptosis protein cellular IAP1 through stabilization with TRAF2. *J. Biol. Chem.* **284**, 20531–9

204. Schwabe, R. F., and Luedde, T. (2018) Apoptosis and necroptosis in the liver: a matter of life and death. *Nat. Rev. Gastroenterol. Hepatol.* **15**, 738–752

205. Chen, J., Kos, R., Garssen, J., and Redegeld, F. (2019) Molecular Insights into the Mechanism of Necroptosis: The Necrosome As a Potential Therapeutic Target. *Cells*. 10.3390/cells8121486

206. Ea, C.-K., Deng, L., Xia, Z.-P., Pineda, G., and Chen, Z. J. (2006) Activation of IKK by TNFalpha requires site-specific ubiquitination of RIP1 and polyubiquitin binding by NEMO. *Mol. Cell*. **22**, 245–57

207. Li, H., Kobayashi, M., Blonska, M., You, Y., and Lin, X. (2006) Ubiquitination of

RIP is required for tumor necrosis factor alpha-induced NF-kappaB activation. *J. Biol. Chem.* **281**, 13636–43

208. Bettermann, K., Vucur, M., Haybaeck, J., Koppe, C., Janssen, J., Heymann, F., Weber, A., Weiskirchen, R., Liedtke, C., Gassler, N., Müller, M., de Vos, R., Wolf, M. J., Boege, Y., Seleznik, G. M., Zeller, N., Erny, D., Fuchs, T., Zoller, S., Cairo, S., Buendia, M.-A., Prinz, M., Akira, S., Tacke, F., Heikenwalder, M., Trautwein, C., and Luedde, T. (2010) TAK1 suppresses a NEMO-dependent but NF-kappaB-independent pathway to liver cancer. *Cancer Cell.* **17**, 481–96

209. Dondelinger, Y., Jouan-Lanhouet, S., Divert, T., Theatre, E., Bertin, J., Gough, P. J., Giansanti, P., Heck, A. J. R., Dejardin, E., Vandenabeele, P., and Bertrand, M. J. M. (2015) NF-κB-Independent Role of IKKα/IKKβ in Preventing RIPK1 Kinase-Dependent Apoptotic and Necroptotic Cell Death during TNF Signaling. *Mol. Cell.* **60**, 63–76

210. Dondelinger, Y., Delanghe, T., Priem, D., Wynosky-Dolfi, M. A., Sorobetea, D., Rojas-Rivera, D., Giansanti, P., Roelandt, R., Gropengiesser, J., Ruckdeschel, K., Savvides, S. N., Heck, A. J. R., Vandenabeele, P., Brodsky, I. E., and Bertrand, M. J. M. (2019) Serine 25 phosphorylation inhibits RIPK1 kinase-dependent cell death in models of infection and inflammation. *Nat. Commun.* **10**, 1729

211. Luedde, T., Beraza, N., Kotsikoris, V., van Loo, G., Nenci, A., De Vos, R., Roskams, T., Trautwein, C., and Pasparakis, M. (2007) Deletion of NEMO/IKKgamma in liver parenchymal cells causes steatohepatitis and hepatocellular carcinoma. *Cancer Cell.* **11**, 119–32

212. Kondylis, V., Polykratis, A., Ehlken, H., Ochoa-Callejero, L., Straub, B. K., Krishna-Subramanian, S., Van, T.-M., Curth, H.-M., Heise, N., Weih, F., Klein, U., Schirmacher, P., Kelliher, M., and Pasparakis, M. (2015) NEMO Prevents Steatohepatitis and Hepatocellular Carcinoma by Inhibiting RIPK1 Kinase Activity-Mediated Hepatocyte Apoptosis. *Cancer Cell*. **28**, 582–598

213. Luedde, T., Heinrichsdorff, J., de Lorenzi, R., De Vos, R., Roskams, T., and Pasparakis, M. (2008) IKK1 and IKK2 cooperate to maintain bile duct integrity in the liver. *Proc. Natl. Acad. Sci. U. S. A.* **105**, 9733–8

214. Amin, P., Florez, M., Najafov, A., Pan, H., Geng, J., Ofengeim, D., Dziedzic, S. A., Wang, H., Barrett, V. J., Ito, Y., LaVoie, M. J., and Yuan, J. (2018) Regulation of a distinct activated RIPK1 intermediate bridging complex I and complex II in TNFα-mediated apoptosis. *Proc. Natl. Acad. Sci. U. S. A.* **115**, E5944–E5953

215. Dondelinger, Y., Darding, M., Bertrand, M. J. M., and Walczak, H. (2016) Poly-ubiquitination in TNFR1-mediated necroptosis. *Cell. Mol. Life Sci.* **73**, 2165–76

216. Bertrand, M. J. M., Milutinovic, S., Dickson, K. M., Ho, W. C., Boudreault, A., Durkin, J., Gillard, J. W., Jaquith, J. B., Morris, S. J., and Barker, P. A. (2008) cIAP1 and cIAP2 facilitate cancer cell survival by functioning as E3 ligases that promote RIP1 ubiquitination. *Mol. Cell*. **30**, 689–700

217. Wang, L., Du, F., and Wang, X. (2008) TNF-alpha induces two distinct caspase-8 activation pathways. *Cell*. **133**, 693–703

218. Petersen, S. L., Wang, L., Yalcin-Chin, A., Li, L., Peyton, M., Minna, J., Harran, P., and Wang, X. (2007) Autocrine TNFalpha signaling renders human cancer

cells susceptible to Smac-mimetic-induced apoptosis. *Cancer Cell*. **12**, 445–56

219. Moulin, M., Anderton, H., Voss, A. K., Thomas, T., Wong, W. W.-L., Bankovacki, A., Feltham, R., Chau, D., Cook, W. D., Silke, J., and Vaux, D. L. (2012) IAPs limit activation of RIP kinases by TNF receptor 1 during development. *EMBO J.* **31**, 1679–91

220. Peltzer, N., Rieser, E., Taraborrelli, L., Draber, P., Darding, M., Pernaute, B., Shimizu, Y., Sarr, A., Draberova, H., Montinaro, A., Martinez-Barbera, J. P., Silke, J., Rodriguez, T. A., and Walczak, H. (2014) HOIP deficiency causes embryonic lethality by aberrant TNFR1-mediated endothelial cell death. *Cell Rep.* **9**, 153–165

221. Tenev, T., Bianchi, K., Darding, M., Broemer, M., Langlais, C., Wallberg, F., Zachariou, A., Lopez, J., MacFarlane, M., Cain, K., and Meier, P. (2011) The Ripoptosome, a signaling platform that assembles in response to genotoxic stress and loss of IAPs. *Mol. Cell*. **43**, 432–48

222. Hakem, R., Hakem, A., Duncan, G. S., Henderson, J. T., Woo, M., Soengas, M. S., Elia, A., de la Pompa, J. L., Kagi, D., Khoo, W., Potter, J., Yoshida, R., Kaufman, S. A., Lowe, S. W., Penninger, J. M., and Mak, T. W. (1998) Differential requirement for caspase 9 in apoptotic pathways in vivo. *Cell*. **94**, 339–52

223. Yoshida, H., Kong, Y. Y., Yoshida, R., Elia, A. J., Hakem, A., Hakem, R., Penninger, J. M., and Mak, T. W. (1998) Apaf1 is required for mitochondrial pathways of apoptosis and brain development. *Cell*. **94**, 739–50

224. Kuida, K., Haydar, T. F., Kuan, C. Y., Gu, Y., Taya, C., Karasuyama, H., Su, M. S., Rakic, P., and Flavell, R. A. (1998) Reduced apoptosis and cytochrome c-

mediated caspase activation in mice lacking caspase 9. *Cell*. **94**, 325–37

225. Yeh, W. C., de la Pompa, J. L., McCurrach, M. E., Shu, H. B., Elia, A. J., Shahinian, A., Ng, M., Wakeham, A., Khoo, W., Mitchell, K., El-Deiry, W. S., Lowe, S. W., Goeddel, D. V, and Mak, T. W. (1998) FADD: essential for embryo development and signaling from some, but not all, inducers of apoptosis. *Science*. **279**, 1954–8

226. Yeh, W. C., Itie, A., Elia, A. J., Ng, M., Shu, H. B., Wakeham, A., Mirtsos, C., Suzuki, N., Bonnard, M., Goeddel, D. V, and Mak, T. W. (2000) Requirement for Casper (c-FLIP) in regulation of death receptor-induced apoptosis and embryonic development. *Immunity*. **12**, 633–42

227. Walsh, C. M., Wen, B. G., Chinnaiyan, A. M., O'Rourke, K., Dixit, V. M., and Hedrick, S. M. (1998) A role for FADD in T cell activation and development. *Immunity*. **8**, 439–49

228. Varfolomeev, E. E., Schuchmann, M., Luria, V., Chiannilkulchai, N., Beckmann, J. S., Mett, I. L., Rebrikov, D., Brodianski, V. M., Kemper, O. C., Kollet, O., Lapidot, T., Soffer, D., Sobe, T., Avraham, K. B., Goncharov, T., Holtmann, H., Lonai, P., and Wallach, D. (1998) Targeted disruption of the mouse Caspase 8 gene ablates cell death induction by the TNF receptors, Fas/Apo1, and DR3 and is lethal prenatally. *Immunity*. **9**, 267–76

229. Salmena, L., Lemmers, B., Hakem, A., Matysiak-Zablocki, E., Murakami, K., Au, P. Y. B., Berry, D. M., Tamblyn, L., Shehabeldin, A., Migon, E., Wakeham, A., Bouchard, D., Yeh, W. C., McGlade, J. C., Ohashi, P. S., and Hakem, R. (2003)

Essential role for caspase 8 in T-cell homeostasis and T-cell-mediated immunity. *Genes Dev.* **17**, 883–95

230. Kabra, N. H., Kang, C., Hsing, L. C., Zhang, J., and Winoto, A. (2001) T cell-specific FADD-deficient mice: FADD is required for early T cell development. *Proc. Natl. Acad. Sci. U. S. A.* **98**, 6307–12

231. Zhang, N., and He, Y.-W. (2005) An essential role for c-FLIP in the efficient development of mature T lymphocytes. *J. Exp. Med.* **202**, 395–404

232. Ch'en, I. L., Beisner, D. R., Degterev, A., Lynch, C., Yuan, J., Hoffmann, A., and Hedrick, S. M. (2008) Antigen-mediated T cell expansion regulated by parallel pathways of death. *Proc. Natl. Acad. Sci. U. S. A.* **105**, 17463–8

233. Ch'en, I. L., Tsau, J. S., Molkentin, J. D., Komatsu, M., and Hedrick, S. M. (2011) Mechanisms of necroptosis in T cells. *J. Exp. Med.* **208**, 633–41

234. Kaiser, W. J., Upton, J. W., Long, A. B., Livingston-Rosanoff, D., Daley-Bauer, L. P., Hakem, R., Caspary, T., and Mocarski, E. S. (2011) RIP3 mediates the embryonic lethality of caspase-8-deficient mice. *Nature.* **471**, 368–72

235. Oberst, A., Dillon, C. P., Weinlich, R., McCormick, L. L., Fitzgerald, P., Pop, C., Hakem, R., Salvesen, G. S., and Green, D. R. (2011) Catalytic activity of the caspase-8-FLIP(L) complex inhibits RIPK3-dependent necrosis. *Nature.* **471**, 363–7

236. Welz, P.-S., Wullaert, A., Vlantis, K., Kondylis, V., Fernández-Majada, V., Ermolaeva, M., Kirsch, P., Sterner-Kock, A., van Loo, G., and Pasparakis, M.

(2011) FADD prevents RIP3-mediated epithelial cell necrosis and chronic intestinal inflammation. *Nature*. **477**, 330–4

237. Bonnet, M. C., Preukschat, D., Welz, P.-S., van Loo, G., Ermolaeva, M. A., Bloch, W., Haase, I., and Pasparakis, M. (2011) The adaptor protein FADD protects epidermal keratinocytes from necroptosis in vivo and prevents skin inflammation. *Immunity*. **35**, 572–82

238. Weinlich, R., Oberst, A., Dillon, C. P., Janke, L. J., Milasta, S., Lukens, J. R., Rodriguez, D. A., Gurung, P., Savage, C., Kanneganti, T. D., and Green, D. R. (2013) Protective roles for caspase-8 and cFLIP in adult homeostasis. *Cell Rep.* **5**, 340–8

239. Pop, C., Oberst, A., Drag, M., Van Raam, B. J., Riedl, S. J., Green, D. R., and Salvesen, G. S. (2011) FLIP(L) induces caspase 8 activity in the absence of interdomain caspase 8 cleavage and alters substrate specificity. *Biochem. J.* **433**, 447–457

240. Kang, T.-B., Oh, G.-S., Scandella, E., Bolinger, B., Ludewig, B., Kovalenko, A., and Wallach, D. (2008) Mutation of a self-processing site in caspase-8 compromises its apoptotic but not its nonapoptotic functions in bacterial artificial chromosome-transgenic mice. *J. Immunol.* **181**, 2522–32

241. Lin, Y., Devin, A., Rodriguez, Y., and Liu, Z. G. (1999) Cleavage of the death domain kinase RIP by caspase-8 prompts TNF-induced apoptosis. *Genes Dev.* **13**, 2514–26

242. Feng, S., Yang, Y., Mei, Y., Ma, L., Zhu, D., Hoti, N., Castanares, M., and Wu, M.

(2007) Cleavage of RIP3 inactivates its caspase-independent apoptosis pathway by removal of kinase domain. *Cell. Signal.* **19**, 2056–67

243. O'Donnell, M. A., Perez-Jimenez, E., Oberst, A., Ng, A., Massoumi, R., Xavier, R., Green, D. R., and Ting, A. T. (2011) Caspase 8 inhibits programmed necrosis by processing CYLD. *Nat. Cell Biol.* **13**, 1437–42

244. Zhang, Y., Su, S. S., Zhao, S., Yang, Z., Zhong, C.-Q., Chen, X., Cai, Q., Yang, Z.-H., Huang, D., Wu, R., and Han, J. (2017) RIP1 autophosphorylation is promoted by mitochondrial ROS and is essential for RIP3 recruitment into necrosome. *Nat. Commun.* **8**, 14329

245. Wang, H., Meng, H., Li, X., Zhu, K., Dong, K., Mookhtiar, A. K., Wei, H., Li, Y., Sun, S.-C., and Yuan, J. (2017) PELI1 functions as a dual modulator of necroptosis and apoptosis by regulating ubiquitination of RIPK1 and mRNA levels of c-FLIP. *Proc. Natl. Acad. Sci. U. S. A.* **114**, 11944–11949

246. Orozco, S., Yatim, N., Werner, M. R., Tran, H., Gunja, S. Y., Tait, S. W. G., Albert, M. L., Green, D. R., and Oberst, A. (2014) RIPK1 both positively and negatively regulates RIPK3 oligomerization and necroptosis. *Cell Death Differ.* **21**, 1511–21

247. Molnár, T., Mázló, A., Tslaf, V., Szöllősi, A. G., Emri, G., and Koncz, G. (2019) Current translational potential and underlying molecular mechanisms of necroptosis. *Cell Death Dis.* **10**, 860

248. Wu, X.-N., Yang, Z.-H., Wang, X.-K., Zhang, Y., Wan, H., Song, Y., Chen, X., Shao, J., and Han, J. (2014) Distinct roles of RIP1-RIP3 hetero- and RIP3-RIP3 homo-interaction in mediating necroptosis. *Cell Death Differ.* **21**, 1709–20

249. Li, J., McQuade, T., Siemer, A. B., Napetschnig, J., Moriwaki, K., Hsiao, Y.-S., Damko, E., Moquin, D., Walz, T., McDermott, A., Chan, F. K.-M., and Wu, H. (2012) The RIP1/RIP3 necrosome forms a functional amyloid signaling complex required for programmed necrosis. *Cell*. **150**, 339–50

250. Fuchslocher Chico, J., Falk-Paulsen, M., Luzius, A., Saggau, C., Ruder, B., Bolik, J., Schmidt-Arras, D., Linkermann, A., Becker, C., Rosenstiel, P., Rose-John, S., and Adam, D. (2018) The enhanced susceptibility of ADAM-17 hypomorphic mice to DSS-induced colitis is not ameliorated by loss of RIPK3, revealing an unexpected function of ADAM-17 in necroptosis. *Oncotarget*. **9**, 12941–12958

251. Onizawa, M., Oshima, S., Schulze-Topphoff, U., Oses-Prieto, J. A., Lu, T., Tavares, R., Prodhomme, T., Duong, B., Whang, M. I., Advincula, R., Agelidis, A., Barrera, J., Wu, H., Burlingame, A., Malynn, B. A., Zamvil, S. S., and Ma, A. (2015) The ubiquitin-modifying enzyme A20 restricts ubiquitination of the kinase RIPK3 and protects cells from necroptosis. *Nat. Immunol.* **16**, 618–27

252. Johnston, A., and Wang, Z. (2018) Necroptosis: MLKL Polymerization. *J. Nat. Sci.*

253. Dondelinger, Y., Declercq, W., Montessuit, S., Roelandt, R., Goncalves, A., Bruggeman, I., Hulpiau, P., Weber, K., Sehon, C. A., Marquis, R. W., Bertin, J., Gough, P. J., Savvides, S., Martinou, J.-C., Bertrand, M. J. M., and Vandenabeele, P. (2014) MLKL compromises plasma membrane integrity by binding to phosphatidylinositol phosphates. *Cell Rep.* **7**, 971–81

254. Hildebrand, J. M., Tanzer, M. C., Lucet, I. S., Young, S. N., Spall, S. K., Sharma, P., Pierotti, C., Garnier, J.-M., Dobson, R. C. J., Webb, A. I., Tripaydonis, A.,

Babon, J. J., Mulcair, M. D., Scanlon, M. J., Alexander, W. S., Wilks, A. F., Czabotar, P. E., Lessene, G., Murphy, J. M., and Silke, J. (2014) Activation of the pseudokinase MLKL unleashes the four-helix bundle domain to induce membrane localization and necroptotic cell death. *Proc. Natl. Acad. Sci. U. S. A.* **111**, 15072–7

255. Sun, L., Wang, H., Wang, Z., He, S., Chen, S., Liao, D., Wang, L., Yan, J., Liu, W., Lei, X., and Wang, X. (2012) Mixed lineage kinase domain-like protein mediates necrosis signaling downstream of RIP3 kinase. *Cell.* **148**, 213–27

256. Nogusa, S., Thapa, R. J., Dillon, C. P., Liedmann, S., Oguin, T. H., Ingram, J. P., Rodriguez, D. A., Kosoff, R., Sharma, S., Sturm, O., Verbist, K., Gough, P. J., Bertin, J., Hartmann, B. M., Sealfon, S. C., Kaiser, W. J., Mocarski, E. S., López, C. B., Thomas, P. G., Oberst, A., Green, D. R., and Balachandran, S. (2016) RIPK3 Activates Parallel Pathways of MLKL-Driven Necroptosis and FADD-Mediated Apoptosis to Protect against Influenza A Virus. *Cell Host Microbe.* **20**, 13–24

257. Reynoso, E., Liu, H., Li, L., Yuan, A. L., Chen, S., and Wang, Z. (2017) Thioredoxin-1 actively maintains the pseudokinase MLKL in a reduced state to suppress disulfide bond-dependent MLKL polymer formation and necroptosis. *J. Biol. Chem.* **292**, 17514–17524

258. Quarato, G., Guy, C. S., Grace, C. R., Llambi, F., Nourse, A., Rodriguez, D. A., Wakefield, R., Frase, S., Moldoveanu, T., and Green, D. R. (2016) Sequential Engagement of Distinct MLKL Phosphatidylinositol-Binding Sites Executes

Necroptosis. *Mol. Cell*. **61**, 589–601

259. Huang, D., Zheng, X., Wang, Z.-A., Chen, X., He, W.-T., Zhang, Y., Xu, J.-G., Zhao, H., Shi, W., Wang, X., Zhu, Y., and Han, J. (2017) The MLKL Channel in Necroptosis Is an Octamer Formed by Tetramers in a Dyadic Process. *Mol. Cell. Biol.* 10.1128/MCB.00497-16

260. Cai, Z., Jitkaew, S., Zhao, J., Chiang, H.-C., Choksi, S., Liu, J., Ward, Y., Wu, L.-G., and Liu, Z.-G. (2014) Plasma membrane translocation of trimerized MLKL protein is required for TNF-induced necroptosis. *Nat. Cell Biol.* **16**, 55–65

261. Chen, X., Li, W., Ren, J., Huang, D., He, W.-T., Song, Y., Yang, C., Li, W., Zheng, X., Chen, P., and Han, J. (2014) Translocation of mixed lineage kinase domain-like protein to plasma membrane leads to necrotic cell death. *Cell Res.* **24**, 105–21

262. Schenk, B., and Fulda, S. (2015) Reactive oxygen species regulate Smac mimetic/TNFα-induced necroptotic signaling and cell death. *Oncogene*. **34**, 5796–806

263. Feoktistova, M., Geserick, P., Kellert, B., Dimitrova, D. P., Langlais, C., Hupe, M., Cain, K., MacFarlane, M., Häcker, G., and Leverkus, M. (2011) cIAPs block Ripoptosome formation, a RIP1/caspase-8 containing intracellular cell death complex differentially regulated by cFLIP isoforms. *Mol. Cell*. **43**, 449–63

264. Geserick, P., Hupe, M., Moulin, M., Wong, W. W.-L., Feoktistova, M., Kellert, B., Gollnick, H., Silke, J., and Leverkus, M. (2009) Cellular IAPs inhibit a cryptic CD95-induced cell death by limiting RIP1 kinase recruitment. *J. Cell Biol.* **187**,

1037–54

265. Netea, M. G., and van der Meer, J. W. M. (2011) Immunodeficiency and genetic defects of pattern-recognition receptors. *N. Engl. J. Med.* **364**, 60–70

266. Takeuchi, O., and Akira, S. (2010) Pattern recognition receptors and inflammation. *Cell*. **140**, 805–20

267. He, S., Liang, Y., Shao, F., and Wang, X. (2011) Toll-like receptors activate programmed necrosis in macrophages through a receptor-interacting kinase-3-mediated pathway. *Proc. Natl. Acad. Sci. U. S. A.* **108**, 20054–9

268. Kaiser, W. J., Sridharan, H., Huang, C., Mandal, P., Upton, J. W., Gough, P. J., Sehon, C. A., Marquis, R. W., Bertin, J., and Mocarski, E. S. (2013) Toll-like receptor 3-mediated necrosis via TRIF, RIP3, and MLKL. *J. Biol. Chem.* **288**, 31268–79

269. Choi, M. E., Price, D. R., Ryter, S. W., and Choi, A. M. K. (2019) Necroptosis: a crucial pathogenic mediator of human disease. *JCI insight*. 10.1172/jci.insight.128834

270. Upton, J. W., Kaiser, W. J., and Mocarski, E. S. (2012) DAI/ZBP1/DLM-1 complexes with RIP3 to mediate virus-induced programmed necrosis that is targeted by murine cytomegalovirus vIRA. *Cell Host Microbe*. **11**, 290–7

271. Thapa, R. J., Nogusa, S., Chen, P., Maki, J. L., Lerro, A., Andrake, M., Rall, G. F., Degterev, A., and Balachandran, S. (2013) Interferon-induced RIP1/RIP3-mediated necrosis requires PKR and is licensed by FADD and caspases. *Proc.*

Natl. Acad. Sci. U. S. A. **110**, E3109-18

272. McComb, S., Cessford, E., Alturki, N. A., Joseph, J., Shutinoski, B., Startek, J. B., Gamero, A. M., Mossman, K. L., and Sad, S. (2014) Type-I interferon signaling through ISGF3 complex is required for sustained Rip3 activation and necroptosis in macrophages. *Proc. Natl. Acad. Sci. U. S. A.* **111**, E3206-13

273. Galluzzi, L., Kepp, O., Chan, F. K.-M., and Kroemer, G. (2017) Necroptosis: Mechanisms and Relevance to Disease. *Annu. Rev. Pathol.* **12**, 103–130

274. Caccamo, A., Branca, C., Piras, I. S., Ferreira, E., Huentelman, M. J., Liang, W. S., Readhead, B., Dudley, J. T., Spangenberg, E. E., Green, K. N., Belfiore, R., Winslow, W., and Oddo, S. (2017) Necroptosis activation in Alzheimer's disease. *Nat. Neurosci.* **20**, 1236–1246

275. Ito, Y., Ofengeim, D., Najafov, A., Das, S., Saberi, S., Li, Y., Hitomi, J., Zhu, H., Chen, H., Mayo, L., Geng, J., Amin, P., DeWitt, J. P., Mookhtiar, A. K., Florez, M., Ouchida, A. T., Fan, J., Pasparakis, M., Kelliher, M. A., Ravits, J., and Yuan, J. (2016) RIPK1 mediates axonal degeneration by promoting inflammation and necroptosis in ALS. *Science*. **353**, 603–8

276. Ofengeim, D., Ito, Y., Najafov, A., Zhang, Y., Shan, B., DeWitt, J. P., Ye, J., Zhang, X., Chang, A., Vakifahmetoglu-Norberg, H., Geng, J., Py, B., Zhou, W., Amin, P., Berlink Lima, J., Qi, C., Yu, Q., Trapp, B., and Yuan, J. (2015) Activation of necroptosis in multiple sclerosis. *Cell Rep.* **10**, 1836–49

277. Lee, S. H., Kwon, J. Y., Kim, S.-Y., Jung, K., and Cho, M.-L. (2017) Interferon-gamma regulates inflammatory cell death by targeting necroptosis in experimental

autoimmune arthritis. *Sci. Rep.* **7**, 10133

278. Jhun, J., Lee, S. H., Kim, S.-Y., Ryu, J., Kwon, J. Y., Na, H. S., Jung, K., Moon, S.-J., Cho, M.-L., and Min, J.-K. (2019) RIPK1 inhibition attenuates experimental autoimmune arthritis via suppression of osteoclastogenesis. *J. Transl. Med.* **17**, 84

279. Oerlemans, M. I. F. J., Liu, J., Arslan, F., den Ouden, K., van Middelaar, B. J., Doevendans, P. A., and Sluijter, J. P. G. (2012) Inhibition of RIP1-dependent necrosis prevents adverse cardiac remodeling after myocardial ischemia-reperfusion in vivo. *Basic Res. Cardiol.* **107**, 270

280. Koshinuma, S., Miyamae, M., Kaneda, K., Kotani, J., and Figueredo, V. M. (2014) Combination of necroptosis and apoptosis inhibition enhances cardioprotection against myocardial ischemia-reperfusion injury. *J. Anesth.* **28**, 235–41

281. Gautheron, J., Vucur, M., Reisinger, F., Cardenas, D. V., Roderburg, C., Koppe, C., Kreggenwinkel, K., Schneider, A. T., Bartneck, M., Neumann, U. P., Canbay, A., Reeves, H. L., Luedde, M., Tacke, F., Trautwein, C., Heikenwalder, M., and Luedde, T. (2014) A positive feedback loop between RIP3 and JNK controls non-alcoholic steatohepatitis. *EMBO Mol. Med.* **6**, 1062–74

282. Roychowdhury, S., McMullen, M. R., Pisano, S. G., Liu, X., and Nagy, L. E. (2013) Absence of receptor interacting protein kinase 3 prevents ethanol-induced liver injury. *Hepatology*. **57**, 1773–83

283. Chauhan, D., Bartok, E., Gaidt, M. M., Bock, F. J., Herrmann, J., Seeger, J. M., Broz, P., Beckmann, R., Kashkar, H., Tait, S. W. G., Müller, R., and Hornung, V.

(2018) BAX/BAK-Induced Apoptosis Results in Caspase-8-Dependent IL-1β Maturation in Macrophages. *Cell Rep.* **25**, 2354-2368.e5

284. Dinarello, C. A. (2011) A clinical perspective of IL-1β as the gatekeeper of inflammation. *Eur. J. Immunol.* **41**, 1203–17

285. Lopez-Castejon, G., and Brough, D. (2011) Understanding the mechanism of IL-1β secretion. *Cytokine Growth Factor Rev.* **22**, 189–95

286. Gurung, P., and Kanneganti, T.-D. (2015) Novel roles for caspase-8 in IL-1β and inflammasome regulation. *Am. J. Pathol.* **185**, 17–25

287. Thornberry, N. A., Bull, H. G., Calaycay, J. R., Chapman, K. T., Howard, A. D., Kostura, M. J., Miller, D. K., Molineaux, S. M., Weidner, J. R., and Aunins, J. (1992) A novel heterodimeric cysteine protease is required for interleukin-1 beta processing in monocytes. *Nature*. **356**, 768–74

288. Kelley, N., Jeltema, D., Duan, Y., and He, Y. (2019) The NLRP3 Inflammasome: An Overview of Mechanisms of Activation and Regulation. *Int. J. Mol. Sci.* 10.3390/ijms20133328

289. Sharma, D., and Kanneganti, T.-D. (2016) The cell biology of inflammasomes: Mechanisms of inflammasome activation and regulation. *J. Cell Biol.* **213**, 617–29

290. Lamkanfi, M., and Dixit, V. M. (2014) Mechanisms and functions of inflammasomes. *Cell*. **157**, 1013–22

291. Manji, G. A., Wang, L., Geddes, B. J., Brown, M., Merriam, S., Al-Garawi, A., Mak, S., Lora, J. M., Briskin, M., Jurman, M., Cao, J., DiStefano, P. S., and Bertin,

J. (2002) PYPAF1, a PYRIN-containing Apaf1-like protein that assembles with ASC and regulates activation of NF-kappa B. *J. Biol. Chem.* **277**, 11570–5

292. Franchi, L., Warner, N., Viani, K., and Nuñez, G. (2009) Function of Nod-like receptors in microbial recognition and host defense. *Immunol. Rev.* **227**, 106–28

293. Lieberman, J., Wu, H., and Kagan, J. C. (2019) Gasdermin D activity in inflammation and host defense. *Sci. Immunol.* 10.1126/sciimmunol.aav1447

294. Liu, X., Zhang, Z., Ruan, J., Pan, Y., Magupalli, V. G., Wu, H., and Lieberman, J. (2016) Inflammasome-activated gasdermin D causes pyroptosis by forming membrane pores. *Nature*. **535**, 153–8

295. Sborgi, L., Rühl, S., Mulvihill, E., Pipercevic, J., Heilig, R., Stahlberg, H., Farady, C. J., Müller, D. J., Broz, P., and Hiller, S. (2016) GSDMD membrane pore formation constitutes the mechanism of pyroptotic cell death. *EMBO J.* **35**, 1766–78

296. Hazuda, D., Webb, R. L., Simon, P., and Young, P. (1989) Purification and characterization of human recombinant precursor interleukin 1 beta. *J. Biol. Chem.* **264**, 1689–93

297. Provoost, S., Maes, T., Pauwels, N. S., Vanden Berghe, T., Vandenabeele, P., Lambrecht, B. N., Joos, G. F., and Tournoy, K. G. (2011) NLRP3/caspase-1-independent IL-1beta production mediates diesel exhaust particle-induced pulmonary inflammation. *J. Immunol.* **187**, 3331–7

298. Kono, H., Orlowski, G. M., Patel, Z., and Rock, K. L. (2012) The IL-1-dependent

sterile inflammatory response has a substantial caspase-1-independent component that requires cathepsin C. *J. Immunol.* **189**, 3734–40

299. Shenderov, K., Riteau, N., Yip, R., Mayer-Barber, K. D., Oland, S., Hieny, S., Fitzgerald, P., Oberst, A., Dillon, C. P., Green, D. R., Cerundolo, V., and Sher, A. (2014) Cutting edge: Endoplasmic reticulum stress licenses macrophages to produce mature IL-1β in response to TLR4 stimulation through a caspase-8- and TRIF-dependent pathway. *J. Immunol.* **192**, 2029–2033

300. Maelfait, J., Vercammen, E., Janssens, S., Schotte, P., Haegman, M., Magez, S., and Beyaert, R. (2008) Stimulation of Toll-like receptor 3 and 4 induces interleukin-1beta maturation by caspase-8. *J. Exp. Med.* **205**, 1967–73

301. Gringhuis, S. I., Kaptein, T. M., Wevers, B. A., Theelen, B., van der Vlist, M., Boekhout, T., and Geijtenbeek, T. B. H. (2012) Dectin-1 is an extracellular pathogen sensor for the induction and processing of IL-1β via a noncanonical caspase-8 inflammasome. *Nat. Immunol.* **13**, 246–54

302. Antonopoulos, C., El Sanadi, C., Kaiser, W. J., Mocarski, E. S., and Dubyak, G. R. (2013) Proapoptotic chemotherapeutic drugs induce noncanonical processing and release of IL-1β via caspase-8 in dendritic cells. *J. Immunol.* **191**, 4789–803

303. Bossaller, L., Chiang, P.-I., Schmidt-Lauber, C., Ganesan, S., Kaiser, W. J., Rathinam, V. A. K., Mocarski, E. S., Subramanian, D., Green, D. R., Silverman, N., Fitzgerald, K. A., Marshak-Rothstein, A., and Latz, E. (2012) Cutting edge: FAS (CD95) mediates noncanonical IL-1β and IL-18 maturation via caspase-8 in an RIP3-independent manner. *J. Immunol.* **189**, 5508–12

304. Zitvogel, L., Kepp, O., Senovilla, L., Menger, L., Chaput, N., and Kroemer, G. (2010) Immunogenic tumor cell death for optimal anticancer therapy: the calreticulin exposure pathway. *Clin. Cancer Res.* **16**, 3100–4

305. Kaufman, R. J. (2002) Orchestrating the unfolded protein response in health and disease. *J. Clin. Invest.* **110**, 1389–98

306. Anand, P. K., Malireddi, R. K. S., and Kanneganti, T.-D. (2011) Role of the nlrp3 inflammasome in microbial infection. *Front. Microbiol.* **2**, 12

307. Kayagaki, N., Warming, S., Lamkanfi, M., Vande Walle, L., Louie, S., Dong, J., Newton, K., Qu, Y., Liu, J., Heldens, S., Zhang, J., Lee, W. P., Roose-Girma, M., and Dixit, V. M. (2011) Non-canonical inflammasome activation targets caspase-11. *Nature*. **479**, 117–21

308. Yi, Y.-S. (2020) Functional crosstalk between non-canonical caspase-11 and canonical NLRP3 inflammasomes during infection-mediated inflammation. *Immunology*. **159**, 142–155

309. Gurung, P., Anand, P. K., Malireddi, R. K. S., Vande Walle, L., Van Opdenbosch, N., Dillon, C. P., Weinlich, R., Green, D. R., Lamkanfi, M., and Kanneganti, T.-D. (2014) FADD and caspase-8 mediate priming and activation of the canonical and noncanonical Nlrp3 inflammasomes. *J. Immunol.* **192**, 1835–46

310. Man, S. M., Tourlomousis, P., Hopkins, L., Monie, T. P., Fitzgerald, K. A., and Bryant, C. E. (2013) Salmonella infection induces recruitment of Caspase-8 to the inflammasome to modulate IL-1β production. *J. Immunol.* **191**, 5239–46

311. Weng, D., Marty-Roix, R., Ganesan, S., Proulx, M. K., Vladimer, G. I., Kaiser, W. J., Mocarski, E. S., Pouliot, K., Chan, F. K.-M., Kelliher, M. A., Harris, P. A., Bertin, J., Gough, P. J., Shayakhmetov, D. M., Goguen, J. D., Fitzgerald, K. A., Silverman, N., and Lien, E. (2014) Caspase-8 and RIP kinases regulate bacteria-induced innate immune responses and cell death. *Proc. Natl. Acad. Sci. U. S. A.* **111**, 7391–6

312. Kang, T.-B., Yang, S.-H., Toth, B., Kovalenko, A., and Wallach, D. (2013) Caspase-8 blocks kinase RIPK3-mediated activation of the NLRP3 inflammasome. *Immunity*. **38**, 27–40

313. Kovalenko, A., Kim, J.-C., Kang, T.-B., Rajput, A., Bogdanov, K., Dittrich-Breiholz, O., Kracht, M., Brenner, O., and Wallach, D. (2009) Caspase-8 deficiency in epidermal keratinocytes triggers an inflammatory skin disease. *J. Exp. Med.* **206**, 2161–77

314. Li, C., Lasse, S., Lee, P., Nakasaki, M., Chen, S.-W., Yamasaki, K., Gallo, R. L., and Jamora, C. (2010) Development of atopic dermatitis-like skin disease from the chronic loss of epidermal caspase-8. *Proc. Natl. Acad. Sci. U. S. A.* **107**, 22249–54

315. Hanahan, D., and Weinberg, R. A. (2011) Hallmarks of cancer: the next generation. *Cell*. **144**, 646–74

316. Fulda, S. (2015) Targeting apoptosis for anticancer therapy. *Semin. Cancer Biol.* **31**, 84–8

317. Deaton, A. M., and Bird, A. (2011) CpG islands and the regulation of transcription.

Genes Dev. **25**, 1010–22

318. Soung, Y. H., Lee, J. W., Kim, S. Y., Sung, Y. J., Park, W. S., Nam, S. W., Kim, S. H., Lee, J. Y., Yoo, N. J., and Lee, S. H. (2005) Caspase-8 gene is frequently inactivated by the frameshift somatic mutation 1225_1226delTG in hepatocellular carcinomas. *Oncogene*. **24**, 141–7

319. Umar, M., Upadhyay, R., Kumar, S., Ghoshal, U. C., and Mittal, B. (2011) CASP8 -652 6N del and CASP8 IVS12-19G>A gene polymorphisms and susceptibility/prognosis of ESCC: a case control study in northern Indian population. *J. Surg. Oncol.* **103**, 716–23

320. Yin, J., Tang, W., Shao, A., Wang, L., Wang, X., Ding, G., Liu, C., Chen, Y., Chen, S., and Gu, H. (2014) Caspase8 rs1035142 G>T polymorphism was associated with an increased risk of esophageal cancer in a Chinese population. *Mol. Biol. Rep.* **41**, 2037–43

321. Iwase, M., Takaoka, S., Uchida, M., Yoshiba, S., Kondo, G., Watanabe, H., Ohashi, M., and Nagumo, M. (2008) Epidermal growth factor receptor inhibitors enhance susceptibility to Fas-mediated apoptosis in oral squamous cell carcinoma cells. *Oral Oncol.* **44**, 361–8

322. Keller, N., Mares, J., Zerbe, O., and Grütter, M. G. (2009) Structural and biochemical studies on procaspase-8: new insights on initiator caspase activation. *Structure*. **17**, 438–48

323. Cursi, S., Rufini, A., Stagni, V., Condò, I., Matafora, V., Bachi, A., Bonifazi, A. P., Coppola, L., Superti-Furga, G., Testi, R., and Barilà, D. (2006) Src kinase

phosphorylates Caspase-8 on Tyr380: a novel mechanism of apoptosis suppression. *EMBO J.* **25**, 1895–905

324. Ekonomopoulou, M. T., Babas, E., Mioglou-Kalouptsi, E., Malandri, M., and Iakovidou-Kritsi, Z. (2011) Changes in activities of caspase-8 and caspase-9 in human cervical malignancy. *Int. J. Gynecol. Cancer.* **21**, 435–8

325. Samaras, V., Tsopanomichalou, M., Stamatelli, A., Arnaoutoglou, C., Samaras, E., Arnaoutoglou, M., Poulias, H., and Barbatis, C. (2009) Is there any potential link among caspase-8, p-p38 MAPK and bcl-2 in clear cell renal cell carcinomas? A comparative immunohistochemical analysis with clinical connotations. *Diagn. Pathol.* **4**, 7

326. Helfer, B., Boswell, B. C., Finlay, D., Cipres, A., Vuori, K., Bong Kang, T., Wallach, D., Dorfleutner, A., Lahti, J. M., Flynn, D. C., and Frisch, S. M. (2006) Caspase-8 promotes cell motility and calpain activity under nonapoptotic conditions. *Cancer Res.* **66**, 4273–8

327. Barbero, S., Mielgo, A., Torres, V., Teitz, T., Shields, D. J., Mikolon, D., Bogyo, M., Barilà, D., Lahti, J. M., Schlaepfer, D., and Stupack, D. G. (2009) Caspase-8 association with the focal adhesion complex promotes tumor cell migration and metastasis. *Cancer Res.* **69**, 3755–63

328. Barbero, S., Barilà, D., Mielgo, A., Stagni, V., Clair, K., and Stupack, D. (2008) Identification of a critical tyrosine residue in caspase 8 that promotes cell migration. *J. Biol. Chem.* **283**, 13031–4

329. Fulda, S. (2015) Promises and Challenges of Smac Mimetics as Cancer

Therapeutics. *Clin. Cancer Res.* **21**, 5030–6

330. Probst, B. L., Liu, L., Ramesh, V., Li, L., Sun, H., Minna, J. D., and Wang, L.
(2010) Smac mimetics increase cancer cell response to chemotherapeutics in a
TNF-α-dependent manner. *Cell Death Differ.* **17**, 1645–54

331. Dineen, S. P., Roland, C. L., Greer, R., Carbon, J. G., Toombs, J. E., Gupta, P.,
Bardeesy, N., Sun, H., Williams, N., Minna, J. D., and Brekken, R. A. (2010)
Smac mimetic increases chemotherapy response and improves survival in mice
with pancreatic cancer. *Cancer Res.* **70**, 2852–61

332. Vellanki, S. H. K., Grabrucker, A., Liebau, S., Proepper, C., Eramo, A., Braun, V.,
Boeckers, T., Debatin, K.-M., and Fulda, S. (2009) Small-molecule XIAP inhibitors
enhance gamma-irradiation-induced apoptosis in glioblastoma. *Neoplasia*. **11**,
743–52

333. Giagkousiklidis, S., Vellanki, S. H., Debatin, K.-M., and Fulda, S. (2007)
Sensitization of pancreatic carcinoma cells for gamma-irradiation-induced
apoptosis by XIAP inhibition. *Oncogene*. **26**, 7006–16

334. Bake, V., Roesler, S., Eckhardt, I., Belz, K., and Fulda, S. (2014) Synergistic
interaction of Smac mimetic and IFNα to trigger apoptosis in acute myeloid
leukemia cells. *Cancer Lett.* **355**, 224–31

335. Eytan, D. F., Snow, G. E., Carlson, S., Derakhshan, A., Saleh, A., Schiltz, S.,
Cheng, H., Mohan, S., Cornelius, S., Coupar, J., Sowers, A. L., Hernandez, L.,
Mitchell, J. B., Annunziata, C. M., Chen, Z., and Van Waes, C. (2016) SMAC
Mimetic Birinapant plus Radiation Eradicates Human Head and Neck Cancers

with Genomic Amplifications of Cell Death Genes FADD and BIRC2. *Cancer Res.* **76**, 5442–5454

336. Yang, L., Kumar, B., Shen, C., Zhao, S., Blakaj, D., Li, T., Romito, M., Teknos, T. N., and Williams, T. M. (2019) LCL161, a SMAC-mimetic, Preferentially Radiosensitizes Human Papillomavirus-negative Head and Neck Squamous Cell Carcinoma. *Mol. Cancer Ther.* **18**, 1025–1035

337. Xiao, R., An, Y., Ye, W., Derakhshan, A., Cheng, H., Yang, X., Allen, C., Chen, Z., Schmitt, N. C., and Van Waes, C. (2019) Dual Antagonist of cIAP/XIAP ASTX660 Sensitizes HPV- and HPV+ Head and Neck Cancers to TNFα, TRAIL, and Radiation Therapy. *Clin. Cancer Res.* **25**, 6463–6474

338. Zhao, M., Sano, D., Pickering, C. R., Jasser, S. A., Henderson, Y. C., Clayman, G. L., Sturgis, E. M., Ow, T. J., Lotan, R., Carey, T. E., Sacks, P. G., Grandis, J. R., Sidransky, D., Heldin, N. E., and Myers, J. N. (2011) Assembly and initial characterization of a panel of 85 genomically validated cell lines from diverse head and neck tumor sites. *Clin. Cancer Res.* **17**, 7248–64

339. Judd, N. P., Winkler, A. E., Murillo-Sauca, O., Brotman, J. J., Law, J. H., Lewis, J. S., Dunn, G. P., Bui, J. D., Sunwoo, J. B., and Uppaluri, R. (2012) ERK1/2 regulation of CD44 modulates oral cancer aggressiveness. *Cancer Res.* **72**, 365–74

340. Campbell, J. D., Yau, C., Bowlby, R., Liu, Y., Brennan, K., Fan, H., Taylor, A. M., Wang, C., Walter, V., Akbani, R., Byers, L. A., Creighton, C. J., Coarfa, C., Shih, J., Cherniack, A. D., Gevaert, O., Prunello, M., Shen, H., Anur, P., Chen, J.,

Cheng, H., Hayes, D. N., Bullman, S., Pedamallu, C. S., Ojesina, A. I., Sadeghi, S., Mungall, K. L., Robertson, A. G., Benz, C., Schultz, A., Kanchi, R. S., Gay, C. M., Hegde, A., Diao, L., Wang, J., Ma, W., Sumazin, P., Chiu, H.-S., Chen, T.-W., Gunaratne, P., Donehower, L., Rader, J. S., Zuna, R., Al-Ahmadie, H., Lazar, A. J., Flores, E. R., Tsai, K. Y., Zhou, J. H., Rustgi, A. K., Drill, E., Shen, R., Wong, C. K., Cancer Genome Atlas Research Network, Stuart, J. M., Laird, P. W., Hoadley, K. A., Weinstein, J. N., Peto, M., Pickering, C. R., Chen, Z., and Van Waes, C. (2018) Genomic, Pathway Network, and Immunologic Features Distinguishing Squamous Carcinomas. *Cell Rep.* **23**, 194-212.e6

341. Gleber-Netto, F. O., Rao, X., Guo, T., Xi, Y., Gao, M., Shen, L., Erikson, K., Kalu, N. N., Ren, S., Xu, G., Fisch, K. M., Akagi, K., Seiwert, T., Gillison, M., Frederick, M. J., Johnson, F. M., Wang, J., Myers, J. N., Califano, J., Skinner, H. D., and Pickering, C. R. (2019) Variations in HPV function are associated with survival in squamous cell carcinoma. *JCI insight*. 10.1172/jci.insight.124762

342. Ran, F. A., Hsu, P. D., Wright, J., Agarwala, V., Scott, D. A., and Zhang, F. (2013) Genome engineering using the CRISPR-Cas9 system. *Nat. Protoc.* **8**, 2281–2308

343. Sigl, R., Ploner, C., Shivalingaiah, G., Kofler, R., and Geley, S. (2014) Development of a multipurpose GATEWAY-based lentiviral tetracycline-regulated conditional RNAi system (GLTR). *PLoS One*. **9**, e97764

344. Ando, M., Kawazu, M., Ueno, T., Fukumura, K., Yamato, A., Soda, M., Yamashita, Y., Choi, Y. L., Yamasoba, T., and Mano, H. (2013) Cancer-associated missense mutations of caspase-8 activate nuclear factor-κB signaling.

Cancer Sci. **104**, 1002–8

345. Tamatani, T., Azuma, M., Motegi, K., Takamaru, N., Kawashima, Y., and Bando, T. (2007) Cepharanthin-enhanced radiosensitivity through the inhibition of radiation-induced nuclear factor-kappaB activity in human oral squamous cell carcinoma cells. *Int. J. Oncol.* **31**, 761–8

346. Kozakai, N., Kikuchi, E., Hasegawa, M., Suzuki, E., Ide, H., Miyajima, A., Horiguchi, Y., Nakashima, J., Umezawa, K., Shigematsu, N., and Oya, M. (2012) Enhancement of radiosensitivity by a unique novel NF-κB inhibitor, DHMEQ, in prostate cancer. *Br. J. Cancer*. **107**, 652–7

347. Zhou, H., Liu, Y., Cheung, L. H., Kim, S., Zhang, W., Mohamedali, K. A., Anand, P., Hittelman, W. N., Aggarwal, B. B., and Rosenblum, M. G. (2010) Characterization and mechanistic studies of a novel melanoma-targeting construct containing IκBa for specific inhibition of nuclear factor-κB activity. *Neoplasia*. **12**, 766–77

348. Li, F., and Sethi, G. (2010) Targeting transcription factor NF-kappaB to overcome chemoresistance and radioresistance in cancer therapy. *Biochim. Biophys. Acta*. **1805**, 167–80

349. Didelot, C., Barberi-Heyob, M., Bianchi, A., Becuwe, P., Mirjolet, J. F., Dauça, M., and Merlin, J. L. (2001) Constitutive NF-kappaB activity influences basal apoptosis and radiosensitivity of head-and-neck carcinoma cell lines. *Int. J. Radiat. Oncol. Biol. Phys.* **51**, 1354–60

350. Balermpas, P., Michel, Y., Wagenblast, J., Seitz, O., Sipek, F., Rödel, F., Rödel,

C., and Fokas, E. (2013) Nuclear NF-κB expression correlates with outcome among patients with head and neck squamous cell carcinoma treated with primary chemoradiation therapy. *Int. J. Radiat. Oncol. Biol. Phys.* **86**, 785–90

351. Kalu, N. N., Mazumdar, T., Peng, S., Shen, L., Sambandam, V., Rao, X., Xi, Y., Li, L., Qi, Y., Gleber-Netto, F. O., Patel, A., Wang, J., Frederick, M. J., Myers, J. N., Pickering, C. R., and Johnson, F. M. (2017) Genomic characterization of human papillomavirus-positive and -negative human squamous cell cancer cell lines. *Oncotarget*. **8**, 86369–86383

352. Skinner, H. D., Sandulache, V. C., Ow, T. J., Meyn, R. E., Yordy, J. S., Beadle, B. M., Fitzgerald, A. L., Giri, U., Ang, K. K., and Myers, J. N. (2012) TP53 disruptive mutations lead to head and neck cancer treatment failure through inhibition of radiation-induced senescence. *Clin. Cancer Res.* **18**, 290–300

353. Nehs, M. A., Lin, C.-I., Kozono, D. E., Whang, E. E., Cho, N. L., Zhu, K., Moalem, J., Moore, F. D., and Ruan, D. T. (2011) Necroptosis is a novel mechanism of radiation-induced cell death in anaplastic thyroid and adrenocortical cancers. *Surgery*. **150**, 1032–9

354. Wang, H.-H., Wu, Z.-Q., Qian, D., Zaorsky, N. G., Qiu, M.-H., Cheng, J.-J., Jiang, C., Wang, J., Zeng, X.-L., Liu, C.-L., Tian, L.-J., Ying, G.-G., Meng, M.-B., Hao, X.-S., and Yuan, Z.-Y. (2018) Ablative Hypofractionated Radiation Therapy Enhances Non-Small Cell Lung Cancer Cell Killing via Preferential Stimulation of Necroptosis In Vitro and In Vivo. *Int. J. Radiat. Oncol. Biol. Phys.* **101**, 49–62

355. Zhou, W., and Yuan, J. (2014) SnapShot: Necroptosis. *Cell*. **158**, 464-464.e1

356. Najafov, A., Zervantonakis, I. K., Mookhtiar, A. K., Greninger, P., March, R. J., Egan, R. K., Luu, H. S., Stover, D. G., Matulonis, U. A., Benes, C. H., and Yuan, J. (2018) BRAF and AXL oncogenes drive RIPK3 expression loss in cancer. *PLoS Biol.* **16**, e2005756

357. Zargarian, S., Shlomovitz, I., Erlich, Z., Hourizadeh, A., Ofir-Birin, Y., Croker, B. A., Regev-Rudzki, N., Edry-Botzer, L., and Gerlic, M. (2017) Phosphatidylserine externalization, "necroptotic bodies" release, and phagocytosis during necroptosis. *PLoS Biol.* **15**, e2002711

358. Koo, G.-B., Morgan, M. J., Lee, D.-G., Kim, W.-J., Yoon, J.-H., Koo, J. S., Kim, S. Il, Kim, S. J., Son, M. K., Hong, S. S., Levy, J. M. M., Pollyea, D. A., Jordan, C. T., Yan, P., Frankhouser, D., Nicolet, D., Maharry, K., Marcucci, G., Choi, K. S., Cho, H., Thorburn, A., and Kim, Y.-S. (2015) Methylation-dependent loss of RIP3 expression in cancer represses programmed necrosis in response to chemotherapeutics. *Cell Res.* **25**, 707–25

359. Morgan, M. J., and Kim, Y.-S. (2015) The serine threonine kinase RIP3: lost and found. *BMB Rep.* **48**, 303–12

360. Pockros, P. J., Schiff, E. R., Shiffman, M. L., McHutchison, J. G., Gish, R. G., Afdhal, N. H., Makhviladze, M., Huyghe, M., Hecht, D., Oltersdorf, T., and Shapiro, D. A. (2007) Oral IDN-6556, an antiapoptotic caspase inhibitor, may lower aminotransferase activity in patients with chronic hepatitis C. *Hepatology*. **46**, 324–9

361. Bonaventura, P., Shekarian, T., Alcazer, V., Valladeau-Guilemond, J., Valsesia-

Wittmann, S., Amigorena, S., Caux, C., and Depil, S. (2019) Cold Tumors: A Therapeutic Challenge for Immunotherapy. *Front. Immunol.* **10**, 168

362. Snyder, A. G., Hubbard, N. W., Messmer, M. N., Kofman, S. B., Hagan, C. E., Orozco, S. L., Chiang, K., Daniels, B. P., Baker, D., and Oberst, A. (2019) Intratumoral activation of the necroptotic pathway components RIPK1 and RIPK3 potentiates antitumor immunity. *Sci. Immunol.* 10.1126/sciimmunol.aaw2004

363. Brumatti, G., Ma, C., Lalaoui, N., Nguyen, N.-Y., Navarro, M., Tanzer, M. C., Richmond, J., Ghisi, M., Salmon, J. M., Silke, N., Pomilio, G., Glaser, S. P., de Valle, E., Gugasyan, R., Gurthridge, M. A., Condon, S. M., Johnstone, R. W., Lock, R., Salvesen, G., Wei, A., Vaux, D. L., Ekert, P. G., and Silke, J. (2016) The caspase-8 inhibitor emricasan combines with the SMAC mimetic birinapant to induce necroptosis and treat acute myeloid leukemia. *Sci. Transl. Med.* **8**, 339ra69

364. Mehta, G., Rousell, S., Burgess, G., Morris, M., Wright, G., McPherson, S., Frenette, C., Cave, M., Hagerty, D. T., Spada, A., and Jalan, R. (2018) A Placebo-Controlled, Multicenter, Double-Blind, Phase 2 Randomized Trial of the Pan-Caspase Inhibitor Emricasan in Patients with Acutely Decompensated Cirrhosis. *J. Clin. Exp. Hepatol.* **8**, 224–234

365. Yang, C., Li, J., Yu, L., Zhang, Z., Xu, F., Jiang, L., Zhou, X., and He, S. (2017) Regulation of RIP3 by the transcription factor Sp1 and the epigenetic regulator UHRF1 modulates cancer cell necroptosis. *Cell Death Dis.* **8**, e3084

366. Gillison, M., Akagi, K., Xiao, W., Jiang, B., Pickerd, R., Li, J., Swanson, B.,

Agrawal, A., Zucker, M., Stache-Crain, B., Emde, A.K., Geiger, H., Robine N., Coombes, K., and Symer, D. (2019) Human papillomavirus and the landscape of secondary genetic alterations in oral cancers. *Genome Res.* **29(1),** 1-17

366. Gillison, M., Trotti, A., Harris, J., Eisbruch, A., Harari, P., Adelstein, D., Jordan R., Dignam, J., and Thu Le, Q. (2019) Radiotherapy plus cetuximab or cisplatin in HPV-positive oropharyngeal cancer (NRG Oncology RTOG 1016): a randomized, multicentre, non-inferiority trial *Lancet* **393(10166),** 40-50

367. Fernandes, Q., Merhi, M., Raza, A., Inchakalody, VP., Abdelouahab, N., Zar Gul, AR., Uddin S., Dermime, S. (2018) Role of Epstein-Barr Virus in the Pathogenesis of Head and Neck Cancers and Its Potential as an Immunutherapeutic Target *Front Oncol.* **8: 257**

368. Krysko, O., Aaes, TL., Kagan, VE., D'Herde, K., Bachert, C.,Leybaert, L., Vandenabeele P., Krysko, DV. (2017) Necroptotis cell death in anti-cancer therapy *Immunol Rev.* **280(1):** 207-219

369. Reed, JC. (2018) Drug insight: cancer therapy strategies based on restoration of endogenous cell death mechanisms. *Nat Clin Pract Oncol.* **3(7):** 388-98

370. Aaes, TL., Kaczmarek, A., Delvaeye, T., De Craene, B., De Koker, S., Heyndrickx, L., Delrue I., Taminau, J., Wiernicki B., De Groote, P., Garg, AD., Leybaert, L., Grooten, J., Bertrand, MJ., Agostinis, P., Berx, G., Declercq, W., Vandenabeele, P., Krysko, DV. (2016) Vaccination with necroptotic cancer cells induces efficient anti-tumor immunity *Cell Rep.* **15(2):** 274-87

371. Schmidt, SV., Seibert, S., Walch-Rückheim, B., Vicinus, B., Kamionka, EM.,

Pahne-Zeppenfeld, J., Solomayer EF., Kim, YJ., Bohle, RM., Smola, S. (2015)

RIPK3 expression in cervical cancer cells is required for PolyIC-induced

necroptosis, IL-1α release, and efficient paracrine dendritic cell activation

Oncotarget **6(11):** 8635-47

VITA

Burak Uzunparmak was born in Antakya-Hatay, Turkey to Vedat and Zeki Uzunparmak. He grew up in Antakya and moved to Ankara-Turkey in 1999 to study at the prestigious Ankara Science High School. After completing his high school studies in 2002, he entered Hacettepe University School of Medicine in Ankara, Turkey. During his medical education, he pursued summer internships in the laboratories of Drs Mark Exley at Beh Israel Deaconess Medical Center (BIDMC), Harvard Medical School, Boston MA and Andrew Scharenberg at Seattle Children's Hospital, University of Washington, Seattle WA in 2005 and 2008, respectively. After receiving his Doctor of Medicine (M.D.) degree from Hacettepe University School of Medicine, Ankara, Turkey in 2009 , he joined Dr Bana Jabri's laboratory at the University of Chicago as a post-doctoral researcher in 2010. At the University of Chicago, while working with medical oncologists and cancer scienctists on a variety of projects, Burak developed an interest in cancer research and he decided to apply for PhD programs. In August 2012, he entered the University of Texas MD Anderson Cancer Center UTHealth Graduate School of Biomedical Sciences, and joined Dr Curtis R. Pickering's laboratory in 2015 as a graduate student where he focused on investigating the role of Caspase-8 mutations in the development and progression of Head and Neck Squamous Carcinoma (HNSCC). Burak is intending to graduate with a PhD degree in Cancer Biology in May 2020.